Astron Astrophys Rev (2018) 26:3
https://doi.org/10.1007/s00159-018-0107-z

REVIEW ARTICLE

Radio jets from young stellar objects

Guillem Anglada[1] · **Luis F. Rodríguez**[2] · **Carlos Carrasco-González**[2]

Received: 19 September 2017 / Published online: 26 June 2018

Abstract Jets and outflows are ubiquitous in the process of formation of stars since outflow is intimately associated with accretion. Free–free (thermal) radio continuum emission in the centimeter domain is associated with these jets. The emission is relatively weak and compact, and sensitive radio interferometers of high angular resolution are required to detect and study it. One of the key problems in the study of outflows is to determine how they are accelerated and collimated. Observations in the cm range are most useful to trace the base of the ionized jets, close to the young central object and the inner parts of its accretion disk, where optical or near-IR imaging is made difficult by the high extinction present. Radio recombination lines in jets (in combination with proper motions) should provide their 3D kinematics at very small scale (near their origin). Future instruments such as the Square Kilometre Array (SKA) and the Next Generation Very Large Array (ngVLA) will be crucial to perform this kind of sensitive observations. Thermal jets are associated with both high and low mass protostars and possibly even with objects in the substellar domain. The ionizing mechanism of these radio jets appears to be related to shocks in the associated outflows, as suggested by the observed correlation between the centimeter luminosity and the outflow momentum rate. From this correlation and that of the centimeter luminosity with the bolometric

✉ Guillem Anglada
guillem@iaa.es

Luis F. Rodríguez
l.rodriguez@irya.unam.mx

Carlos Carrasco-González
c.carrasco@irya.unam.mx

1 Instituto de Astrofísica de Andalucía, CSIC, Glorieta de la Astronomía s/n, 18008 Granada, Spain

2 Instituto de Radioastronomía y Astrofísica, UNAM, Apdo. Postal 3-72, 58089 Morelia, Michoacán, Mexico

luminosity of the system it will be possible to discriminate between unresolved HII regions and jets, and to infer additional physical properties of the embedded objects. Some jets associated with young stellar objects (YSOs) show indications of non-thermal emission (negative spectral indices) in part of their lobes. Linearly polarized synchrotron emission has been found in the jet of HH 80–81, allowing one to measure the direction and intensity of the jet magnetic field, a key ingredient to determine the collimation and ejection mechanisms. As only a fraction of the emission is polarized, very sensitive observations such as those that will be feasible with the interferometers previously mentioned are required to perform studies in a large sample of sources. Jets are present in many kinds of astrophysical scenarios. Characterizing radio jets in YSOs, where thermal emission allows one to determine their physical conditions in a reliable way, would also be useful in understanding acceleration and collimation mechanisms in all kinds of astrophysical jets, such as those associated with stellar and supermassive black holes and planetary nebulae.

Keywords Radiation mechanisms: non-thermal · Radiation mechanisms: thermal · Stars: pre-main sequence · ISM: Herbig–Haro objects · Radio lines: stars

1 Introduction

Until around 1980, the process of star formation was believed to be dominated by infall motions from an ambient cloud that made the forming star at its center grow in mass. Several papers published at that time indicated that powerful bipolar ejections of high-velocity molecular (Snell et al. 1980; Rodriguez et al. 1980a) and ionized (Herbig and Jones 1981) gas were also present. The star formation paradigm changed from one of pure infall to one in which infall and outflow coexisted. As a matter of fact, both processes have a symbiotic relation: the rotating disk by which the star accretes provides the energy for the outflow, while this latter process removes the excess of angular momentum that otherwise will impede further accretion.

Early studies of centimeter radio continuum from visible T Tau stars made mostly with the Very Large Array (VLA) showed that emission was sometimes detected in them (e.g., Cohen et al. 1982). Later studies made evident that in these more evolved stars the emission could have a thermal (free–free) origin but that most frequently the emission was dominated by a nonthermal (gyrosynchrotron) process (Feigelson and Montmerle 1985) produced in the active magnetospheres of the stars. These non-thermal radio stars are frequently time-variable (e.g., Rivilla et al. 2015) and its compact radio size makes them ideal for the determination of accurate parallaxes using Very Long Baseline Interferometry (VLBI) observations (e.g., Kounkel et al. 2017).

In contrast, the youngest low-mass stars, the so-called Class 0 and I objects (Lada 1991; Andre et al. 1993) frequently exhibit free–free emission at weak but detectable levels (Anglada et al. 1992). In the best studied cases, the sources are resolved angularly at the sub-arcsec scale and found to be elongated in the direction of the large-scale tracers of the outflow (e.g., Rodriguez et al. 1990; Anglada 1996), indicating that they trace the region, very close to the exciting star, where the outflow phenomenon

originates. The spectral index at centimeter wavelengths α (defined as $S_\nu \propto \nu^\alpha$), usually rises slowly with frequency and can be understood with the free–free jet models of Reynolds (1986). Given its morphology and spectrum, these radio sources are sometimes referred to as "thermal radio jets". It should be noted that there are a few Class I objects where the emission seems to be dominantly gyrosynchrotron (Feigelson et al. 1998; Dzib et al. 2013). These cases might be due to a favorable geometry (that is, the protostar is seen nearly pole-on or nearly edge-on, where the free–free opacity might be reduced; Forbrich et al. 2007), or to clearing of circumstellar material by tidal forces in a tight binary system (Dzib et al. 2010)

In the last years it has become clear that the radio jets are present in young stars across the stellar spectrum, from O-type protostars (Garay et al. 2003) and possibly to brown dwarfs (Palau et al. 2014), suggesting that the disk–jet scenario that explains the formation of solar-type stars extends to all stars and even into the sub-stellar regime. The observed centimeter radio luminosities (taken to be $S_\nu d^2$, with d being the distance) go from ~ 100 mJy kpc^2 for massive young stars to $\sim 3 \times 10^{-3}$ mJy kpc^2 for young brown dwarfs.

High sensitivity studies of Herbig–Haro systems revealed that a large fraction of them showed the presence of central centimeter continuum sources (Rodriguez and Reipurth 1998). With the extraordinary sensitivity of the Jansky VLA (JVLA) and planed future instrumentation it is expected that all nearby (a few kpc) young stellar objects (YSOs) known to be associated with outflows, both molecular and/or optical/infrared, will be detectable as centimeter sources (Anglada et al. 2015).

The topic of radio jets from young stars has been reviewed by Anglada (1996), Anglada et al. (2015) and Rodríguez (1997, 2011). The more general theme of multifrequency jets and outflows from young stars has been extensively reviewed in the literature, with the most recent contributions being Frank et al. (2014) and Bally (2016). In this review we concentrate on radio results obtained over the last two decades, emphasizing possible lines of study feasible with the improved capabilities of current and future radio interferometers.

2 Information from radio jets

The study of radio jets associated with young stars has several astronomical uses. Given the large obscuration present towards the very young stars, the detection of the radio jet provides so far the best way to obtain their accurate positions. These observations also provide information on the direction and collimation of the gas ejected by the young system in the last few years and allow a comparison with the gas in the molecular outflows and optical/infrared HH jets, that trace the ejection over timescales one to two orders of magnitude larger. This comparison allows to make evident changes in the ejection direction possibly resulting from precession or orbital motions in binary systems (Rodríguez et al. 2010; Masqué et al. 2012).

In some sources it has been possible to establish the proper motions of the core of the jet and to confirm its association with the region studied (Loinard et al. 2002; Rodríguez et al. 2003a; Lim and Takakuwa 2006; Carrasco-González et al. 2008a; Loinard et al. 2010; Rodríguez et al. 2012a, b). In the case of the binary jet systems

L1551 IRS5 and YLW 15, the determination of its orbital motions (Lim and Takakuwa 2006; Curiel et al. 2004) allows one to confirm that they are solar-mass systems and that they are very overluminous with respect to the corresponding main sequence luminosity, as expected for objects that are accreting strongly.

The free–free radio emission at cm wavelengths has been used for a long time to estimate important physical properties of YSO jets (see below). Recently, the observation of the radio emission from jets has reached much lower frequencies, as in the recent Low Frequency ARray (LOFAR) observations at 149 GHz (2 m) of T Tau (Coughlan et al. 2017). These observations have revealed the low-frequency turnover of the free–free spectrum, a result that has allowed the degeneracy between emission measure and electron density to be broken.

3 Observed properties of radio jets

3.1 Properties of currently known angularly resolved radio jets

In Table 1 we present the parameters of selected radio jets that have been angularly resolved. Several trends can be outlined. The spectral index, α, is moderately positive, going from values of 0.1 to ~ 1, with a median of 0.45. The opening angle of the radio jet near its origin, θ_0, is typically in the few tens of degrees. In contrast, if we consider the HH objects or knots located relatively far from the star, an opening angle an order of magnitude smaller is derived. This result has been taken to suggest that there is recollimation at scales of tens to hundreds of au. The jet velocity is typically in the 100 to 1000 km s^{-1} range. The ionized mass loss rate, $\dot{M}_{ion}$, is found to be typically an order of magnitude smaller than that determined from the large-scale molecular outflow, and as derived from atomic emission lines, a result that has been taken to imply that the radio jet is only partially ionized ($\sim$ 1–10%; Rodriguez et al. 1990; Hartigan et al. 1994; Bacciotti et al. 1995) and that the mass loss rates determined from them are only lower limits. In Fig. 1 we show images of several selected radio jets.

3.2 Proper motions in the jet

As noted above, comparing observations taken with years of separation it has been possible in a few cases to determine the proper motions of the core of the jet, whose centroid is believed to coincide within a few au's with the young star (e.g., Curiel et al. 2003; Chandler et al. 2005; Rodríguez et al. 2012b, a). These proper motions are consistent with those of other stars in the region.

It is also possible to follow the birth and proper motions of new radio knots ejected by the star (Marti et al. 1995; Curiel et al. 2006; Pech et al. 2010; Carrasco-González et al. 2010a, 2012a; Gómez et al. 2013; Rodríguez-Kamenetzky et al. 2016; Osorio et al. 2017). When radio knots are detected very near the protostar, these are most probably due to internal shocks in the jet resulting from changes in the velocity of the material with time. These shocks are weak, and the emission mechanism seems to be free–free emission from (partially) ionized gas. Their proper motions are directly related to the

Table 1 Properties of selected angularly resolved radio jets in YSOs

Source	$L_{\rm bol}$ ($L_\odot$)	$M_\star$ ($M_\odot$)	d (kpc)	S_ν (mJy)	α	θ_0 (deg)	Size (au)	v_j (km s^{-1})	$t_{\rm dyn}$ (year)	ϵ	$\dot{M}_{ion}$ ($M_\odot$ year^{-1})	r_0 (au)	Refs.
HH 1–2 VLA1	20	~ 1	0.4	1	0.3	19	200	270	2	0.7	1×10^{-8}	≤ 11	1, 2, 3, 4
NGC 2071-IRS3	~ 500	4	0.4	3	0.6	40	200	400[a]	1	1.0	2×10^{-7}	≤ 18	5, 6, 2, 7
Cep A HW2	1×10^4	15	0.7	10	0.7	14	400	460	2	0.9	5×10^{-7}	≤ 60	8, 9, 10, 11, 12
HH 80–81	2×10^4	15	1.7	5	0.2	34	1500	1000	4	0.6	1×10^{-6}	≤ 25	13, 14, 15, 16, 17, 18
IRAS 16547-4247	6×10^4	20	2.9	11	0.5	25	3000	900[a]	8	0.9	8×10^{-6}	≤ 310	19, 20, 21, 22
Serpens	300	3	0.42	2.8	0.2	< 34	280	300	2	0.6	3×10^{-8}	≤ 9	23, 24, 25, 26, 27
AB Aur	38	2.4	0.14	0.14	1.1	< 39	24	300[a]	0.2	3.5	2×10^{-8}	≤ 3	28, 29, 30
L1551 IRS5[b]	20	0.6	0.14	0.8	0.1	36	39	150[a]	0.6	0.6	1×10^{-9}	≤ 1	31, 32, 33
HH 111[c]	25	1.3	0.4	0.8	~ 1	< 79	110	400	0.7	2.3	2×10^{-7}	≤ 12	34, 35, 36, 37, 38
HL Tau	7	1.3	0.14	0.3	~ 0.3	69	27	230[a]	0.3	0.7	2×10^{-9}	~ 1.5	39, 40, 41
IC 348-SMM2E	0.1	0.03	0.24	0.02	~ 0.4	45[d]	< 100	~ 50[a]	< 2	0.8	2×10^{-10}	≤ 1	42, 43, 44
W75N VLA3	750	6[d]	2.0	4.0	0.6	37	420	220	4.6	1.0	6×10^{-7}	≤ 70	45, 46
OMC2 VLA11	360	4[d]	0.42	2.2	0.3	10	200	100	4.6	1.0	6×10^{-7}	≤ 70	2, 47, 48
Re50N	250	4[d]	0.42	1.1	0.7	33	450	400	2.7	1.2	8×10^{-8}	≤ 13	2, 49, 50

References: (1) Fischer et al. (2010); (2) Menten et al. (2007); (3) Rodriguez et al. (1990); (4) Rodríguez et al. (2000); (5) Butner et al. (1990); (6) Carrasco-González et al. (2012a); (7) Torrelles et al. (1998); (8) Hughes et al. (1995); (9) Patel et al. (2005); (10) Dzib et al. (2011); (11) Curiel et al. (2006); (12) Rodriguez et al. (1994b); (13) Aspin and Geballe (1992); (14) Fernández-López et al. (2011); (15) Rodríguez et al. (1980b); (16) Marti et al. (1995); (17) Marti et al. (1993); (18) Carrasco-González et al. (2012b); (19) Zapata et al. (2015b); (20) Garay et al. (2003); (21) Rodríguez et al. (2008); (22) Rodríguez et al. (2005); (23) Dzib et al. (2010); (24) Rodriguez et al. (1989a); (25) Harvey et al. (1984); (26) Curiel et al. (1993); (27) Rodríguez-Kamenetzky et al. (2016); (28) DeWarf et al. (2003); (29) van den Ancker et al. (1997); (30) Rodríguez et al. (2014a); (31) Liseau (2005); (32) Rodríguez et al. (2003b); (33) Rodríguez et al. (1998); (34) Reipurth (1989); (35) Lee (2010); (36) Gómez et al. (2013); (37) Rodriguez and Reipurth (1994); (38) Cernicharo and Reipurth (1996); (39) Cohen (1983); (40) ALMA Partnership (2015); (41) A. M. Lumbreras et al., in preparation (42) Palau et al. (2014); (43) Forbrich et al. (2015); (44) Rodríguez et al. (2014b); (45) Persi et al. (2006); (46) Carrasco-González et al. (2010a); (47) Adams et al. (2012); (48) Osorio et al. (2017); (49) Chiang et al. (2015); (50) L. F. Rodríguez et al., in preparation

[a] Calculated using Eq. (12)

[b] Binary twin jet system. The values listed are the mean value of the two jets

[c] Binary jet system. The values listed are for the dominant east-west jet

[d] Assumed

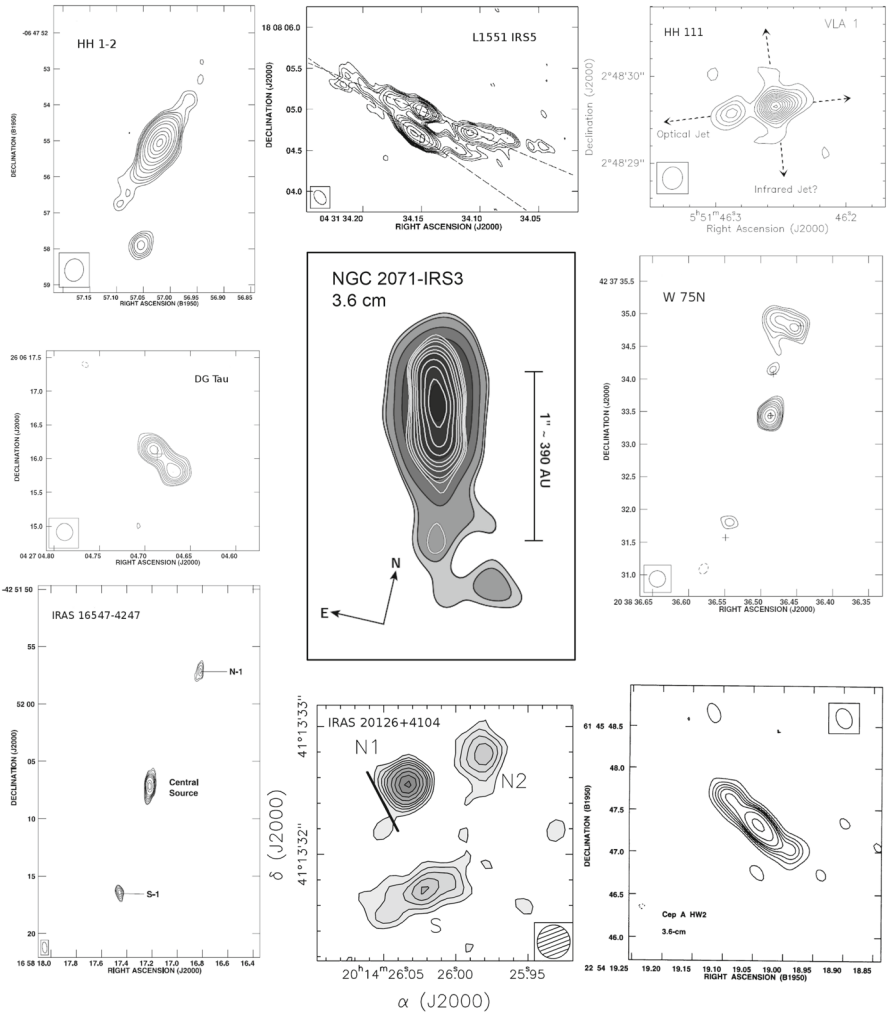

Fig. 1 Images of selected radio jets. From left to right, and top to bottom: HH 1–2 (Rodríguez et al. 2000); L1551-IRS5 (Rodríguez et al. 2003b); HH 111 (Gómez et al. 2013); DG Tau (Rodríguez et al. 2012b); NGC2071-IRS3 (Carrasco-González et al. 2012a); W75N (Carrasco-González et al. 2010a); IRAS 16547−4247 (Rodríguez et al. 2005); IRAS 20126+4104 (Hofner et al. 2007); Cep A HW2 (Rodriguez et al. 1994b). Jets from low- and intermediate-mass protostars are shown in the top and middle panels, while those from high-mass protostars are shown in the bottom panels

velocity of the jet material as it arises from the protostar. The observed proper motions of these internal shocks suggest velocities of the jet that go from $\sim$ 100 km s^{-1} in the low mass stars up to $\sim$ 1000 km s^{-1} in the most massive objects. So far, in some sources there is also evidence of deceleration far from the protostar. The radio knots observed by Marti et al. (1995) close to the star in the HH 80–81 system move at velocities of $\sim$ 1000 km s^{-1} in the plane of the sky, while the more distant optical HH objects show velocities of order 350 km s^{-1} (Heathcote et al. 1998; Masqué et al.

2015). A similar case has been observed in the triple source in Serpens, where knots near the protostar appear to be ejected at very high velocities ($\sim 500\,\mathrm{km\,s^{-1}}$), while radio knots far from the protostar move at slower velocities ($\sim 200\,\mathrm{km\,s^{-1}}$; Rodríguez-Kamenetzky et al. 2016). These results suggest that radio knots far from the star are then most probably tracing the shocks of the jet against the ambient medium. In some cases, when the velocity of the jet is high, the emission of these outer knots seems to be of synchrotron nature (negative spectral indices), implying that a mechanism of particle acceleration can take place at these termination shocks. This topic is discussed in more detail below (Sect. 6).

3.3 Variability

Since thermal radio jets are typically detected over scales of $\sim$ 100 au and have velocities in the order of 300 km s^{-1}, one expects that if variations are present they will be detectable on timescales of the order of the travel time ($\sim$ a few years) or longer.

The first attempts to detect time variability suggested that modest variations, of order 10–20%, could be present in some sources (Martí et al. 1998; Rodríguez et al. 1999, 2000).

However, over time a few examples of more extreme variability were detected. The 3.5 cm flux density of the radio source powering the HH 119 flow in B335 was 0.21 ± 0.03 mJy in 1990 (Anglada et al. 1992), dropping to $\leq 0.08 \pm 0.02$ mJy in 1994 (Avila et al. 2001), and finally increasing to 0.39 ± 0.02 mJy in 2001 (Reipurth et al. 2002). C. Carrasco-González et al. (in preparation) report a factor of two increase in the 1.0 cm flux density of the southern component of XZ Tau over a few months. This increase in radio flux density has been related by these authors to an optical/infrared outburst (Krist et al. 2008) attributed to the periastron passage in a close binary system.

The radio source associated with DG Tau A presented an important increase in its 3.5 cm flux density, that was 0.41 ± 0.04 mJy in 1994 to 0.84 ± 0.05 mJy in 1996 (Rodríguez et al. 2012b). The radio source associated with DG Tau B decreased from a total 3.5 cm flux density of 0.56 ± 0.07 mJy in 1994 to 0.32 ± 0.05 mJy in 1996 (Rodríguez et al. 2012a). In the source IRAS 16293–2422A2, Pech et al. (2010) observed an increase in the 3.5 cm flux density from 1.35 ± 0.08 mJy in 2003 to > 2.2 mJy en 2009. In these last three sources the observed variations were clearly associated with the appearance or disappearance of bright radio knots in the systems.

Despite these remarkable cases, most of the radio jets that have been monitored show no evidence of variability above the 10–20% level (e.g., Rodríguez et al. 2008; Loinard et al. 2010; Carrasco-González et al. 2012a, 2015; Rodríguez et al. 2014a; see Fig. 2). If ejections are present in these systems, they are not as bright as the cases discussed in the previous paragraph.

Given that accretion and outflow are believed to be correlated, the variations in the radio continuum emission (tracing the ionized outflow) and in the compact infrared and millimeter continuum emissions (tracing the accretion to the star) are expected to present some degree of temporal correlation. The correlation of the [OI] jet brightness with the mid-infrared excess from the inner disk and with the optical excess from the

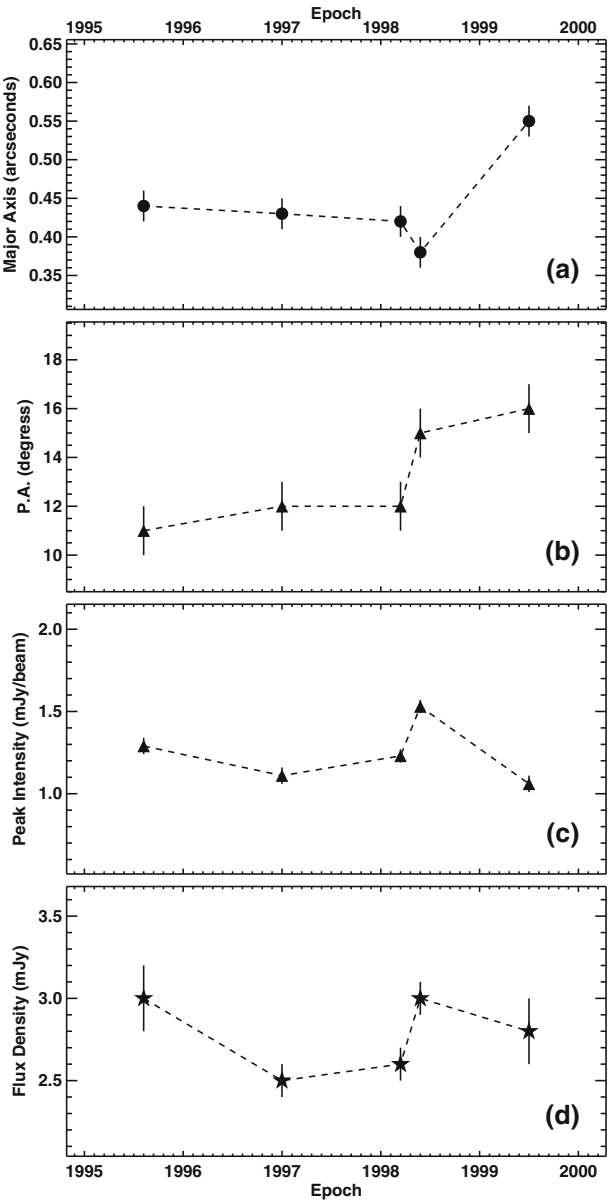

Fig. 2 Monitoring of the deconvolved size of the major axis (**a**), position angle (**b**), peak intensity (**c**), and flux density (**d**) of NGC2071 IRS 3 at 3.6 cm. Image reproduced with permission from Carrasco-González et al. (2012a), copyright by AAS

hot accretion layer has been considered as evidence that jets are powered by accretion (Cabrit 2007 and references therein; see also the recent work by Nisini et al. 2018). Also the correlation between the radio and bolometric luminosities (see Sect. 8.1) in very young objects supports this hypothesis. In these objects this correlation is expected

since most of the luminosity comes from accretion, while the radio continuum traces the outflow.

However, temporal correlations between the variations in the bolometric luminosity and the radio continuum have not been clearly observed. For example, the infrared source HOPS 383 in Orion was reported to have a large bolometric luminosity increase between 2004 and 2008 (Safron et al. 2015), while the radio continuum monitoring at several epochs before and after the outburst (from 1998 to 2014) shows no significant variation in the flux density (Galván-Madrid et al. 2015). Ellerbroek et al. (2014) could not establish a relation between outflow and accretion variability in the Herbig Ae/Be star HD 163296, the former being measured from proper motions and radial velocities of the jet knots, whereas the latter was measured from near-infrared photometric and Brγ variability. Similarly, Connelley and Greene (2014) monitored a sample of 19 embedded (class I) YSOs with near-IR spectroscopy and found that, on average, accretion tracers such as Brγ are not correlated in time to wind tracers such as the H_2 and [Fe II] lines. The infrared source LRLL 54361 shows a periodic variation in its infrared luminosity, increasing by a factor of 10 over roughly 1 week every 25.34 days. However, the sensitive JVLA observations of Forbrich et al. (2015) show no correlation with the infrared variations.

3.4 Outflow rotation

At the scale of the molecular outflows, several cases have been found that show a suggestion of rotation, with a small velocity gradient perpendicular to the major axis of the outflow (e.g., Chrysostomou et al. 2008; Launhardt et al. 2009; Lee et al. 2009; Zapata et al. 2010; Choi et al. 2011; Pech et al. 2012; Hara et al. 2013; Chen et al. 2016; Bjerkeli et al. 2016). Evidence of outflow rotation has also been found in optical/IR microjets from T Tauri stars (e.g., Bacciotti et al. 2002; Anderson et al. 2003; Pesenti et al. 2004; Coffey et al. 2004, 2007). The observed velocity difference across the minor axis of the molecular outflow is typically a few km s^{-1}, while in the case of optical/IR microjets (that trace the inner, more collimated component) it can reach a few tens of km s^{-1}. These signatures of jet rotation about its symmetry axis are very important because they represent the best way to test the hypothesis that jets extract angular momentum from the star-disk systems. However, there is considerable debate on the actual nature and origin of these gradients (Frank et al. 2014; De Colle et al. 2016). The presence of precession, asymmetric shocks or multiple sources could also produce apparent jet rotation. Also, it is possible that most of the angular momentum could be stored in magnetic form, rather than in rotation of matter (Coffey et al. 2015). To ensure that the true jet rotation is being probed it should be checked that rotation signatures are consistent at different positions along the jet, and that the jet gradient goes in the same direction as that of the disk. This kind of tests have been carried out only in very few objects (see Coffey et al. 2015) with disparate results. In the case of the rotating outflow associated with HH 797 (Pech et al. 2012) a double radio source with angular separation of $\sim 3''$ is found at its core (Forbrich et al. 2015), suggesting an explanation in terms of a binary jet system.

It is important that the jet is observed as close as possible to the star, where any evidence of angular momentum transfer is still preserved, since far from the star the interaction with the environment can hide and confuse rotation signatures. Therefore, high angular resolution observations of radio recombination lines from radio jets, reaching the region closer to the star, could help to solve these problems. In principle, it could be possible to observe the jet near its launch region and compare the velocity gradients with those observed al larger scales. However, these observations are very difficult and can be feasible only with new instruments such as the Atacama Large Millimeter/submillimeter Array (ALMA) and in the future the Next Generation Very Large Array (ngVLA) and the Square Kilometre Array (SKA).

4 Free–free continuum emission from radio jets

4.1 Frequency dependences

Reynolds (1986) modeled the free–free emission from an ionized jet. He assumed that the ionized flow begins at an injection radius r_0 with a circular cross section with initial half-width w_0. He adopted power-law dependences with radius r, so that the half-width of the jet is given by

$$w = w_0 \left(\frac{r}{r_0} \right)^{\epsilon}. \tag{1}$$

The case of $\epsilon = 1$ corresponds to a conical (constant opening angle) jet. The electron temperature, velocity, density, and ionized fraction were taken to vary as r/r_0 to the powers q_T, q_v, q_n, and q_x, respectively. In general. the jets are optically thick close to the origin and optically thin at large r. The jet axis is assumed to have an inclination angle i with respect to the line of sight. In consequence, the optical depth along a line of sight through the jet follows a power law with index:

$$q_\tau = \epsilon + 2q_x + 2q_n - 1.35q_T. \tag{2}$$

Assuming flux continuity

$$q_\tau = -3\epsilon + 2q_x - 2q_v - 1.35q_T. \tag{3}$$

Assuming the case of an isothermal jet with constant velocity and ionization fraction ($q_T = q_v = q_x = 0$), the flux density increases with frequency as

$$S_\nu \propto \nu^\alpha, \tag{4}$$

where the spectral index α is given by

$$\alpha = 1.3 - \frac{0.7}{\epsilon}. \tag{5}$$

The angular size of the major axis of the jet decreases with frequency as

$$\theta_\nu \propto \nu^{-0.7/\epsilon} = \nu^{\alpha-1.3}. \tag{6}$$

The previous discussion is valid for frequencies below the turnover frequency ν_m, which is related to the injection radius r_0. At high enough frequencies, $\nu > \nu_m$, the whole jet becomes optically thin and the spectral index becomes -0.1.

4.2 Physical parameters from radio continuum emission

Following Reynolds (1986) the injection radius and ionized mass loss rate are given by:

$$\left(\frac{r_0}{\text{au}}\right) = 26 \left[\frac{(2-\alpha)(0.1+\alpha)}{1.3-\alpha}\right]^{0.5} \left[\left(\frac{S_\nu}{\text{mJy}}\right)\left(\frac{\nu}{10\ \text{GHz}}\right)^{-\alpha}\right]^{0.5} \left(\frac{\nu_m}{10\ \text{GHz}}\right)^{0.5\alpha-1} \times \left(\frac{\theta_0 \sin i}{\text{rad}}\right)^{-0.5} \left(\frac{d}{\text{kpc}}\right)\left(\frac{T}{10^4\ \text{K}}\right)^{-0.5}, \tag{7}$$

$$\left(\frac{\dot{M}_{\text{ion}}}{10^{-6}\ M_\odot\ \text{year}^{-1}}\right) = 0.108 \left[\frac{(2-\alpha)(0.1+\alpha)}{1.3-\alpha}\right]^{0.75} \left[\left(\frac{S_\nu}{\text{mJy}}\right)\left(\frac{\nu}{10\ \text{GHz}}\right)^{-\alpha}\right]^{0.75} \times \left(\frac{v_j}{200\ \text{km s}^{-1}}\right)\left(\frac{\nu_m}{10\ \text{GHz}}\right)^{0.75\alpha-0.45} \left(\frac{\theta_0}{\text{rad}}\right)^{0.75} (\sin i)^{-0.25} \times \left(\frac{d}{\text{kpc}}\right)^{1.5} \left(\frac{T}{10^4\ \text{K}}\right)^{-0.075}, \tag{8}$$

where $\theta_0 = 2w_0/r_0$ is the injection opening angle of the jet, that usually is roughly estimated using

$$\theta_0 = 2\ \arctan(\theta_{\text{min}}/\theta_{\text{maj}}), \tag{9}$$

where θ_{min} and θ_{maj} are the deconvolved minor and major axes of the jet. We note that the dimensions of the jet are very compact, comparable or smaller than the beam and as a consequence the value of θ_0 is uncertain. The opening angle determined on larger scales (for example using Herbig–Haro knots along the flow away from the jet core) is usually smaller and at present it is not known if this is the result of recollimation or of an overestimate in the measurement of θ_0.

In the case of a conical ($\alpha = 0.6$) jet, Eqs. (7) and (8) simplify to:

$$\left(\frac{r_0}{\text{au}}\right) = 31 \left[\left(\frac{S_\nu}{\text{mJy}}\right)\left(\frac{\nu}{10\ \text{GHz}}\right)^{-0.6}\right]^{0.5} \left(\frac{\nu_m}{10\ \text{GHz}}\right)^{-0.7} \times \left(\frac{\theta_0 \sin i}{\text{rad}}\right)^{-0.5} \left(\frac{d}{\text{kpc}}\right)\left(\frac{T}{10^4\ \text{K}}\right)^{-0.5}, \tag{10}$$

$$\left(\frac{\dot{M}_{\rm ion}}{10^{-6}\ M_\odot\ {\rm year}^{-1}}\right) = 0.139\left[\left(\frac{S_\nu}{\rm mJy}\right)\left(\frac{\nu}{10\ {\rm GHz}}\right)^{-0.6}\right]^{0.75} \times \left(\frac{v_j}{200\ {\rm km\ s}^{-1}}\right)\left(\frac{\theta_0}{\rm rad}\right)^{0.75}(\sin i)^{-0.25} \times \left(\frac{d}{\rm kpc}\right)^{1.5}\left(\frac{T}{10^4\ {\rm K}}\right)^{-0.075}, \quad (11)$$

Usually a value of $T = 10^4$ K is adopted. In a few cases there is information on the jet velocity, but in general one has to assume a velocity typically in the range from 100 km s^{-1} to 1000 km s^{-1}, depending on the mass of the young star. Following Panoglou et al. (2012) and assuming a launch radius of about 0.5 au (Estalella et al. 2012), the jet velocity can be crudely estimated from

$$\left(\frac{v_j}{\rm km\ s^{-1}}\right) \simeq 140\left(\frac{M_*}{0.5\ M_\odot}\right)^{1/2}. \quad (12)$$

Until recently, the turnover frequency has not been determined directly from observations and is estimated that it will appear above 40 GHz. Only in the case of HL Tau, the detailed multifrequency observations and modeling suggest a value of $\sim$ 1.5 au (A.M. Lumbreras et al., in preparation). Determining ν_m is difficult because at high frequencies dust emission from the associated disk starts to become dominant. Future observations at high frequencies made with high angular resolution should allow to separate the compact free–free emission from the base of the jet to that of the more extended dust emission in the disk and give more determinations of ν_m and of the morphology and size of the gap between the star and the injection radius of the jet. Anyhow, the dependence of r_0 on ν_m is not critical, that is, in order to change r_0 one order of magnitude, the turnover frequency should typically change a factor of $\sim$ 30. Assuming a lower limit of $\sim$ 10 GHz for the turnover frequency, upper limits of $\sim$ 10 au have been obtained for r_0 (Anglada et al. 1998; Beltrán et al. 2001).

In the case of $\dot{M}_{\rm ion}$ the dependence on ν_m is almost negligible and disappears for the case of a conical jet ($\alpha = 0.6$). Using this technique, ionized mass loss rates in the range of $10^{-10}\ M_\odot$ year^{-1} (low-mass objects) to $10^{-5}\ M_\odot$ year^{-1} (high-mass objects) have been determined (Rodriguez et al. 1994b; Beltrán et al. 2001; Guzmán et al. 2016, 2012; see Table 1).

5 Radio recombination lines from radio jets

5.1 LTE formulation

Following Reynolds (1986), the flux density at frequency ν, S_ν, from a jet is given by

$$S_\nu = \int_0^\infty B_\nu(T)(1 - \exp[-\tau_\nu])\,{\rm d}\Omega, \quad (13)$$

where $B_\nu(T)$ is the source function (taken to be Planck's function since we are assuming LTE), τ_ν is the optical depth along a line of sight through the jet, and $\mathrm{d}\Omega$ is the differential of solid angle.

Since

$$\mathrm{d}\Omega = \frac{2w(r)}{d^2}\,\mathrm{d}y, \tag{14}$$

where d is the distance to the source and $y = r\sin i$ is the projected distance in the plane of the sky. Assuming an isothermal jet, the continuum emission is given by

$$S_\mathrm{C} = B_\nu(T)\int_0^\infty \frac{2w(r)}{d^2}(1-\exp[-\tau_\mathrm{C}])\,\mathrm{d}y, \tag{15}$$

while the line plus continuum emission will be given by

$$S_\mathrm{L+C} = B_\nu(T)\int_0^\infty \frac{2w(r)}{d^2}(1-\exp[-\tau_\mathrm{L+C}])\,\mathrm{d}y. \tag{16}$$

The line-to-continuum ratio will be given by

$$\frac{S_\mathrm{L}}{S_\mathrm{C}} = \frac{S_\mathrm{L+C}}{S_\mathrm{C}} - 1. \tag{17}$$

Using the power law dependences of the variables and noting that the line and the continuum opacities have the same radial dependence, we obtain

$$\frac{S_\mathrm{L}}{S_\mathrm{C}} = \frac{\int_0^\infty y^\epsilon(1-\exp[-\tau_\mathrm{L+C}(r_0)y^{\epsilon+2q_x+2q_n}/\sin i])\,\mathrm{d}y}{\int_0^\infty y^\epsilon(1-\exp[-\tau_\mathrm{C}(r_0)y^{\epsilon+2q_x+2q_n}/\sin i])\,\mathrm{d}y} - 1. \tag{18}$$

Using the definite integral (Gradshteyn and Ryzhik 1994)

$$\int_0^\infty [1-\exp(-\mu x^p)]\,x^{t-1}\,\mathrm{d}x = -\frac{1}{|p|}\,\mu^{-\frac{t}{p}}\,\Gamma\left(\frac{t}{p}\right), \tag{19}$$

valid for $0 < t < -p$ for $p < 0$ and with Γ being the Gamma function.

We then obtain

$$\frac{S_\mathrm{L}}{S_\mathrm{C}} = \left[\frac{\tau_\mathrm{L+C}(r_0)}{\tau_\mathrm{C}(r_0)}\right]^{-(\epsilon+1)/(\epsilon+2q_x+2q_n)} - 1. \tag{20}$$

Finally,

$$\frac{S_\mathrm{L}}{S_\mathrm{C}} = \left[\frac{\kappa_\mathrm{L}}{\kappa_\mathrm{C}} + 1\right]^{-(\epsilon+1)/(\epsilon+2q_x+2q_n)} - 1, \tag{21}$$

where κ_L and κ_C are the line and continuum absorption coefficients at the frequency of observation, respectively. Substituting the LTE ratio of these coefficients (Mezger and Hoglund 1967; Gordon 1969; Quireza et al. 2006), we obtain:

$$\frac{S_L}{S_C} = \left[0.28 \left(\frac{\nu_L}{\mathrm{GHz}} \right)^{1.1} \left(\frac{T}{10^4\ \mathrm{K}} \right)^{-1.1} \left(\frac{\Delta v}{\mathrm{km\ s^{-1}}} \right)^{-1} (1+Y^+)^{-1} + 1 \right]^{-(\epsilon+1)/(\epsilon+2q_x+2q_n)} - 1, \tag{22}$$

where ν_L is the frequency of the line, Δv the full width at half maximum of the line, and Y^+ is the ionized helium to ionized hydrogen ratio.

For a standard biconical jet with constant velocity and ionized fraction, the equation becomes

$$\frac{S_L}{S_C} = \left[0.28 \left(\frac{\nu_L}{\mathrm{GHz}} \right)^{1.1} \left(\frac{T}{10^4\ \mathrm{K}} \right)^{-1.1} \left(\frac{\Delta v}{\mathrm{km\ s^{-1}}} \right)^{-1} (1+Y^+)^{-1} + 1 \right]^{2/3} - 1. \tag{23}$$

In the centimeter regime, the first term inside the brackets is smaller than 1 and using a Taylor expansion the equation can be approximated by

$$\frac{S_L}{S_C} = 0.19 \left(\frac{\nu_L}{\mathrm{GHz}} \right)^{1.1} \left(\frac{T}{10^4\ \mathrm{K}} \right)^{-1.1} \left(\frac{\Delta v}{\mathrm{km\ s^{-1}}} \right)^{-1} (1+Y^+)^{-1}. \tag{24}$$

Are these relatively weak RRLs detectable with the next generation of radio interferometers? Let us assume that we attempt to observe the H86α line at 10.2 GHz and adopt an electron temperature of 10^4 K and an ionized helium to ionized hydrogen ratio of 0.1. The line width expected for these lines is poorly known. If the jet is highly collimated, the line width could be a few tens of km s^{-1}, similar to those observed in HII regions and dominated by the microscopic velocity dispersion of the gas. Under these circumstances, we expect to see two relatively narrow lines separated by the projected difference in radial velocity of the two sides of the jet. However, if the jet is highly turbulent and/or has a large opening angle we expect a single line with a width of a few hundreds of km s^{-1}. Since for a constant area under the line it is easier to detect narrow lines (the signal-to-noise ratio improves as $\Delta v^{-1/2}$), we will conservatively (perhaps pessimistically) assume a line width of 200 km s^{-1}.

Using Eq. (24) we obtain that the line-to-continuum ratio will be $S_L/S_C = 0.011$. The brightest thermal jets (see Table 1) have continuum flux densities of about 5 mJy, so we expect a peak line flux density of 55 μJy. These are indeed weak lines. However, the modern wide-band receivers allow the simultaneous detection of many recombination lines. For example, in the X band (8–12 GHz) there are 11 α lines (from the H92α at 8.3 GHz to the H82α at 11.7 GHz). Stacking N different lines will improve the signal-to-noise ratio by $N^{1/2}$, so we expect a gain of a factor of 3.3 from this averaging.

At present, the Jansky VLA will give, for a frequency of 10.2 GHz, a channel width of 100 km s^{-1} and, with an on-source integration time of $\sim$ 45 h, an rms noise of $\sim$ 11 μJy beam^{-1}, sufficient to detect the H86α emission at the 5σ level from a handful of bright jets. Line stacking will improve this signal-to-noise ratio by 3.3. In

contrast, the ngVLA is expected to be 10 times as sensitive as the Jansky VLA, which means that a similar sensitivity will be achieved with 1/100 of the time, that is about 0.5 h. For an on-source integration time of about 14 hours the ngVLA will have an rms noise of ~ 2 μJy beam^{-1} in the line mode previously described and will be able to detect the RRLs from the more typical 1 mJy continuum jet at the 5σ level. Line stacking will increase this detection to a very robust $\sim 16\sigma$. This will allow to start resolving the jets into at least a few pixels and start studying the detailed kinematics of the jet. Then, a program of a few hundred hours with the ngVLA will characterize the RRL emission from a wide sample of thermal jets. Similar on-source integration times would be required with the expected sensitivity of the SKA (see Anglada et al. 2015).

5.2 Stark broadening

The collisions between the electrons and the atoms produce a line broadening, known as Stark or pressure broadening, that depends strongly on the electron density of the medium and in particular on the level of the transition. For an RRL with principal quantum number n, quantum number decrement Δn in a medium with electron density $N_{\rm e}$ and electron temperature $T_{\rm e}$, the Stark broadening is given by (Walmsley 1990):

$$\left(\frac{\delta_S}{\rm km\ s^{-1}}\right) = 2.72 \left(\frac{n}{42}\right)^{7.5} \Delta n^{-1} \left(\frac{N_{\rm e}}{10^7\ {\rm cm^{-3}}}\right) \left(\frac{T_{\rm e}}{10^4\ {\rm K}}\right)^{-0.1}. \quad (25)$$

Stark broadening has been detected in the case of HII regions (e.g., Smirnov et al. 1984; Alexander and Gulyaev 2016) and slow ionized winds (e.g., Guzmán et al. 2014). Would it be an important effect in the case of RRLs from ionized jets? In contrast with HII regions, where a uniform electron density can approximately describe the object, thermal jets are characterized by steep gradients in the electron density, that is expected to decrease typically as the distance to the star squared (see discussion above). On the other hand, the inner parts of a thermal jet are optically thick in the continuum and do not contribute to the recombination line emission. All the line emission comes from radii external to the line of sight where the free–free continuum opacity, $\tau_{\rm C}$, is ~ 1.

The length of the jets along its major axis is of the order of twice the radius at which $\tau_{\rm C} \simeq 1$. From Table 1 we estimate that at cm wavelengths the distance from the star where $\tau_{\rm C} \simeq 1$ is in the range of 100 to 500 au. Assuming a typical opening angle of 30° we find that the physical depth of the jet, $2w$, at this position ranges from 50 to 250 au. The free–free opacity is given approximately by (Mezger et al. 1967):

$$\tau_{\rm C} \simeq 1.59 \times 10^{-10} \left(\frac{T_{\rm e}}{10^4\ {\rm K}}\right)^{-1.35} \left(\frac{\nu}{\rm GHz}\right)^{-2.1} \left(\frac{N_{\rm e}}{\rm cm^{-3}}\right)^{2} \left(\frac{2w}{100\ {\rm au}}\right). \quad (26)$$

Adopting $T_{\rm e} = 10^4$ K, $\nu = 10.2$ GHz (the H86α line) and $\tau_{\rm C} = 1$, we find that the electron density at this position will be in the range of 5.7×10^5 cm^{-3} to 1.3×10^6 cm^{-3}. The recombination line emission will be coming from regions with electron densities equal or smaller than these values. Finally, using the equation for

the Stark broadening given above, we find that the broadening will be in the range of 33–167 km s^{-1}. We then conclude that Stark broadening will be important in the case that the line widths are of the order of the microscopic velocity dispersion (tens of km s^{-1}), but it will not be dominant in the case that the line widths have a value similar to that of the jet speed.

5.3 Non-LTE radio recombination lines

The treatment presented here assumes that the recombination line emission is in LTE, which seems to be a reasonable approach. There are, however, cases where the LTE treatment is clearly insufficient and a detailed modeling of the line transfer is required. The more clear case is that of MWC 349A, a photoevaporating disk located some 1.2 kpc away (Gordon 1994). Even when this source is not a jet properly but a photoevaporated wind, we discuss it briefly since it is the best case known of non-LTE radio recombination lines.

At centimeter wavelengths, the line emission from MWC 349A is consistent with LTE conditions (Rodriguez and Bastian 1994). However, at the millimeter wavelengths, below 3 mm, this source presents strong, double-peaked hydrogen recombination lines (Martin-Pintado et al. 1989). These spectra arise from a dense Keplerian-rotating disk, that is observed nearly edge-on (Weintroub et al. 2008; Báez-Rubio et al. 2014). The flux density of these features is an order or magnitude larger than expected from the LTE assumption and the inference that maser emission is at work seems well justified. However, the nature of MWC 349A remains controversial, with some groups considering it a young object, while others attribute to it an evolved nature (Strelnitski et al. 2013).

Extremely broad millimeter recombination lines of a possible maser nature have been reported from the high-velocity ionized jet Cep A HW2 (Jiménez-Serra et al. 2011). In this case, the difference between the LTE and non-LTE models is less than a factor of two and in some of the transitions it is necessary to multiply the non-LTE model intensities by a factor of several to agree with the observations. The source Mon R2-IRS2 could be a case of weakly amplified radio recombination lines in a young massive star. Jiménez-Serra et al. (2013) report toward this source a double-peaked spectrum. with the peaks separated by about 40 km s^{-1}. However, the line intensity is only $\sim$ 50% larger than expected from LTE. Jiménez-Serra et al. (2013) propose that the radio recombination lines arise from a dense and collimated jet embedded in a cylindrical ionized wind, oriented nearly along the line of sight. In the case of LkHα101, Thum et al. (2013) find the millimeter RRLs to be close to LTE and to show non-Gaussian wings that can be used to infer the velocity of the wind, in this case 55 km s^{-1}. Finally, Guzmán et al. (2014) detect millimeter recombination lines from the high-mass young stellar object G345.4938+01.4677. The hydrogen recombination lines exhibit Voigt profiles, which is a strong signature of Stark broadening. The continuum and line emissions can be successfully reproduced with a simple model of a slow ionized wind in LTE.

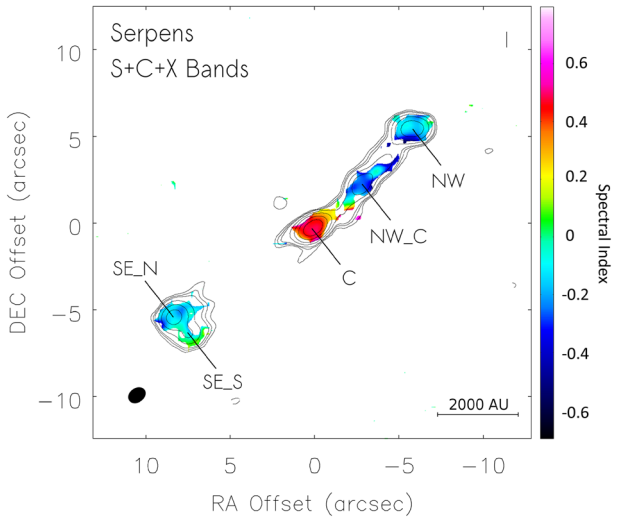

Fig. 3 Image of the non-thermal radio jet in Serpens. The radio continuum image is shown in contours and was made by combining the data from the S, C, and X bands. This image is superposed on the spectral index image (color contours). Image reproduced with permission from Rodríguez-Kamenetzky et al. (2016), copyright by AAS

6 Non-thermal emission from radio jets

As commented above, jets from YSOs have been long studied at radio wavelengths through their thermal free–free emission which traces the base of the ionized jet, and shows a characteristic positive spectral index (the intensity of the emission increases with the frequency, e.g., Rodriguez 1995, 1996; Anglada 1996). However, in the early 1990s, sensitive observations started to reveal that non-thermal emission at centimeter wavelengths might be also present in several YSO jets (e.g., Rodriguez et al. 1989a; Rodríguez et al. 2005; Marti et al. 1993; Garay et al. 1996; Wilner et al. 1999). This non-thermal emission is usually found in relatively strong radio knots, away from the core, showing negative spectral indices at centimeter wavelengths (see Fig. 3). Oftentimes, these non-thermal radio knots appear in pairs, moving away from the central protostar at velocities of several hundred kilometers per second (e.g., the triple source in Serpens; Curiel et al. 1993). Because of these characteristics, it was proposed that these knots could be tracing strong shocks of the jet against dense material in the surrounding molecular cloud where the protostar is forming. Their non-thermal nature was interpreted as synchrotron emission from a small population of relativistic particles that would be accelerated in the ensuing strong shocks. This scenario is supported by several theoretical studies, showing the feasibility of strong shocks in protostellar jets as efficient particle accelerators (e.g., Araudo et al. 2007; Bosch-Ramon et al. 2010; Padovani et al. 2015, 2016; Cécere et al. 2016).

The possibility of protostellar jets as efficient particle accelerators has been confirmed only recently, with the detection and mapping of linearly polarized emission from the YSO jet in HH 80–81 (Carrasco-González et al. 2010b; see Fig. 4). This

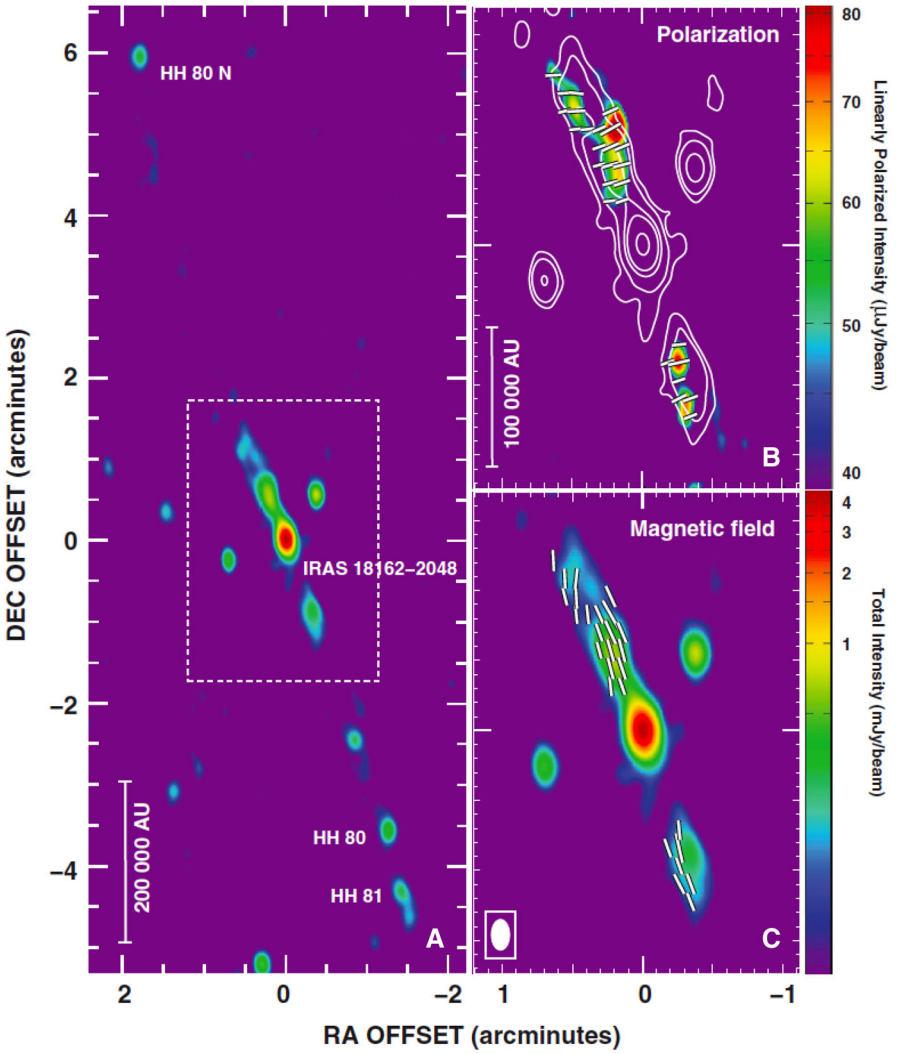

Fig. 4 Images of the non-thermal HH 80–81 radio jet. The left panel (**a**) shows in color scale the total intensity at 6 cm extending from the central source to the HH objects. The upper right panel (**b**) shows a close-up of the central region with the total intensity in contours and the linearly polarized emission in colors. The white bars indicate the direction of the polarization. The bottom right panel (**c**) shows the direction of the magnetic field. Image reproduced with permission from Carrasco-González et al. (2010b), copyright by AAAS

result provided for the first time conclusive evidence for the presence of synchrotron emission in a jet from a YSO, and then, the presence of relativistic particles.

At centimeter wavelengths, where most of the radio jet studies have been carried out, the emission of the non-thermal lobes is usually weaker than that of the thermal core of the jet. Consequently, most of the early detections of non-thermal radio knots were obtained through very sensitive observations resulting from unusually long projects,

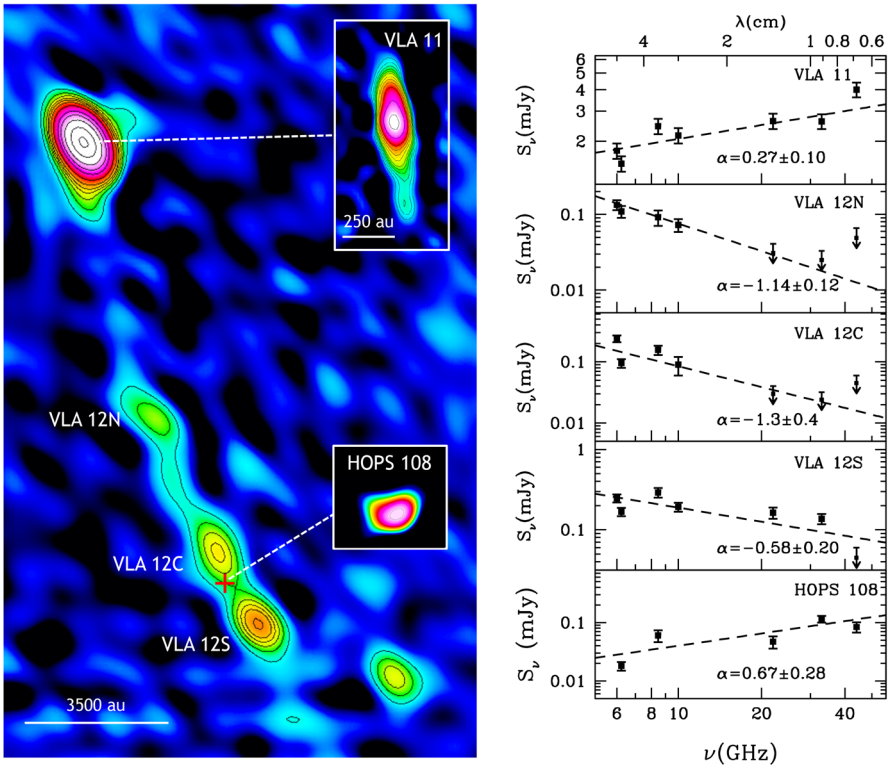

Fig. 5 The non-thermal radio jet from the intermediate-mass YSO FIR3 (VLA 11) in OMC-2. The left panel shows the 3 cm continuum emission (angular resolution $\sim 2''$) of the thermal core (VLA 11) and the non-thermal lobe (VLA 12N, 12C, 12S) of the FIR3 radio jet. Insets show the 5 cm emission at higher angular resolution ($\sim 0.3''$) of the thermal core of the FIR3 radio jet and of the Class 0 protostar HOPS 108. The right panels show the spectra of the radio sources. Image adapted from Osorio et al. (2017)

mainly carried out at the VLA. After the confirmation in 2010 of synchrotron emission in the HH 80–81 radio jet, the improvement in sensitivity of radio interferometers has facilitated higher sensitivity observations at multiple wavelengths of star forming regions, and new non-thermal protostellar jet candidates are emerging (e.g., Purser et al. 2016; Osorio et al. 2017; Hunter et al. 2018; Tychoniec et al. 2018; see Fig. 5). It is then expected that the next generation of ultra-sensitive radio interferometers (LOFAR, SKA, ngVLA) will produce very detailed studies on the nature of non-thermal emission in protostellar jets.

It is worth noting that, even when non-thermal emission is brighter at lower frequencies, most of the proposed detections have been performed at relatively high frequencies, typically in the 4–10 GHz range. One reason is that studies of radio jets have been focused preferentially on the detection of thermal emission, which is dominant at higher frequencies. Another reason is the lack of sensitivity at low frequencies, specially below 1 GHz, in most of the available interferometers. However, despite the small number of sensitive observations performed at low frequencies, they have pro-

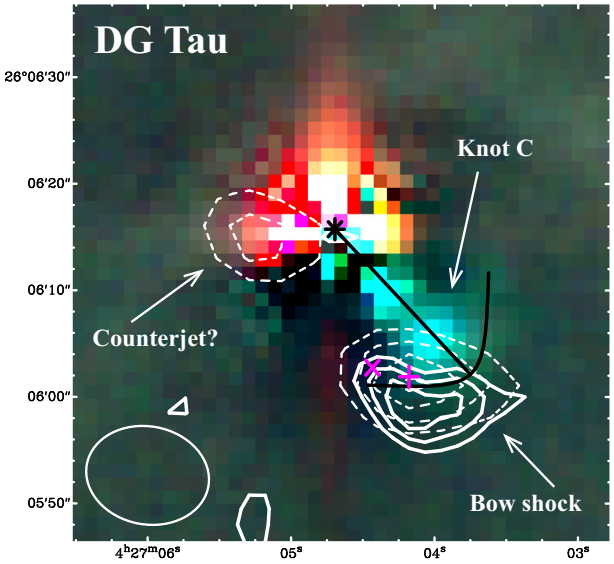

Fig. 6 GMRT image at 325 MHz (dashed contours) and 610 MHz (solid contours) overlaid on a composite RGB image (I, Hα and [SII]) of the DG Tau jet. The VLA positions of the bow shock at 5.4 and 8.5 GHz are shown as a plus (+) and a cross (×), respectively. The optical stellar position is shown as an asterisk (∗) and the optical jet axis and bow shock are shown as solid black lines. Image reproduced with permission from Ainsworth et al. (2014), copyright by AAS

duced very interesting results. For example, the only non-thermal radio jet candidate associated with a low-mass protostar known so far has been identified through Giant Metrewave Radio Telescope (GMRT) observations of DG Tau in the 300–700 MHz range (Ainsworth et al. 2014; see Fig. 6). Very recent GMRT observations of HH 80–81 (Vig et al. 2018) at 325 and 610 MHz found negative spectral indices steeper than previous studies at higher frequencies. This has been interpreted as indicating that an important free–free contribution is present at high frequencies even in the non-thermal radio knots. We should then expect more interesting results from low-frequency observations using the next generation of low-frequency interferometers, such as the Low Wavelength Array (LWA), and the aforementioned LOFAR and SKA.

At present, the best studied cases of particle acceleration in protostellar jets are the triple source in Serpens and HH 80–81 (Rodríguez-Kamenetzky et al. 2016, 2017). These sources were observed very recently with the VLA combining high angular resolution and very high sensitivity in the 1–10 GHz frequency range. These observations resolve both jets at all observed frequencies, allowing to study the different emission mechanisms present in the jet in a spatially resolved way. In both cases, strong non-thermal emission is detected at the termination points of the jets, which is consistent with particle acceleration in strong shocks against a very dense ambient medium. Additionally, in the case of HH 80–81, non-thermal emission is observed at several positions along the very well collimated radio jet, suggesting that this object is able to accelerate particles also in internal shocks (Rodríguez-Kamenetzky et al. 2017). Overall, these studies have found that the necessary conditions to accelerate

particles in a protostellar jet are high velocities ($\gtrsim 500\,\mathrm{km\,s^{-1}}$) and an ambient medium denser than the jet. These conditions are probably well satisfied in the case of very young protostellar jets, which are still deeply embedded in their parental cloud.

The discovery of linearly polarized emission in the HH 80–81 radio jet by Carrasco-González et al. (2010b) opened the interesting possibility of studying magnetic fields in protostellar jets. Detection of linearly polarized emission at several wavelengths would allow one to infer the properties of the magnetic field in these jets in a way similar to that commonly employed in AGN jets. The magnetic field strength can be estimated from the spectral energy distribution at cm wavelengths (e.g., Pacholczyk 1970; Beck and Krause 2005), while the magnetic field morphology can be obtained from the properties of the linear polarization (polarization angle, polarization degree and Faraday rotation). For non-relativistic jets, the apparent magnetic field (magnetic field averaged along the line-of-sight) is perpendicular to the direction of the linear polarization. Moreover, theoretical models of helical magnetic fields predict gradients of the polarization degree and Faraday rotation measurements along and across the jet (Lyutikov et al. 2005). Thus, by comparing the observational results with theoretical models, the 3D morphology of the magnetic field can be inferred.

Mapping the polarization in a set of YSO jets in combination with detailed theoretical modeling may lead to a deeper understanding of the overall jet phenomenon. However, radio synchrotron emission in YSO jets seems to be intrinsically much weaker and difficult to study than in relativistic jets (e.g., AGN and microquasar jets). So far, only in the case of HH 80–81, one of the brightest and most powerful YSO jets known, it has been possible to obtain enough sensitivity to detect and study its linear polarization, which is only a fraction of the total continuum emission. Subsequent higher sensitivity studies (Rodríguez-Kamenetzky et al. 2016, 2017) have not been able to detect polarization in YSO jets. One of the reasons of this is that, due to the presence of thermal electrons mixed with the relativistic particles, we expect strong Faraday rotation. At the moment, high sensitivities in radio interferometers are obtained by averaging data in large bandwidths. Within these bandwidths, we expect large rotations of the polarization angle, resulting in strong depolarization when the emission is averaged. Then, it is still necessary to observe using long integration times in order to obtain enough sensitivity to detect polarization in smaller frequency ranges. Note that using the Faraday RM-Synthesis tool (Brentjens and Bruyn 2005) to determine the rotation measure to account for this effect is also hampered by the poor signal-to-noise ratio over narrow frequency ranges in these weak sources. At the moment, probably HH 80–81 is the only object bright enough to perform a study of polarization at several wavelengths; and even in this object, polarization would be detected only after observations of several tens of hours long. Therefore, we will probably have to wait for new ultra-sensitive interferometers in order to perform a polarization study in a large sample of protostellar jets.

7 Masers as tracers of jets

Molecular maser emission at cm wavelengths (e.g., H_2O, CH_3OH, OH) is often found in the early evolutionary stages of massive protostars. Such maser emission is usu-

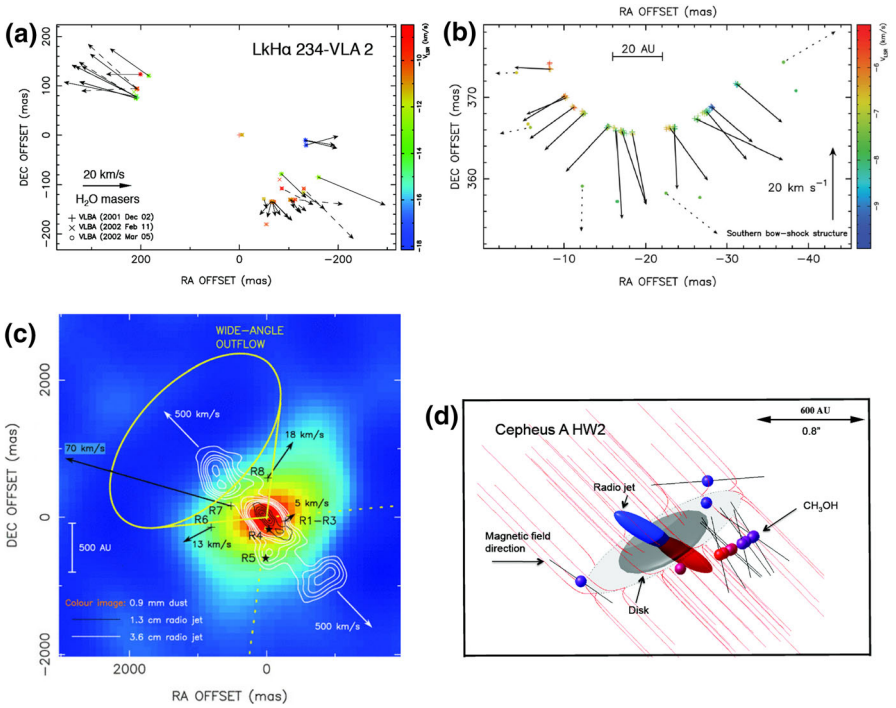

Fig. 7 **a** Distribution and proper motions of H_2O masers showing a very compact ($\sim$ 180 au), short-lived ($\sim$ 40 year), bipolar jet from a very embedded protostar of unknown nature in the LkHα 234 star-forming region (Torrelles et al. 2014). **b** Micro-bow shock traced by water masers in AFGL2591 VLA 3-N. Arrows indicate the measured proper motions (Trinidad et al. 2013). **c** Maser microstructures tracing a low-collimation outflow around the radio jet associated with the massive protostar Cep A HW2 (Torrelles et al. 2011). **d** Magnetic field structure around the protostar–disk–jet system of Cep A HW2. Spheres indicate the CH_3OH masers and black vectors the magnetic field direction. Image adapted from Vlemmings et al. (2010)

ally very compact and strong, with brightness temperatures exceeding in some cases 10^{10} K, allowing the observation of outflows at milliarcsecond (mas) scales (1 mas = 1 au at a distance of 1 kpc) using Very Long Baseline Interferometry (VLBI). Sensitive VLBI observations show, in some sources, thousands of maser spots forming microstructures that reveal the 3D kinematics of outflows and disks at small scale (e.g., Sanna et al. 2015). This kind of observations have given a number of interesting results: the discovery of short-lived, episodic non-collimated outflow events (e.g., Torrelles et al. 2001, 2003; Surcis et al. 2014); detection of infall motions in accretion disks around massive protostars (Sanna et al. 2017); the imaging of young ($<$ 100 year) small-scale (a few 100 au) bipolar jets of masers (Sanna et al. 2012, Torrelles et al. 2014; Fig. 7a), and even allowed to analyze the small-scale (1–20 au) structure of the micro bow-shocks (Uscanga et al. 2005; Trinidad et al. 2013; Fig. 7b); the simultaneous presence of a wide-angle outflow and a collimated jet in a massive protostar (Torrelles et al. 2011; see Fig. 7c); and polarization studies have determined the distribution and strength of the magnetic field very close to protostars allowing to better

understand its role in the star formation processes (Surcis et al. 2009; Vlemmings et al. 2010; Sanna et al. 2015; Fig. 7d).

In particular, the combination of continuum and maser studies in Cep A HW2 has been useful to provide one of the best examples of the two-wind model for outflows from massive protostars (Torrelles et al. 2011; Fig. 7c). In this source the water masers trace the presence of a relatively slow ($\sim$ 10–70 km s^{-1}) wide-angle outflow (opening angle of $\sim$ 102°), while the thermal jet traces a fast ($\sim$ 500 km s^{-1}) highly collimated radio jet (opening angle of $\sim$ 18°). This two-wind phenomenon had been previously imaged only in low mass protostars such as L1551-IRS5 (Itoh et al. 2000, Pyo et al. 2005), HH 46/47 (Velusamy et al. 2007), HH 211 (Gueth and Guilloteau 1999, Hirano et al. 2006) and IRAS 04166+2706 (Santiago-García et al. 2009). An extensive study of the connection between high-velocity collimated jets and slow un-collimated winds in a large sample of low-mass class II objects has been carried out recently by Nisini et al. (2018); this work has been performed from the analysis of [OI]6300 Å line profiles under the working hypothesis that the low velocity component traces a wide wind and the high-velocity component a collimated jet.

8 Nature of the centimeter continuum emission in thermal radio jets

8.1 Observational properties: radio to bolometric luminosity correlation

Photoionization does not appear to be the ionizing mechanism of radio jets since, in the sources associated with low-luminosity objects, the rate of ionizing UV photons ($\lambda < 912$ Å) from the star is clearly insufficient to produce the ionization required to account for the observed radio continuum emission (e.g., Rodriguez et al. 1989b; Anglada 1995). For low-luminosity objects ($1 \lesssim L_{\rm bol} \lesssim 1000\ L_\odot$), the observed flux densities at cm wavelengths are several orders of magnitude higher than those expected by photoionization (see Fig. 8 and left panel in Fig. 5 of Anglada 1995). Ionization by shocks in a strong stellar wind or in the jet itself has been proposed as the most likely possibility (Torrelles et al. 1985; Curiel et al. 1987, 1989; Anglada et al. 1992; see below). Detailed simulations of the two-shock internal working surfaces traveling down the jet flow, and the expected emission of the ionized material at shorter wavelengths have been performed (e.g., the Hα and [OI]6300 Å line emission of a radiative jet model with a variable ejection velocity by Raga et al. 2007).

In Fig. 8 we plot the observed cm luminosity ($S_\nu d^2$) as a function of the bolometric luminosity for the sources listed in Table 2 (squares, dots, and triangles correspond, respectively, to very low, low, and high luminosity objects). For most of the sources in this plot, S_ν is the flux density at 3.6 cm, but some data at 6, 2, and 1.3 cm are included to construct a larger sample; these data points are used to estimate the 3.6 cm luminosity using the spectral index, when known, or assuming a value of $\sim$ 0.5. As can be seen in Fig. 8, the observed cm luminosity (data points) is uncorrelated with the cm luminosity expected from photoionization (dot-dashed line), further indicating that this is not the ionizing mechanism. However, as the figure shows, the observed cm luminosity is indeed correlated with the bolometric luminosity ($L_{\rm bol}$). A fit to the 48 data points with $1\ L_\odot \lesssim L_{\rm bol} \lesssim 1000\ L_\odot$ (dots) gives:

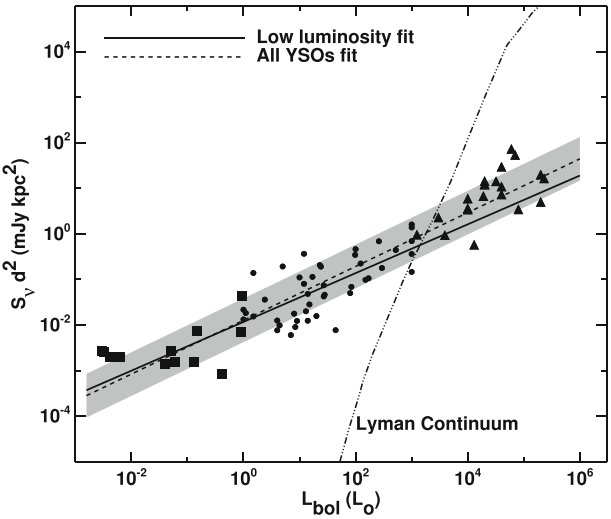

Fig. 8 Empirical correlation between the bolometric luminosity and the radio continuum luminosity at cm wavelengths. Data are taken from Table 2. Triangles correspond to high luminosity objects ($L_{\rm bol} > 1000\ L_\odot$), dots correspond to low-luminosity objects ($1 \leq L_{\rm bol} \leq 1000\ L_\odot$), and squares to very low-luminosity objects ($L_{\rm bol} < 1\ L_\odot$). The dashed line is a least-squares fit to all the data points and the grey area indicates the residual standard deviation of the fit. The solid line is a fit to the low-luminosity objects alone. The dot-dashed line corresponds to the expected radio luminosity of an optically thin region photoionized by the Lyman continuum of the star

$$\left(\frac{S_\nu d^2}{\rm mJy\ kpc^2}\right) = 10^{-1.93\pm0.14} \left(\frac{L_{\rm bol}}{L_\odot}\right)^{0.54\pm0.08} . \tag{27}$$

As can be seen in the figure, the correlation also holds for both the most luminous (triangles) and the very low luminosity (squares) objects, suggesting that the mechanism that relates the bolometric and cm luminosities is shared by all the YSOs. A fit to all the 81 data points ($10^{-2}\ L_\odot \lesssim L_{\rm bol} \lesssim 10^6\ L_\odot$) gives a better fit, with a similar result,

$$\left(\frac{S_\nu d^2}{\rm mJy\ kpc^2}\right) = 10^{-1.90\pm0.07} \left(\frac{L_{\rm bol}}{L_\odot}\right)^{0.59\pm0.03} . \tag{28}$$

A correlation between bolometric and cm luminosities was noted by Cabrit and Bertout (1992) from a set of ~ 25 outflow sources, quoting a slope of ~ 0.8 in a log-log plot. Skinner et al. (1993) suggested a correlation between the 3.6 cm luminosity and the bolometric luminosity with a slope of 0.9 by fitting a sample of Herbig Ae/Be stars and candidates with 11 detections and 7 upper limits. The fit to the 29 outflow sources presented in Anglada (1995) gives a slope of 0.6 (after updating some distances and flux densities; a slope of 0.7 was obtained with the values originally listed in Table 1 of that paper), similar to the value given in Eq. (28). Shirley et al. (2007) obtained separate fits for the 3.6 cm and for the 6 cm data, obtaining slopes of 0.7 and 0.9, respectively (although these fits are probably affected by a few outliers with anomalously high

Table 2 Sample of YSOs associated with outflows and radio continuum emission

Source	d (kpc)	$L_{\rm bol}$ ($L_\odot$)	S_ν (mJy)	$\dot{P}$ ($M_\odot$ year^{-1} km s^{-1})	Refs.
J041757	0.140	0.003	0.14	···	79, 83, 84
J041836	0.140	0.0033	0.13	···	84
J041847	0.140	0.0041	0.10	···	84
J041938	0.140	0.0062	0.10	···	84
IRAM04191	0.140	0.05	0.14	1.5×10^{-5}	70, 71, 72
L1014IRS	0.260	0.15	0.11	1.3×10^{-7}	70, 73, 74, 75
L1148-IRS	0.140	0.13	0.080	1.0×10^{-7}	70, 76, 77
L1521F-IRS	0.140	0.04	0.07	1.1×10^{-6}	77, 78, 79
IC348-SMM2E	0.240	0.06	0.027	1.1×10^{-7}	79, 80, 81, 82
HH30	0.140	0.42	0.042	7.5×10^{-7}	85, 86, 87
L1262	0.2	1.0	0.33	4.0×10^{-5}	47, 50, 51, 142, 46
VLA1623	0.16	1.5	0.6	4.5×10^{-4}	16, 35
L723	0.3	2.4	0.4	3.2×10^{-4}	10, 11, 33, 28, 132, 155
L1489	0.14	4.4	0.5	2.0×10^{-7}	3, 4, 24, 137
B335	0.25	4	0.2	2.0×10^{-5}	10, 12, 24, 22, 58, 140, 142
NGC2264G	0.8	5	0.3	3.0×10^{-3}	17, 18, 36
AS353A	0.3	8.4	0.1	4.5×10^{-4}	1, 23, 52, 12
L1448C	0.35	9	0.1	4.5×10^{-4}	14, 15, 34
L1448N(A)	0.35	10	0.9	1.2×10^{-4}	14, 15, 35, 129, 130, 140
RNO43	0.4	12	0.5	2.1×10^{-4}	12, 22, 39
L483	0.2	14	0.31	1.5×10^{-5}	47, 45, 24
L1251B	0.2	14	1.2	4.9×10^{-5}	48, 142, 49
TTAU	0.14	17	5.8	4.1×10^{-5}	5, 6, 25, 26, 19, 1, 27
HH111	0.46	24	0.9	5.0×10^{-5}	20, 21, 23
IRAS16293	0.16	27	2.9	1.6×10^{-3}	8, 9, 30, 31, 32
L1251A	0.3	27	0.47	8.6×10^{-5}	48, 45, 49
HARO4-255FIR	0.48	28	0.2	1.3×10^{-4}	12, 19, 37, 38
L1551-IRS5	0.14	20	0.8	1.0×10^{-4}	1, 6, 28, 101, 102, 103
HLTAU	0.16	44	0.3	1.4×10^{-6}	5, 19, 1, 29, 23, 7, 119
L1228	0.20	7	0.15	5.4×10^{-6}	53, 94, 198
PVCEP	0.5	80	0.2	1.0×10^{-4}	12, 13, 19, 27
L1641N	0.42	170	0.6	9.0×10^{-4}	43, 37, 44, 142
FIRSSE101	0.45	123	1.1	2.0×10^{-3}	37, 40, 41
HH7-11 VLA3	0.35	150	0.8	1.1×10^{-3}	1, 2, 23, 69
RE50	0.46	295	0.84	3.0×10^{-4}	42, 37, 40, 23, 41, 116
SERPENS	0.415	98	2.0	5.3×10^{-4}	110, 111, 112, 156, 92, 93
IRAS22198	1.3	1240	0.57	2.3×10^{-4}	88, 89
NGC2071-IRS3	0.39	520	2.9	1.5×10^{-2}	54, 90, 91, 136
HH34	0.42	15	0.160	3.0×10^{-6}	59, 94, 95
AF5142 CM1	2.14	10 000	1.3	2.4×10^{-3}	96, 108

Table 2 continued

Source	d (kpc)	$L_{\rm bol}$ ($L_\odot$)	S_ν (mJy)	$\dot{P}$ ($M_\odot$ year^{-1} km s^{-1})	Refs.
AF5142 CM2	2.14	1000	0.35	2.4×10^{-3}	96, 108
CepAHW2	0.725	10000	6.9	5.4×10^{-3}	104, 105, 106, 107
IRAS20126	1.7	13000	0.2	6.0×10^{-3}	152, 153, 199
HH80–81	1.7	20000	5.0	1.0×10^{-3}	98, 113, 114, 115
V645Cyg	3.5	40000	0.6	7.0×10^{-4}	122, 129, 137
IRAS16547	2.9	60000	8.7	4.0×10^{-1}	149, 150, 151
IRAS18566 B	6.7	80000	0.077	7.2×10^{-3}	99, 100, 167
IRAS04579	2.5	3910	0.15	9.0×10^{-4}	88, 148, 194
GGD14-VLA7	0.9	1000	0.18	1.6×10^{-3}	55, 65, 66, 67, 68, 97
IRAS23139	4.8	20000	0.53	8.0×10^{-4}	123, 124, 125
N7538-IRS9	2.8	40000	3.8	2.1×10^{-2}	88, 126, 127
N7538-IRS9 A1	2.8	40000	1.4	3.0×10^{-2}	88, 126, 127
IRAS16562	1.6	70000	21.1	3.0×10^{-2}	131, 133
I18264-1152 F	3.5	10000	0.28	1.4×10^{-2}	99, 100, 123
G31.41	7.9	200 000	0.32	6.0×10^{-2}	134, 135, 143, 147
AF2591-VLA3	3.3	230000	1.52	7.7×10^{-3}	121, 172, 195
I18182-1433b	4.5	20000	0.6	2.8×10^{-3}	99, 196
I18089-1732(1)a	3.6	32000	1.1	···	196
G28S-JVLA1	4.8	100	0.02	···	197
G28N-JVLA2N	4.8	1000	0.06	···	197
G28N-JVLA2S	4.8	1000	0.03	···	197
L1287	0.85	1000	0.5	3.3×10^{-4}	192, 193, 116, 118
DG Tau B	0.15	0.9	0.31	6.0×10^{-6}	60, 61, 157, 158
Z CMa	1.15	3000	1.74	1.0×10^{-4}	122, 159, 160
W3IRS5(d)	1.83	200000	1.5	3.0×10^{-2}	128, 161, 162
YLW 16A	0.16	13	0.78	3.4×10^{-6}	137, 163
YLW 15 VLA1	0.12	1	1.5	1.1×10^{-5}	138, 164, 165, 166
L778	0.25	0.93	0.69	1.9×10^{-6}	4, 137, 168
W75N(B)VLA1	1.3	19000	4.0	1.2×10^{-2}	139, 169, 170, 171, 172, 154
NGC1333 VLA2	0.235	1.5	2.5	4.9×10^{-4}	140, 141, 173, 174, 175
NGC1333 IRAS4A1	0.235	8	0.32	1.5×10^{-4}	140, 173, 176, 177, 178
NGC1333 IRAS4B	0.235	1.1	0.33	4.1×10^{-5}	140, 173, 177, 178
L1551 NE-A	0.14	4.0	0.39	1.5×10^{-5}	140, 179, 180, 181, 61, 62
Haro 6-10 VLA1	0.14	0.5	1.1	9.4×10^{-6}	146, 12, 182, 183, 184
L1527 VLA1	0.14	1.9	1.1	1.6×10^{-4}	144, 145, 146, 179, 184
OMC 2/3 VLA4	0.414	40	0.83	5.2×10^{-4}	146, 185
HH1–2 VLA1	0.414	23	1.2	4.6×10^{-5}	186, 187, 188, 109
HH1–2 VLA3	0.414	84	0.40	5.7×10^{-4}	186, 187, 188
OMC2 VLA11	0.414	360	2.16	3.2×10^{-3}	189, 190, 191

Table 2 continued

Source	d (kpc)	$L_{\rm bol}$ ($L_\odot$)	S_ν (mJy)	$\dot{P}$ ($M_\odot$ year^{-1} km s^{-1})	Refs.
HH46/47	0.45	12	1.8	2.0×10^{-4}	23, 56, 57, 117, 120
IRAS20050	0.7	260	1.4	5.0×10^{-3}	63, 64

References: (1) Edwards and Snell (1984); (2) Bachiller and Cernicharo (1990); (3) Rodriguez et al. (1989b); (4) Myers et al. (1988); (5) Calvet et al. (1983); (6) Cohen et al. (1982); (7) Brown et al. (1985); (8) Wootten and Loren (1987); (9) Estalella et al. (1991); (10) Goldsmith et al. (1984); (11) Anglada et al. (1991); (12) Anglada et al. (1992) (13) Levreault (1984); (14) Bachiller et al. (1990); (15) Curiel et al. (1990); (16) Andre et al. (1990); (17) Margulis et al. (1988); (18) Gómez et al. (1994); (19) Levreault (1988); (20) Reipurth and Olberg (1991); (21) Rodriguez and Reipurth (1994); (22) Cabrit et al. (1988); (23) Reipurth et al. (1993); (24) Ladd et al. (1991); (25) Schwartz et al. (1986); (26) Edwards and Snell (1982); (27) Evans et al. (1986); (28) Mozurkewich et al. (1986); (29) Torrelles et al. (1987); (30) Mundy et al. (1986); (31) Mizuno et al. (1990); (32) Walker et al. (1988); (33) Avery et al. (1990); (34) Bachiller et al. (1991); (35) Andre et al. (1993); (36) Ward-Thompson et al. (1995); (37) Morgan et al. (1991); (38) Morgan and Bally (1991); (39) Cohen and Schwartz (1987); (40) Fukui (1989); (41) Morgan et al. (1990); (42) Reipurth and Bally (1986); (43) Fukui et al. (1988); (44) Chen et al. (1995); (45) Beltrán et al. (2001); (46) Terebey et al. (1989); (47) Parker et al. (1988); (48) Sato et al. (1994); (49) Kun and Prusti (1993); (50) Yun and Clemens (1994); (51) Parker (1991); (52) Cohen and Bieging (1986); (53) Haikala and Laureijs (1989); (54) Snell et al. (1984); (55) Rodriguez et al. (1982); (56) Chernin and Masson (1991); (57) S. Curiel, private communication; (58) Moriarty-Schieven and Snell (1989); (59) Antoniucci et al. (2008); (60) Mitchell et al. (1994); (61) Rodriguez et al. (1995); (62) Moriarty-Schieven et al. (1995); (63) Bachiller et al. (1995); (64) Wilking et al. (1989); (65) Little et al. (1990); (66) Gómez et al. (2000); (67) Gómez et al. (2002); (68) Harvey et al. (1985); (69) Rodríguez et al. (1997); (70) Dunham et al. (2008); (71) Choi et al. (2014); (72) André et al. (1999); (73) Bourke et al. (2005); (74) Shirley et al. (2007); (75) Maheswar et al. (2011); (76) Kauffmann et al. (2011); (77) AMI Consortium et al. (2011a); (78) Takahashi et al. (2013); (79) Palau et al. (2014); (80) Rodríguez et al. (2014b); (81) Hirota et al. (2008); (82) Hirota et al. (2011); (83) Palau et al. (2012); (84) Morata et al. (2015); (85) Cotera et al. (2001); (86) Pety et al. (2006); (87) G. Anglada et al., in preparation; (88) Sánchez-Monge et al. (2008); (89) Zhang et al. (2005); (90) Carrasco-González et al. (2012a); (91) Stojimirović et al. (2008); (92) Kristensen et al. (2012); (93) van Kempen et al. (2016); (94) Rodríguez and Reipurth (1996); (95) Chernin and Masson (1995); (96) Zhang et al. (2007); (97) Dzib et al. (2016); (98) Benedettini et al. (2004); (99) Beuther et al. (2002); (100) Rosero et al. (2016); (101) Rodríguez et al. (2003b); (102) Bieging and Cohen (1985); (103) Rodriguez et al. (1986); (104) Hughes (1988); (105) Rodriguez et al. (1994b); (106) Gómez et al. (1999); (107) Curiel et al. (2006); (108) Hunter et al. (1995); (109) Rodriguez et al. (1990); (110) Rodriguez et al. (1989a); (111) Curiel et al. (1993); (112) Curiel (1995); (113) Rodríguez and Reipurth (1989); (114) Marti et al. (1993); (115) Marti et al. (1995); (116) Anglada (1995); (117) Arce et al. (2013); (118) Anglada et al. (1994); (119) Rodriguez et al. (1994a); (120) Zhang et al. (2016); (121) Hasegawa and Mitchell (1995); (122) Skinner et al. (1993); (123) Sridharan et al. (2002); (124) Wouterloot et al. (1989); (125) Trinidad et al. (2006); (126) Tamura et al. (1991); (127) Sandell et al. (2005); (128) Claussen et al. (1994); (129) Girart et al. (1996a); (130) Girart et al. (1996b); (131) Guzmán et al. (2016); (132) Anglada et al. (1996); (133) Guzmán et al. (2011); (134) Osorio et al. (2009); (135) Cesaroni et al. (2010); (136) Torrelles et al. (1998); (137) Girart et al. (2002); (138) Girart et al. (2000); (139) Torrelles et al. (1997); (140) Reipurth et al. (2002); (141) Rodríguez et al. (1999); (142) Anglada et al. (1998); (143) Cesaroni et al. (2011); (144) Rodriguez and Reipurth (1998); (145) Loinard et al. (2002); (146) Reipurth et al. (2004); (147) Mayen-Gijon (2015); (148) Molinari et al. (1996); (149) Garay et al. (2003); (150) Brooks et al. (2003); (151) Rodríguez et al. (2005); (152) Hofner et al. (1999); (153) Trinidad et al. (2005); (154) Torrelles et al. (2003); (155) Carrasco-González et al. (2008b); (156) Rodríguez-Kamenetzky et al. (2016); (157) Rodríguez et al. (2012b); (158) Zapata et al. (2015a); (159) Evans et al. (1994); (160) Velázquez and Rodríguez (2001); (161) Imai et al. (2000); (162) Hasegawa et al. (1994); (163) Sekimoto et al. (1997); (164) Girart et al. (2004); (165) van Kempen et al. (2009); (166) Bontemps et al. (1996); (167) Hofner et al. (2017); (168) Rodriguez et al. (1989b); (169) Hunter et al. (1994); (170) Shepherd et al. (2003); (171) Carrasco-González et al. (2010a); (172) Rygl et al. (2012); (173) Plunkett et al. (2013); (174) Sadavoy et al. (2014); (175) Downes and Cabrit (2007); (176) Dunham et al. (2014); (177) Ching et al. (2016); (178) Yıldız et al. (2012); (179) Froebrich (2005); (180) Lim et al. (2016); (181) Takakuwa et al. (2017); (182) Doppmann et al. (2008); (183) Roccatagliata et al. (2011); (184) Hogerheijde et al. (1998); (185) Yu et al. (2000); (186) Fischer et al. (2010); (187) Rodríguez et al. (2000); (188) Correia et al. (1997); (189) Furlan et al. (2016); (190) Osorio et al. (2017); (191) Takahashi et al. (2008); (192) Yang et al. (1991); (193) Wu et al. (2010); (194) Xu et al. (2012); (195) Johnston et al. (2013); (196) Zapata et al. (2006); (197) C. Carrasco-González et al., in preparation; (198) Skinner et al. (2014); (199) Shepherd et al. (2000)

values of the flux density, taken from the compilation of Furuya et al. 2003). Because radio jets have positive spectral indices with typical values around ~ 0.4, it is expected that the 3.6 cm flux densities are $\sim 20\%$ higher than the 6 cm flux densities, but the slopes of the luminosity correlations are expected to be similar, provided the scattering in the values of the spectral index is small. L. Tychoniec et al. (in preparation) analyze a large homogeneous sample of low-mass protostars in Perseus, obtaining similar slopes of ~ 0.7 for data at 4.1 and 6.4 cm. These authors note, however, that the correlations are weak for these sources that cover a relatively small range of luminosities. These results suggest that there is a general trend over a wide range of luminosities, but with an intrinsic dispersion.

Recently, Moscadelli et al. (2016) derived a slope of 0.5 from a small sample (8 sources) of high luminosity objects with outflows traced by masers. Also, recent surveys targeted towards high-mass protostellar candidates (but without a confirmed association with an outflow) also show radio continuum to bolometric luminosity correlations with similar slopes of ~ 0.7 (Purser et al. 2016). Recently, Tanaka et al. (2016) modeled the evolution of a massive protostar and its associated jet as it is being photoionized by the protostar, making predictions for the free–free continuum and RRL emissions. These authors find global properties of the continuum emission similar to those of radio jets. The radio continuum luminosities of the photoionized outflows predicted by the models are somewhat higher than those obtained from the empirical correlations for jets but much lower than those expected for optically thin HII regions. When including an estimate of the ionization of the ambient clump by photons that escape along the outflow cavity the predicted properties get closer to those of the observed UC/HC HII regions. Photoevaporation has not been included. This kind of models, including additional effects such as the photoevaporation, are a promising tool to investigate the transition from jets to HII regions in massive protostars. Purser et al. (2016) found a number of objects with radio luminosities intermediate between optically thin HII regions and radio jets that these authors interpret as optically thick HII regions. We note that this kind of objects could be in an evolutionary stage intermediate between the jet and the HII region phases, and their properties could be predicted by models similar to those of Tanaka et al. (2016).

From a sample of outflow sources of low and very low bolometric luminosity, but using low angular resolution data ($\sim 30''$) at 1.8 cm, a correlation between the cm luminosity and the internal luminosity[1] with a slope of either 0.5 or 0.6 was found (AMI Consortium et al. 2011a, b), depending, respectively, on the use of either the bolometric luminosity or the IR luminosity as an estimate of the internal luminosity. Morata et al. (2015) report cm emission from four proposed proto-brown dwarf (proto-BD) candidates, that appear to follow the general trend of the luminosity correlation but showing some excess of radio emission. Further observations are required to confirm the nature of these objects as proto-BDs, to better determine their properties such as distance and intrinsic luminosity, as well as their radio jet morphology. If confirmed as bona fide proto-BDs that follow the correlation, this would suggest that the same mechanisms are at work for YSOs and proto-BDs, supporting the idea that the intrinsic

[1] The internal luminosity is the luminosity in excess of that supplied by the interstellar radiation field.

properties of proto-BDs are a continuation to smaller masses of the properties of low-mass YSOs. It is interesting that the only two *bona fide* young brown dwarfs detected in the radio continuum fall well in this correlation (Rodríguez et al. 2017).

Recently, it has been realized that young stars in more advanced stages, such as those surrounded by transitional disks[2] are also associated with radio jets that have become detectable with the improved sensitivity of the JVLA (Rodríguez et al. 2014a; Macías et al. 2016). In these objects, accretion is very low but high enough to produce outflow activity detectable through the associated radio emission at a level of $\lesssim 0.1$ mJy. These radio jets follow the general trend of the luminosity correlation but appear to be radio underluminous with respect to the correlation that was established from data corresponding to younger objects. This fact has been interpreted as indicating that it is the accretion component of the luminosity that is correlated with the outflow (and, thus, with the radio flux of the jet). Accretion luminosity is dominant in the youngest objects, from which the correlation was derived, while in more evolved objects the stellar contribution (which is not expected to be correlated with the radio emission) to the total luminosity becomes more important. Thus, it is expected that in more evolved objects the observed radio luminosity is correlated with only a fraction of the bolometric luminosity.

In summary, the radio luminosity ($S_\nu d^2$) of thermal jets associated with very young stellar objects is correlated with their bolometric luminosity ($L_{\rm bol}$). This correlation is valid for objects of a wide range of luminosities, from high to very low luminosity objects, and likely even for proto-BDs. This suggests that accretion and outflow processes work in a similar way for objects of a wide range of masses and luminosities. Accretion appears to be correlated with outflow (which is traced by the radio luminosity). As the young star evolves, accretion decreases and so does the radio luminosity. However, for these more evolved objects the accretion luminosity represents a smaller fraction of the bolometric luminosity (the luminosity of the star becomes more important) and they become radio underluminous with respect to the empirical correlation, which was derived for younger objects.

8.2 Observational properties: radio luminosity to outflow momentum rate correlation

The radio luminosity of thermal radio jets is also correlated with the properties of the associated outflows. A correlation between the momentum rate (force) in the outflow, $\dot{P}$, derived from observations, and the observed radio continuum luminosity at centimeter wavelengths, $S_\nu d^2$, was first noted by Anglada et al. (1992) and by Cabrit and Bertout (1992). Anglada et al. (1992) considered a sample of 16 sources of low bolometric luminosity (to avoid a contribution from photoionization) and found a correlation $(S_\nu d^2/\text{mJy kpc}^2) = 10^{2.4\pm1.0}\,(\dot{P}/M_\odot\ \text{year}^{-1})^{0.9\pm0.3}$. Since the outflow momentum rate estimates have considerable uncertainties (more than one order of magnitude, typically), $\dot{P}$ was fitted (in the log-log space) taking $S_\nu d^2$ as the indepen-

[2] Transitional disks are accretion disks with central cavities or gaps in the dust distribution that are attributed to disk clearing by still forming planets.

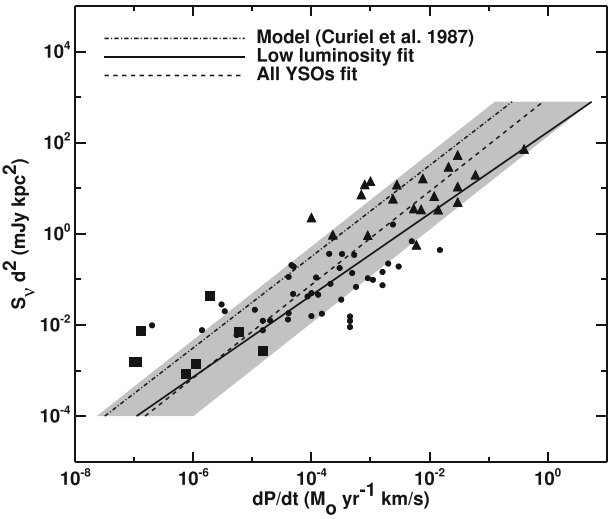

Fig. 9 Empirical correlation between the outflow momentum rate and the radio continuum luminosity at cm wavelengths. Data are taken from Table 2. Triangles correspond to high luminosity objects ($L_{\rm bol} > 1000\ L_\odot$), dots correspond to low-luminosity objects ($1 \leq L_{\rm bol} \leq 1000\ L_\odot$), and squares to very low-luminosity objects ($L_{\rm bol} < 1\ L_\odot$). The dashed line is a least-squares fit to all the data points and the grey area indicates the residual standard deviation of the fit. The solid line is a fit to the low-luminosity objects alone. The dot-dashed line corresponds to the radio luminosity predicted by the models of Curiel et al. (1987, 1989)

dent variable, as it was considered to be less affected by observational uncertainties. The correlation was confirmed with fits to larger samples (Anglada 1995, 1996; Anglada et al. 1998; Shirley et al. 2007; AMI Consortium et al. 2011a,b, 2012). The best fit to the low-luminosity sources ($1 \lesssim L_{\rm bol} \lesssim 1000\ L_\odot$) presented in Table 2 gives (see also Fig. 9):

$$\left(\frac{S_\nu d^2}{\rm mJy\ kpc^2}\right) = 10^{2.22\pm0.46} \left(\frac{\dot{P}}{M_\odot\ {\rm year}^{-1}\ {\rm km\ s}^{-1}}\right)^{0.89\pm0.16}. \quad (29)$$

This correlation between the outflow momentum rate and the radio luminosity has been interpreted as evidence that shocks are the ionizing mechanism of jets. Curiel et al. (1987, 1989) modeled the scenario in which a neutral stellar wind is ionized as a result of a shock against the surrounding high-density material, assuming a plane-parallel shock. From the results obtained in this model, ignoring further details about the radiative transfer and geometry of the emitting region, and assuming that the free–free emission is optically thin, a relationship between the momentum rate in the outflow and the centimeter luminosity can be obtained (see Anglada 1996; Anglada et al. 1998):

$$\left(\frac{S_\nu d^2}{\rm mJy\ kpc^2}\right) = 10^{3.5}\ \eta \left(\frac{\dot{P}}{M_\odot\ {\rm year}^{-1}\ {\rm km\ s}^{-1}}\right), \quad (30)$$

where $\eta = \Omega/4\pi$ is an efficiency factor that can be taken to equal the fraction of the stellar wind that is shocked and produces the observed radio continuum emission. Despite the limitations of the model, and the simplicity of the assumptions used to derive Eq. (30), its predictions agree quite well with the results obtained from a large number of observations (Eq. 29), for an efficiency $\eta \simeq 0.1$. González and Cantó (2002) present a model in which the ionization is produced by internal shocks in a wind, resulting of periodic variations of the velocity of the wind at injection.

Cabrit and Bertout (1992) and Rodríguez et al. (2008) noted that high-mass protostars driving molecular outflows appear to follow the same radio luminosity to outflow momentum rate correlation as the sources of low luminosity. As can be seen in Fig. 9, high luminosity objects fall close to the fit determined by the low luminosity objects. Actually, a fit including all the sources in the sample of Table 2, including both low and high luminosity objects, gives a quite similar result,

$$\left(\frac{S_\nu d^2}{\mathrm{mJy\ kpc^2}}\right) = 10^{2.97\pm0.27}\left(\frac{\dot{P}}{M_\odot\ \mathrm{year^{-1}\ km\ s^{-1}}}\right)^{1.02\pm0.08}, \tag{31}$$

as it was also the case for the bolometric luminosity correlation (Fig. 8). Thus, radio jets in massive protostars appear to be ionized by a mechanism similar to that acting in low luminosity objects. Radio jets would represent a stage in massive star formation previous to the onset of photoionization and the development of an HII region. Actually, the correlations can be used as a diagnostic tool to discriminate between photoionized (HII regions) versus shock-ionized (jets) sources (see Tanaka et al. 2016 and the previous discussion in Sect. 8.1).

As in the radio to bolometric luminosity correlation, the very low luminosity objects also fall in the outflow momentum rate correlation. These results are interpreted as indicating that the mechanisms for accretion, ejection and ionization of outflows are very similar for all kind of YSOs, from very low to high luminosity protostars.

A direct measure of the outflow momentum rate is difficult for objects in the last stages of the star formation process, when accretion has decreased to very small values and outflows are hard to detect. For these objects, the weak radio continuum emission can be used as a tracer of the outflow. Recent results obtained for sources associated with transitional disks (Rodríguez et al. 2014a; Macías et al. 2016) indicate that the observed radio luminosities are consistent with the outflow momentum rate to radio luminosity correlation being valid and the ratio between accretion, and outflow being similar in these low accretion objects than in younger protostars.

8.3 On the origin of the correlations

As has been shown above, the observable properties of the cm continuum outflow sources indicate that these sources trace thermal free–free emission from ionized collimated outflows (jets). Both theoretical and observational results suggest that the ionization in thermal jets is only partial ($\sim$ 1–10%; Rodriguez et al. 1990; Hartigan et al. 1994; Bacciotti et al. 1995). The mechanism that is able to produce the required ionization, even at these relatively low levels, is still not fully understood. As photoion-

ization cannot account for the observed radio continuum emission of low-luminosity objects (see above), shock ionization has been proposed as a viable alternative mechanism (Curiel et al. 1987; González and Cantó 2002).

The correlations described in Sects. 8.1 and 8.2 are related to the well-known correlation between the momentum rate observed in molecular outflows and the bolometric luminosity of the driving sources, first noted by Rodriguez et al. (1982). More recent determinations of this correlation give $(\dot{P}/M_\odot \text{ year}^{-1} \text{ km s}^{-1}) = 10^{-4.36\pm0.12} (L_{\rm bol}/L_\odot)^{0.69\pm0.05}$ (Cabrit and Bertout 1992) or $(\dot{P}/M_\odot \text{ year}^{-1} \text{ km s}^{-1}) = 10^{-4.24\pm0.32} (L_{\rm bol}/L_\odot)^{0.67\pm0.13}$ (Maud et al. 2015, for a sample of massive protostars). The empirical correlations with cm emission described by Eqs. 28 and 31 result in an expected correlation $(\dot{P}/M_\odot \text{ year}^{-1} \text{ km s}^{-1}) = 10^{-4.77\pm0.14} (L_{\rm bol}/L_\odot)^{0.58\pm0.08}$, which is in agreement with the results obtained directly from the observations. We interpreted the correlation of the outflow momentum rate with the radio luminosity (Eq. 31) as a consequence of the shock ionization mechanism working in radio jets, and the correlation of the bolometric and radio luminosities (Eq. 28) as a consequence of the accretion and outflow relationship. In this context, the well-known correlation between the momentum rate of molecular outflows and the bolometric luminosity of their driving sources can be interpreted as a natural consequence of the other two correlations.

9 Additional topics

9.1 Fossil outflows

In the case of regions of massive star formation there are also clear examples of jets that show the morphology and spectral index characteristic of this type of sources. Furthermore, these massive jets fall in the correlations previously discussed.

However, there is a significant number of molecular outflows in regions of massive star formation where it has not been possible to detect the jet. Instead, ultracompact HII regions are found near the center of these outflows (e.g., G5.89−0.39, Zijlstra et al. 1990; G25.65+1.05 and G240.31+0.07, Shepherd and Churchwell 1996; G45.12+0.13 and G45.07+0.13, Hunter et al. 1997; G192.16−3.82, Devine et al. 1999; G213.880−11.837, Qin et al. 2008; G10.6−0.4, Liu et al. 2010; G24.78+0.08, Codella et al. 2013; G35.58−0.03, Zhang et al. 2014).

We can think of two explanations for this result. One is that the central source has evolved and the jet has been replaced by an ultracompact HII region. From momentum conservation the outflow will continue coasting for a large period of time, becoming a fossil outflow in the sense that it now lacks an exciting source of energy. The alternative explanation is that a centimeter jet is present in the region but that the much brighter HII region makes it difficult to detect it. This is a problem that requires further research.

It should also be noted that in two of the best studied cases, G25.65+1.05 and G240.31+0.07, high angular resolution radio observations (Kurtz et al. 1994; Chen 2007; Trinidad 2011) have revealed fainter sources in the region that could be the true energizing sources of the molecular outflows. If this is the case, the outflows cannot be considered as fossil since they would have an associated active jet.

9.2 Jets or ionized disks?

The presence in star forming regions of an elongated centimeter source is usually interpreted as indicating the presence of a thermal jet. This interpretation is typically confirmed by showing that the outflow traced at larger scales by molecular outflows and/or optical/IR HH objects aligns with the small-scale radio jet. In the sources where the true dust disk is detected and resolved, it is found to align perpendicular to the outflow axis. However, in a few massive objects there is evidence that the elongated centimeter source actually traces a photoionized disk (S106IR: Hoare et al. 1994; S140-IRS: Hoare 2006; Orion Source I: Reid et al. 2007; see Fig. 10). These objects show a similar centimeter spectral index to that of jets and one cannot discriminate using this criterion. There is also the case of NGC 7538 IRS1, a source that has been interpreted as an ionized jet (Sandell et al. 2009) or modeled as a photoionized accretion disk (Lugo et al. 2004), although it is usually referred to as an ultracompact HII region (Zhu et al. 2013).

A possible way to favor one of the interpretations is to locate the object in a radio luminosity versus bolometric luminosity diagram as has been discussed above. It is expected that a photoionized disk will fall in between the regions of thermal jets and UC HII regions in such a diagram. Another test to discriminate between thermal jets and photoionized disks would be to eventually detect radio recombination lines from the source. In the case of photoionized disks lines with widths of tens of km s^{-1} are expected, while in the case of thermal jets the lines could exhibit widths an order of magnitude larger. It should be noted, however, that in the case of very collimated jets the velocity dispersion and, thus, the observed line widths, will be narrow.

The possibility of an ionized disk is also present in the case of low mass protostars. The high resolution images of GM Aur presented by Macías et al. (2016) show that, after subtracting the expected dust emission from the disk, the centimeter emission from this source is composed of an ionized radio jet and a photoevaporative wind arising from the disk perpendicular to the jet (see Fig. 11). It is believed that extreme-UV (EUV) radiation from the star is the main ionizing mechanism of the disk surface. Dust emission at cm wavelengths is supposed to arise mainly from grains that have grown up to reach pebble sizes (e.g., Guzmán et al. 2016).

10 Conclusions

The study of jets associated with young stars has contributed in an important manner to our understanding of the process of star formation. We list below the main conclusions that arise from these studies:

1. Free–free radio jets are typically found in association with the forming stars that can also power optical or molecular large-scale outflows. While the jets trace the outflow over the last few years, the optical and molecular outflows integrate in time over centuries or even millenia.
2. The radio jets provide a means to determine accurately the position and proper motions of the stellar system in regions of extremely high obscuration.

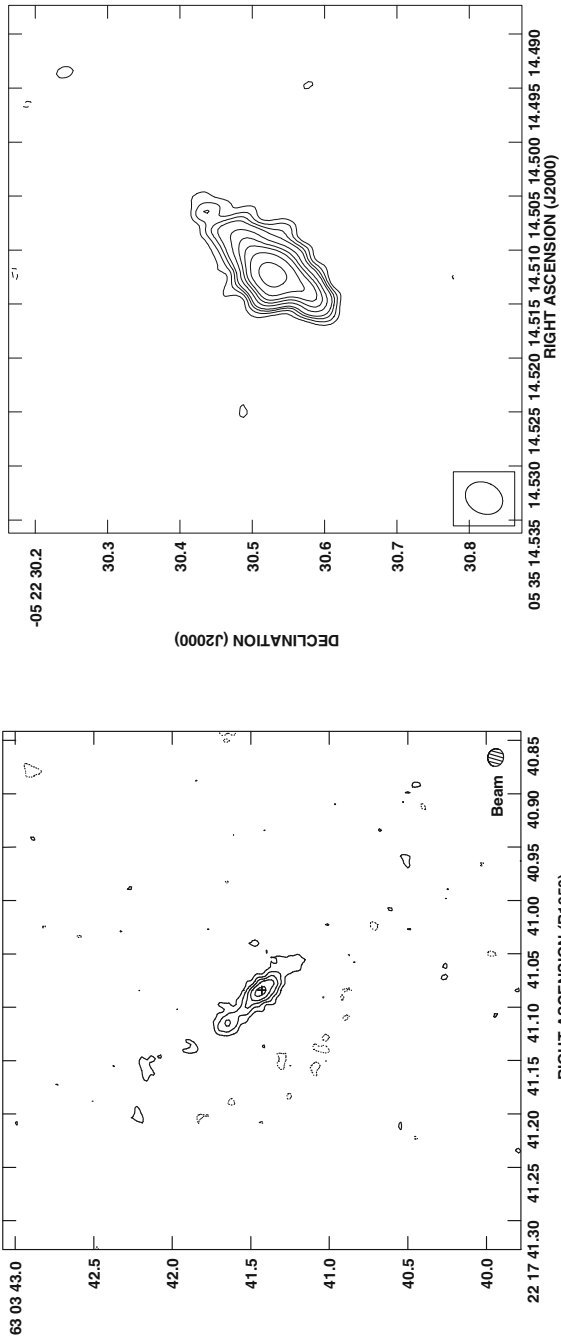

Fig. 10 The radio sources associated with S140 IRS1 and with source I in Orion. These sources of radio continuum emission are believed to trace photoionized disks and not jets. Image reproduced with permission from [left] Hoare (2006), copyright by AAS; and [right] based on Reid et al. (2007)

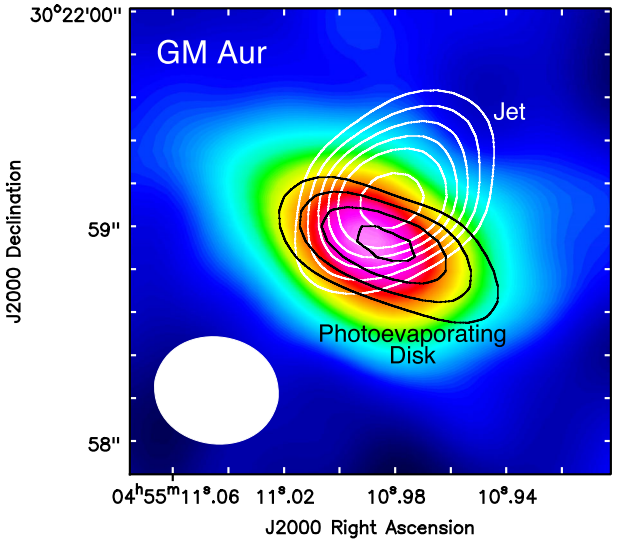

Fig. 11 Decomposition of the emission of GM Aur at cm wavelengths. The free–free emission at 3 cm of the radio jet is shown in white contours and that of the photoevaporative wind from the disk is shown in black contours. The dust emission from the disk at 7 mm is shown in color scale. The free–free emission of the two ionized components was separated by fitting two Gaussians to the 3 cm image after subtraction of the contribution at 3 cm of the dust of the disk, estimated by scaling the 7 mm image with the dust spectral index obtained from a fit to the spectral energy distribution. Image reproduced with permission from Macías et al. (2016), copyright by AAS

3. The core of these jets emits as a partially optically thick free–free source. However, in knots along the jet (notably in the more massive protostars) optically thin synchrotron emission could be present. Studies of this non-thermal emission will provide important information on the role of magnetic fields in these jets.
4. At present there are only tentative detections of radio recombination lines from the jets. Future instruments such as SKA and the ngVLA will allow a new avenue of research using this observational tool.
5. The radio luminosity of the jets is well correlated both with the bolometric luminosity and the outflow momentum rate of the optical or molecular outflow. This is a result that can be understood theoretically for sources that derive most of its luminosity from accretion and where the ionization of the jet is due to shocks with the ambient medium. These correlations extend from massive young stars to the sub-stellar domain, suggesting a common formation mechanism for all stars.

Acknowledgements GA acknowledges support from MINECO (Spain) AYA2014-57369-C3-3-P and AYA2017-84390-C2-1-R grants (co-funded by FEDER). LFR acknowledges support from CONACyT, Mexico and DGAPA, UNAM. CC-G acknowledges support from UNAM-DGAPA-PAPIIT grant numbers IA102816 and IN108218. We thank an anonymous referee for his/her useful comments and suggestions.

References

Adams JD, Herter TL, Osorio M, Macias E, Megeath ST, Fischer WJ, Ali B, Calvet N, D'Alessio P, De Buizer JM, Gull GE, Henderson CP, Keller LD, Morris MR, Remming IS, Schoenwald J, Shuping RY, Stacey G, Stanke T, Stutz A, Vacca W (2012) First Science Observations with SOFIA/FORCAST: Properties of Intermediate-luminosity Protostars and Circumstellar Disks in OMC-2. Astrophys J 74:L24. https://doi.org/10.1088/2041-8205/749/2/L24

Ainsworth RE, Scaife AMM, Ray TP, Taylor AM, Green DA, Buckle JV (2014) Tentative evidence for relativistic electrons generated by the jet of the young Sun-like star DG Tau. Astrophys J 792:L18. https://doi.org/10.1088/2041-8205/792/1/L18

Alexander J, Gulyaev S (2016) Stark broadening of high-order radio recombination lines toward the Orion Nebula. Astrophys J 828:40. https://doi.org/10.3847/0004-637X/828/1/40

ALMA Partnership, Brogan CL, Pérez LM, Hunter TR, Dent WRF, Hales AS Hills RE, Corder S, Fomalont EB, Vlahakis C, Asaki Y, Barkats D, Hirota A, Hodge JA, Impellizzeri CMV, Kneissl R, Liuzzo E, Lucas R, Marcelino N, Matsushita S, Nakanishi K, Phillips N, Richards AMS, Toledo I, Aladro R, Broguiere D, Cortes JR, Cortes PC, Espada D, Galarza F, Garcia-Appadoo D, Guzman-Ramirez L, Humphreys EM, Jung T, Kameno S, Laing RA, Leon S, Marconi G, Mignano A, Nikolic B, Nyman L-A Radiszcz M, Remijan A, Rodón JA, Sawada T, Takahashi S, Tilanus RPJ, Vila Vilaro B, Watson LC, Wiklind T, Akiyama E, Chapillon E, de Gregorio-Monsalvo I, Di Francesco J, Gueth F, Kawamura A, Lee C-F, Nguyen Luong Q, Mangum J, Pietu V, Sanhueza P, Saigo K, Takakuwa S, Ubach C, van Kempen T, Wootten A, Castro-Carrizo A, Francke H, Gallardo J, Garcia J, Gonzalez S, Hill T, Kaminski T, Kurono Y, Liu H-Y, Lopez C, Morales F, Plarre K, Schieven G, Testi L, Videla L, Villard E, Andreani P, Hibbard JE, Tatematsu K (2015) The 2014 ALMA Long Baseline Campaign: First Results from High Angular Resolution Observations toward the HL Tau Region. Astrophys J 808:L3. https://doi.org/10.1088/2041-8205/808/1/L3

AMI Consortium, Scaife AMM, Curtis EI, Davies M, Franzen TMO, Grainge KJB, Hobson MP, Hurley-Walker N, Lasenby AN, Olamaie M, Pooley GG, Rodríguez-Gonzálvez C, Saunders RDE, Schammel M, Scott PF, Shimwell T, Titterington D, Waldram E, Zwart JTL (2011a) AMI Large Array radio continuum observations of Spitzer c2d small clouds and cores. Mon Not R Astron Soc 410:2662–2678. https://doi.org/10.1111/j.1365-2966.2010.17644.x

AMI Consortium, Scaife AMM, Hatchell J, Davies M, Franzen TMO, Grainge KJB, Hobson MP, Hurley-Walker N, Lasenby AN, Olamaie M, Perrott YC, Pooley GG, Rodríguez-Gonzálvez C, Saunders RD, Schammel MP, Scott PF, Shimwell T, Titterington D, Waldram E (2011b) AMI-LA radio continuum observations of Spitzer c2d small clouds and cores: Perseus region. Mon Not R Astron Soc 415:893–910. https://doi.org/10.1111/j.1365-2966.2011.18755.x

AMI Consortium, Ainsworth RE, Scaife AMM, Ray TP, Buckle JV, Davies M, Franzen TMO, Grainge KJB, Hobson MP, Hurley-Walker N, Lasenby AN, Olamaie M, Perrott YC, Pooley GG, Richer JS, Rodríguez-Gonzálvez C, Saunders RDE, Schammel MP, Scott PF, Shimwell T, Titterington D, Waldram E (2012) AMI radio continuum observations of young stellar objects with known outflows. Mon Not R Astron Soc 423:1089–1108. https://doi.org/10.1111/j.1365-2966.2012.20935.x

Anderson JM, Li Z-Y, Krasnopolsky R, Blandford RD (2003) Locating the launching region of T Tauri winds: the case of DG Tauri. Astrophys J 590:L107–L110. https://doi.org/10.1086/376824

Andre P, Martin-Pintado J, Despois D, Montmerle T (1990) Discovery of a remarkable bipolar flow and exciting source in the Rho Ophiuchi cloud core. Astron Astrophys 236:180–192

Andre P, Ward-Thompson D, Barsony M (1993) Submillimeter continuum observations of Rho Ophiuchi A: the candidate protostar VLA 1623 and prestellar clumps. Astrophys J 406:122–141. https://doi.org/10.1086/172425

André P, Motte F, Bacmann A (1999) Discovery of an extremely young accreting protostar in Taurus. Astrophys J 513:L57–L60. https://doi.org/10.1086/311908

Anglada G (1995) Centimeter continuum emission from outflow sources. Rev Mex Astron Astrof Ser Conf 1:67

Anglada G (1996) Radio jets in young stellar objects. In: Taylor AR, Paredes JM (eds) Radio emission from the stars and the Sun. Astronomical Society of the Pacific Conference Series, vol 93, pp 3–14

Anglada G, Estalella R, Rodriguez LF, Torrelles JM, Lopez R, Canto J (1991) A double radio source at the center of the outflow in L723. Astrophys J 376:615–617. https://doi.org/10.1086/170309

Anglada G, Rodriguez LF, Canto J, Estalella R, Torrelles JM (1992) Radio continuum from the powering sources of the RNO 43, HARO 4–255 FIR, B335, and PV Cephei outflows and from the Herbig–Haro object 32A. Astrophys J 395:494–500. https://doi.org/10.1086/171670
Anglada G, Rodriguez LF, Girart JM, Estalella R, Torrelles JM (1994) A radio candidate for the exciting source of the L1287 bipolar outflow. Astrophys J 420:L91–L93. https://doi.org/10.1086/187170
Anglada G, Rodriguez LF, Torrelles JM (1996) A thermal radio jet associated with the quadrupolar molecular outflow in L723. Astrophys J 473:L123. https://doi.org/10.1086/310408
Anglada G, Villuendas E, Estalella R, Beltrán MT, Rodríguez LF, Torrelles JM, Curiel S (1998) Spectral indices of centimeter continuum sources in star-forming regions: implications on the nature of the outflow exciting sources. Astron J 116:2953–2964. https://doi.org/10.1086/300637
Anglada G, Rodríguez LF, Carrasco-Gonzalez C (2015) Radio jets in young stellar objects with the SKA. In: Advancing Astrophysics with the Square Kilometre Array. Proceedings of Science, PoS(AASKA14)121
Antoniucci S, Nisini B, Giannini T, Lorenzetti D (2008) Accretion and ejection properties of embedded protostars: the case of HH26, HH34, and HH46 IRS. Astron Astrophys 479:503–514. https://doi.org/10.1051/0004-6361:20077468
Araudo AT, Romero GE, Bosch-Ramon V, Paredes JM (2007) Gamma-ray emission from massive young stellar objects. Astron Astrophys 476:1289–1295. https://doi.org/10.1051/0004-6361:20077636
Arce HG, Mardones D, Corder SA, Garay G, Noriega-Crespo A, Raga AC (2013) ALMA observations of the HH 46/47 molecular outflow. Astrophys J 774:39. https://doi.org/10.1088/0004-637X/774/1/39
Aspin C, Geballe TR (1992) Mid-IR spectroscopy of GGD 27-IRS: Evidence for a PMS stellar cluster. Astron Astrophys 266:219–224
Avery LW, Hayashi SS, White GJ (1990) The unusual morphology of the high-velocity gas in L723: one outflow or two? Astrophys J 357:524–530. https://doi.org/10.1086/168939
Avila R, Rodríguez LF, Curiel S (2001) VLA detection of the exciting sources of the HH 211 and HH 68 outflows. Rev Mex Astron Astrof 37:201–211
Bacciotti F, Chiuderi C, Oliva E (1995) The structure of optical stellar jets: a phenomenological analysis. Astron Astrophys 296:185
Bacciotti F, Ray TP, Mundt R, Eislöffel J, Solf J (2002) Hubble space telescope/STIS spectroscopy of the optical outflow from DG Tauri: indications for rotation in the initial jet channel. Astrophys J 576:222–231. https://doi.org/10.1086/341725
Bachiller R, Cernicharo J (1990) Extremely high-velocity emission from molecular jets in NGC 6334 I and NGC 1333 (HH 7–11). Astron Astrophys 239:276–286
Bachiller R, Martin-Pintado J, Tafalla M, Cernicharo J, Lazareff B (1990) High-velocity molecular bullets in a fast bipolar outflow near L1448/IRS3. Astron Astrophys 231:174–186
Bachiller R, Andre P, Cabrit S (1991) Detection of the exciting source of the spectacular molecular outflow L1448 at lambda lambda 1–3 mm. Astron Astrophys 241:L43–L46
Bachiller R, Fuente A, Tafalla M (1995) An extremely high velocity multipolar outflow around IRAS 20050 + 2720. Astrophys J 445:L51–L54. https://doi.org/10.1086/187887
Báez-Rubio A, Martín-Pintado J, Thum C, Planesas P, Torres-Redondo J (2014) Origin of the ionized wind in MWC 349A. Astron Astrophys 571:L4. https://doi.org/10.1051/0004-6361/201424389
Bally J (2016) Protostellar outflows. Annu Rev Astron Astrophys 54:491–528. https://doi.org/10.1146/annurev-astro-081915-023341
Beck R, Krause M (2005) Revised equipartition and minimum energy formula for magnetic field strength estimates from radio synchrotron observations. Astronomische Nachrichten 326:414–427. https://doi.org/10.1002/asna.200510366
Beltrán MT, Estalella R, Anglada G, Rodríguez LF, Torrelles JM (2001) Radio spectral indices of the powering sources of outflows. Astron J 121:1556–1568. https://doi.org/10.1086/319394
Benedettini M, Molinari S, Testi L, Noriega-Crespo A (2004) Millimetre observations of the IRAS 18162–2048 outflow: evidence for cloud disruption around an intermediate-mass protostar. Mon Not R Astron Soc 347:295–306. https://doi.org/10.1111/j.1365-2966.2004.07212.x
Beuther H, Schilke P, Sridharan TK, Menten KM, Walmsley CM, Wyrowski F (2002) Massive molecular outflows. Astron Astrophys 383:892–904. https://doi.org/10.1051/0004-6361:20011808
Bieging JH, Cohen M (1985) Multifrequency radio images of L1551 IRS 5. Astrophys J 289:L5–L8. https://doi.org/10.1086/184423
Bjerkeli P, van der Wiel MHD, Harsono D, Ramsey JP, Jørgensen JK (2016) Resolved images of a protostellar outflow driven by an extended disk wind. Nature 540:406–409. https://doi.org/10.1038/nature20600

Bontemps S, Andre P, Terebey S, Cabrit S (1996) Evolution of outflow activity around low-mass embedded young stellar objects. Astron Astrophys 311:858–872
Bosch-Ramon V, Romero GE, Araudo AT, Paredes JM (2010) Massive protostars as gamma-ray sources. Astron Astrophys 511:A8. https://doi.org/10.1051/0004-6361/200913488
Bourke TL, Crapsi A, Myers PC, Evans NJ II, Wilner DJ, Huard TL, Jørgensen JK, Young CH (2005) Discovery of a low-mass bipolar molecular outflow from L1014-IRS with the submillimeter array. Astrophys J 633:L129–L132. https://doi.org/10.1086/498449
Brentjens MA, de Bruyn AG (2005) Faraday rotation measure synthesis. Astron Astrophys 441:1217–1228. https://doi.org/10.1051/0004-6361:20052990
Brooks KJ, Garay G, Mardones D, Bronfman L (2003) A parsec-scale flow associated with the IRAS 16547–4247 radio jet. Astrophys J 594:L131–L134. https://doi.org/10.1086/378626
Brown A, Drake SA, Mundt R (1985) Radio continuum emission from premain sequence stars and associated structures. Radio Stars 116:105–110. https://doi.org/10.1007/978-94-009-5420-5_15
Butner HM, Evans NJ II, Harvey PM, Mundy LG, Natta A, Randich MS (1990) High-resolution, far-infrared observations of NGC 2071. Astrophys J 364:164–172. https://doi.org/10.1086/169398
Cabrit S (2007) The accretion-ejection connexion in T Tauri stars: jet models vs. observations. In: Bouvier J, Appenzeller I (eds) Star-Disk Interaction in Young Stars. IAU Symposium, vol 243, pp 203–214. https://doi.org/10.1017/S1743921307009568
Cabrit S, Bertout C (1992) CO line formation in bipolar flows. III. The energetics of molecular flows and ionized winds. Astron Astrophys 261:274–284
Cabrit S, Goldsmith PF, Snell RL (1988) Identification of RNO 43 and B335 as two highly collimated bipolar flows oriented nearly in the plane of the sky. Astrophys J 334:196–208. https://doi.org/10.1086/166830
Calvet N, Cantó J, Rodríguez LF (1983) Stellar winds and molecular clouds: T Tauri stars. Astrophys J 268:739–752. https://doi.org/10.1086/160996
Carrasco-González C, Anglada G, Rodríguez LF, Torrelles JM, Osorio M (2008a) Proper motions of thermal radio sources near HH 7–11 in the NGC 1333 star-forming region. Astron J 136:2238–2243. https://doi.org/10.1088/0004-6256/136/6/2238
Carrasco-González C, Anglada G, Rodríguez LF, Torrelles JM, Osorio M, Girart JM (2008b) A multiple system of radio sources at the core of the L723 multipolar outflow. Astrophys J 676:1073–1081
Carrasco-González C, Rodríguez LF, Torrelles JM, Anglada G, González-Martín O (2010a) A bright radio HH object with large proper motions in the massive star-forming region W75N. Astron J 139:2433–2439. https://doi.org/10.1088/0004-6256/139/6/2433
Carrasco-González C, Rodríguez LF, Anglada G, Martí J, Torrelles JM, Osorio M (2010b) A magnetized jet from a massive protostar. Science 330:1209. https://doi.org/10.1126/science.1195589
Carrasco-González C, Osorio M, Anglada G, D'Alessio P, Rodríguez LF, Gómez JF, Torrelles JM (2012a) Multiplicity, disks, and jets in the NGC 2071 star-forming region. Astrophys J 746:71. https://doi.org/10.1088/0004-637X/746/1/71
Carrasco-González C, Galván-Madrid R, Anglada G, Osorio M, D'Alessio P, Hofner P, Rodríguez LF, Linz H, Araya ED (2012b) Resolving the circumstellar disk around the massive protostar driving the HH 80–81 jet. Astrophys J 752:L29. https://doi.org/10.1088/2041-8205/752/2/L29
Carrasco-González C, Torrelles JM, Cantó J, Curiel S, Surcis G, Vlemmings WHT, van Langevelde HJ, Goddi C, Anglada G, Kim S-W, Kim J-S, Gómez JF (2015) Observing the onset of outflow collimation in a massive protostar. Science 348:114–117. https://doi.org/10.1126/science.aaa7216
Cécere M, Velázquez PF, Araudo AT, De Colle F, Esquivel A, Carrasco-González C, Rodríguez LF (2016) A study of radio polarization in protostellar jets. Astrophys J 816:64. https://doi.org/10.3847/0004-637X/816/2/64
Cernicharo J, Reipurth B (1996) Herbig-Haro Jets, CO Flows, and CO Bullets: The Case of HH 111. Astrophys J 460:L57. https://doi.org/10.1086/309967
Cesaroni R, Hofner P, Araya E, Kurtz S (2010) The structure of hot molecular cores over 1000 AU. Astron Astrophys 509:A50. https://doi.org/10.1051/0004-6361/200912877
Cesaroni R, Beltrán MT, Zhang Q, Beuther H, Fallscheer C (2011) Dissecting a hot molecular core: the case of G31.41+0.31. Astron Astrophys 533:A73. https://doi.org/10.1051/0004-6361/201117206
Chandler CJ, Brogan CL, Shirley YL, Loinard L (2005) IRAS 16293–2422: proper motions, jet precession, the hot core, and the unambiguous detection of infall. Astrophys J 632:371–396. https://doi.org/10.1086/432828

Chen H, Zhao J-H, Ohashi N (1995) Dust emission from L1641N: an optically thick circumstellar disk? Astrophys J 450:L71. https://doi.org/10.1086/316773
Chen H-R, Su Y-N, Liu S-Y, Hunter TR, Wilner DJ, Zhang Q, Lim J, Ho PTP, Ohashi N, Hirano N (2007) 654 GHz Continuum and $C^{18}O$(6–5) Observations of G240.31+0.07 with the Submillimeter Array. Astrophys J 654:L87–L90. https://doi.org/10.1086/510715
Chen X, Arce HG, Zhang Q, Launhardt R, Henning T (2016) Rotating bullets from a variable protostar. Astrophys J 824:72. https://doi.org/10.3847/0004-637X/824/2/72
Chernin LM, Masson CR (1991) A nearly unipolar CO outflow from the HH 46–47 system. Astrophys J 382:L93–L96. https://doi.org/10.1086/186220
Chernin LM, Masson CR (1995) Powerful jets and weak outflows: HH 1–2 and HH 34. Astrophys J 443:181–186. https://doi.org/10.1086/175512
Chiang H-F, Reipurth B, Walawender J, Connelley MS, Pessev P, Geballe TR, Best WMJ, Paegert M (2015) The Brightening of Re50N: Accretion Event or Dust Clearing? Astrophys J 805:54. https://doi.org/10.1088/0004-637X/805/1/54
Ching T-C, Lai S-P, Zhang Q, Yang L, Girart JM, Rao R (2016) Helical magnetic fields in the NGC 1333 IRAS 4A protostellar outflows. Astrophys J 819:159. https://doi.org/10.3847/0004-637X/819/2/159
Choi M, Kang M, Tatematsu K (2011) Rotation of the NGC 1333 IRAS 4A2 protostellar jet. Astrophys J 728:L34. https://doi.org/10.1088/2041-8205/728/2/L34
Choi M, Lee J-E, Kang M (2014) Radio variability survey of very low luminosity protostars. Astrophys J 789:8. https://doi.org/10.1088/0004-637X/789/1/9
Chrysostomou A, Bacciotti F, Nisini B, Ray TP, Eislöffel J, Davis CJ, Takami M (2008) Investigating the transport of angular momentum from young stellar objects. Do H2 jets from class I YSOs rotate? Astron Astrophys 482:575–583. https://doi.org/10.1051/0004-6361:20078494
Claussen MJ, Gaume RA, Johnston KJ, Wilson TL (1994) The W3 IRS 5 cluster: radio continuum and water maser observations. Astrophys J 424:L41–L44. https://doi.org/10.1086/187270
Codella C, Beltrán MT, Cesaroni R, Moscadelli L, Neri R, Vasta M, Zhang Q (2013) SiO collimated outflows driven by high-mass YSOs in G24.78+0.08. Astron Astrophys 550:A81. https://doi.org/10.1051/0004-6361/201219900
Coffey D, Bacciotti F, Woitas J, Ray TP, Eislöffel J (2004) Rotation of jets from young stars: new clues from the Hubble Space Telescope imaging spectrograph. Astrophys J 604:758–765. https://doi.org/10.1086/382019
Coffey D, Bacciotti F, Ray TP, Eislöffel J, Woitas J (2007) Further indications of jet rotation in new ultraviolet and optical Hubble Space Telescope STIS spectra. Astrophys J 663:350–364. https://doi.org/10.1086/518100
Coffey D, Dougados C, Cabrit S, Pety J, Bacciotti F (2015) A search for consistent jet and disk rotation signatures in RY Tau. Astrophys J 804:2. https://doi.org/10.1088/0004-637X/804/1/2
Cohen M (1983) HL Tauri and its circumstellar disk. Astrophys J 270:L69–L71. https://doi.org/10.1086/184072
Cohen M, Bieging JH (1986) Radio variability and structure of T Tauri stars. Astron J 92:1396–1402. https://doi.org/10.1086/114273
Cohen M, Schwartz RD (1987) IRAS observations of the exciting stars of Herbig–Haro objects. Astrophys J 316:311–314. https://doi.org/10.1086/165203
Cohen M, Bieging JH, Schwartz PR (1982) VLA observations of mass loss from T Tauri stars. Astrophys J 253:707–715. https://doi.org/10.1086/159671
Connelley MS, Greene TP (2014) Near-IR spectroscopic monitoring of class I protostars: variability of accretion and wind indicators. Astron J 147:125. https://doi.org/10.1088/0004-6256/147/6/125
Correia JC, Griffin M, Saraceno P (1997) High resolution observations of molecular outflows in the HH 1–2 region. Astron Astrophys 322:L25–L28
Cotera AS, Whitney BA, Young E, Wolff MJ, Wood K, Povich M, Schneider G, Rieke M, Thompson R (2001) High-resolution near-infrared images and models of the circumstellar disk in HH 30. Astrophys J 556:958–969. https://doi.org/10.1086/321627
Coughlan CP, Ainsworth RE, Eislöffel J, Hoeft M, Drabent A, Scaife AMM, Ray TP, Bell ME, Broderick JW, Corbel S, Grießmeier J-M, van der Horst AJ, van Leeuwen J, Markoff S, Pietka M, Stewart AJ, Wijers RAMJ, Zarka P (2017) A LOFAR Detection of the Low-mass Young Star T Tau at 149 MHz. Astrophys J 834:206. https://doi.org/10.3847/1538-4357/834/2/206
Curiel S (1995) Radio continuum observations of Herbig–Haro objects. Rev Mex Astron Astrof Ser Conf 1:59

Curiel S, Canto J, Rodriguez LF (1987) A model for the thermal radio continuum emission produced by a shock wave and its application to the Herbig–Haro objects 1 and 2. Rev Mex Astron Astrof 14:595–602
Curiel S, Rodriguez LF, Bohigas J, Roth M, Canto J, Torrelles JM (1989) Extended radio continuum emission associated with V645 Cyg and MWC1080. Astrophys Lett Commun 27:299–309
Curiel S, Raymond JC, Moran JM, Rodriguez LF, Canto J (1990) The exciting source of the bipolar outflow in L1448. Astrophys J 365:L85–L88. https://doi.org/10.1086/185894
Curiel S, Rodriguez LF, Moran JM, Canto J (1993) The triple radio continuum source in Serpens: the birth of a Herbig–Haro system? Astrophys J 415:191–203. https://doi.org/10.1086/173155
Curiel S, Girart JM, Rodríguez LF, Cantó J (2003) Very large array observations of proper motions in YLW 15. Astrophys J 582:L109–L113. https://doi.org/10.1086/367631
Curiel S, Girart JM, Rodríguez LF, Cantó J (2004) VLA observations of orbital motions in YLW 15. Rev Mex Astron Astrof 21:137–138
Curiel S, Ho PTP, Patel NA, Torrelles JM, Rodríguez LF, Trinidad MA, Cantó J, Hernández L, Gómez JF, Garay G, Anglada G (2006) Large proper motions in the jet of the high-mass YSO Cepheus A HW2. Astrophys J 638:878–886. https://doi.org/10.1086/498931
De Colle F, Cerqueira AH, Riera A (2016) Transverse velocity shifts in protostellar jets: rotation or velocity asymmetries? Astrophys J 832:152. https://doi.org/10.3847/0004-637X/832/2/152
Devine D, Bally J, Reipurth B, Shepherd D, Watson A (1999) A giant Herbig–Haro flow from a massive young star in G192.16−3.82. Astron J 117:2919–2930. https://doi.org/10.1086/300871
DeWarf LE, Sepinsky JF, Guinan EF, Ribas I, Nadalin I (2003) Intrinsic Properties of the Young Stellar Object SU Aurigae. Astrophys J 590:357–367. https://doi.org/10.1086/374979
Doppmann GW, Najita JR, Carr JS (2008) Stellar and circumstellar properties of the pre-main-sequence binary GV Tau from infrared spectroscopy. Astrophys J 685:298–312. https://doi.org/10.1086/590328
Downes TP, Cabrit S (2007) Jet-driven molecular outflows from class 0 sources: younger and stronger than they seem? Astron Astrophys 471:873–884. https://doi.org/10.1051/0004-6361:20066921
Dunham MM, Crapsi A, Evans NJ II, Bourke NJ II, Bourke TL, Huard TL, Myers PC, Kauffmann J (2008) Identifying the low-luminosity population of embedded protostars in the c2d observations of clouds and cores. Astrophys J Suppl Ser 179:249–282. https://doi.org/10.1086/591085
Dunham MM, Arce HG, Mardones D, Lee J-E, Matthews BC, Stutz AM, Williams JP (2014) Molecular outflows driven by low-mass protostars. I. Correcting for underestimates when measuring outflow masses and dynamical properties. Astrophys J 783:29. https://doi.org/10.1088/0004-637X/783/1/29
Dzib S, Loinard L, Mioduszewski AJ, Boden AF, Rodríguez LF, Torres RM (2010) VLBA determination of the distance to nearby star-forming regions. IV. A preliminary distance to the proto-Herbig AeBe Star EC 95 in the Serpens core. Astrophys J 718:610–619. https://doi.org/10.1088/0004-637X/718/2/610
Dzib S, Loinard L, Rodríguez LF, Mioduszewski AJ, Torres RM (2011) VLBA Determination of the Distance to Nearby Star-forming Regions. VI. The Distance to the Young Stellar Object HW 9 in Cepheus A. Astrophys J 733:71. https://doi.org/10.1088/0004-637X/733/1/71
Dzib SA, Loinard L, Mioduszewski AJ, Rodríguez LF, Ortiz-León GN, Pech G, Rivera JL, Torres RM, Boden AF, Hartmann L, Evans NJ II, Briceño C, Tobin J (2013) The Gould's belt Very Large Array survey. I. The Ophiuchus complex. Astrophys J 775:63. https://doi.org/10.1088/0004-637X/775/1/63
Dzib SA, Ortiz-León GN, Loinard L, Mioduszewski AJ, Rodríguez LF, Torres RM, Deller A (2016) VLBA determination of the distance to nearby star-forming regions. VII. Monoceros R2. Astrophys J 826:201. https://doi.org/10.3847/0004-637X/826/2/201
Edwards S, Snell RL (1982) A search for high-velocity molecular gas around T Tauri stars. Astrophys J 261:151–160. https://doi.org/10.1086/160326
Edwards S, Snell RL (1984) A survey of high-velocity molecular gas near Herbig–Haro objects. II. Astrophys J 281:237–249. https://doi.org/10.1086/162093
Ellerbroek LE, Podio L, Dougados C, Cabrit S, Sitko ML, Sana H, Kaper L, de Koter A, Klaassen PD, Mulders GD, Mendigutía I, Grady CA, Grankin K, van Winckel H, Bacciotti F, Russell RW, Lynch DK, Hammel HB, Beerman LC, Day AN, Huelsman DM, Werren C, Henden A, Grindlay J (2014) Relating jet structure to photometric variability: the Herbig Ae star HD 163296. Astron Astrophys 563:A87. https://doi.org/10.1051/0004-6361/201323092
Estalella R, Anglada G, Rodriguez LF, Garay G (1991) Multifrequency VLA observations of radio continuum from IRAS 16293–2422. Astrophys J 371:626–630. https://doi.org/10.1086/169927

Estalella R, López R, Anglada G, Gómez G, Riera A, Carrasco-González C (2012) The counterjet of HH 30: new light on its binary driving source. Astron J 144:61. https://doi.org/10.1088/0004-6256/144/2/61

Evans NJ II, Levreault RM, Harvey PM (1986) Far-infrared photometry of low-mass pre-main-sequence stars with broad CO wings. Astrophys J 301:894–900. https://doi.org/10.1086/163954

Evans NJ II, Balkum S, Levreault RM, Hartmann L, Kenyon S (1994) Molecular outflows from FU Orionis stars. Astrophys J 424:793–799. https://doi.org/10.1086/173931

Feigelson ED, Montmerle T (1985) An extremely variable radio star in the rho Ophiuchi cloud. Astrophys J 289:L19–L23. https://doi.org/10.1086/184426

Feigelson ED, Carkner L, Wilking BA (1998) Circularly polarized radio emission from an X-ray protostar. Astrophys J 494:L215. https://doi.org/10.1086/311190

Fernández-López M, Girart JM, Curiel S, Gómez Y, Ho PTP, Patel N (2011) A Rotating Molecular Disk Toward IRAS 18162–2048, the Exciting Source of HH 80–81. Astron J 142:97. https://doi.org/10.1088/0004-6256/142/4/97

Fischer WJ, Megeath ST, Ali B, Tobin JJ, Osorio M, Allen LE, Kryukova E, Stanke T, Stutz AM, Bergin E, Calvet N, di Francesco J, Furlan E, Hartmann L, Henning T, Krause O, Manoj P, Maret S, Muzerolle J, Myers P, Neufeld D, Pontoppidan K, Poteet CA, Watson DM, Wilson T (2010) Herschel–PACS imaging of protostars in the HH 1–2 outflow complex. Astron Astrophys 518:L122. https://doi.org/10.1051/0004-6361/201014636

Forbrich J, Massi M, Ros E, Brunthaler A, Menten KM (2007) Searching for coronal radio emission from protostars using very-long-baseline interferometry. Astron Astrophys 469:985–992. https://doi.org/10.1051/0004-6361:20077113

Forbrich J, Rodríguez LF, Palau A, Zapata LA, Muzerolle J, Gutermuth RA (2015) Radio monitoring of the periodically variable IR source LRLL 54361: no direct correlation between the radio and IR emissions. Astrophys J 814:15. https://doi.org/10.1088/0004-637X/814/1/15

Frank A, Ray TP, Cabrit S, Hartigan P, Arce HG, Bacciotti F, Bally J, Benisty M, Eislöffel J, Güdel M, Lebedev S, Nisini B, Raga A (2014) Jets and outflows from star to cloud: observations confront theory. Protostars Planets VI:451–474. https://doi.org/10.2458/azu_uapress_9780816531240-ch020

Froebrich D (2005) Which are the youngest protostars? Determining properties of confirmed and candidate class 0 sources by broadband photometry. Astrophys J Suppl Ser 156:169–177. https://doi.org/10.1086/426441

Fukui Y (1989) Molecular outflows: their implications on protostellar evolution. In: Reipurth B (ed) Low mass star formation and pre-main-sequence objects. ESO Conference and Workshop Proceedings, vol 33, pp 95–117

Fukui Y, Takaba H, Iwata T, Mizuno A (1988) A bipolar outflow: L1641-north and its ambient dense cloud. Astrophys J 325:L13–L15. https://doi.org/10.1086/185099

Furlan E, Fischer WJ, Ali B, Stutz AM, Stanke T, Tobin JJ, Megeath ST, Osorio M, Hartmann L, Calvet N, Poteet CA, Booker J, Manoj P, Watson DM, Allen L (2016) The Herschel Orion Protostar Survey: spectral energy distributions and fits using a grid of protostellar models. Astrophys J Suppl Ser 224:5. https://doi.org/10.3847/0067-0049/224/1/5

Furuya RS, Kitamura Y, Wootten A, Claussen MJ, Kawabe R (2003) Water maser survey toward low-mass young stellar objects in the northern sky with the Nobeyama 45 meter telescope and the Very Large Array. Astrophys J Suppl Ser 144:71–134. https://doi.org/10.1086/342749

Galván-Madrid R, Rodríguez LF, Liu HB, Costigan G, Palau A, Zapata LA, Loinard L (2015) Pre- and post-burst radio observations of the class 0 protostar HOPS 383 in Orion. Astrophys J 806:L32. https://doi.org/10.1088/2041-8205/806/2/L32

Garay G, Ramirez S, Rodriguez LF, Curiel S, Torrelles JM (1996) The nature of the radio sources within the Cepheus A star-forming region. Astrophys J 459:193. https://doi.org/10.1086/176882

Garay G, Brooks KJ, Mardones D, Norris RP (2003) A triple radio continuum source associated with IRAS 16547–4247: a collimated stellar wind emanating from a massive protostar. Astrophys J 587:739–747. https://doi.org/10.1086/368310

Girart JM, Curiel S, Raymond J, Rodriguez LF, Canto J (1996a) Matching-beam 2 and 6 cm radio continuum observations in molecular and optical outflows. In: Taylor AR, Paredes JM (eds) Radio emission from the stars and the Sun. Astronomical Society of the Pacific Conference Series, vol 93, p 38

Girart JM, Curiel S, Raymond J, Rodriguez LF, Canto J (1996b) High angular resolution radio continuum observations in molecular and optical outflows. In: Taylor AR, Paredes JM (eds) Radio emission from the stars and the Sun. Astronomical Society of the Pacific Conference Series, vol 93, p 41

Girart JM, Rodríguez LF, Curiel S (2000) A subarcsecond binary radio source associated with the X-ray-emitting young stellar object YLW 15. Astrophys J 544:L153–L156. https://doi.org/10.1086/317302
Girart JM, Curiel S, Rodríguez LF, Cantó J (2002) Radio continuum observations towards optical and molecular outflows. Rev Mex Astron Astrof 38:169–186
Girart JM, Curiel S, Rodríguez LF, Honda M, Cantó J, Okamoto YK, Sako S (2004) On the evolutionary state of the components of the YLW 15 binary system. Astron J 127:2969–2977. https://doi.org/10.1086/383551
Goldsmith PF, Snell RL, Hemeon-Heyer M, Langer WD (1984) Bipolar outflows in dark clouds. Astrophys J 286:599–608. https://doi.org/10.1086/162635
Gómez JF, Curiel S, Torrelles JM, Rodríguez LF, Anglada G, Girart JM (1994) The molecular core and the powering source of the bipolar molecular outflow in NGC 2264G. Astrophys J 436:749–753. https://doi.org/10.1086/174948
Gómez JF, Sargent AI, Torrelles JM, Ho PTP, Rodríguez LF, Cantó J, Garay G (1999) Disk and outflow in Cepheus A-HW2: interferometric SiO and HCO^+ observations. Astrophys J 514:287–295. https://doi.org/10.1086/306916
Gómez Y, Rodríguez LF, Garay G (2000) A cluster of radio sources near GGD 14. Astrophys J 531:861–867. https://doi.org/10.1086/308496
Gómez Y, Rodríguez LF, Garay G (2002) The nature of the cluster of radio sources in GGD 14. Astrophys J 571:901–905. https://doi.org/10.1086/340067
Gómez L, Rodríguez LF, Loinard L (2013) A one-sided knot ejection at the core of the HH 111 outflow. Rev Mex Astron Astrof 49:79–85
González RF, Cantó J (2002) Radio-continuum emission from shocked stellar winds in low-mass stars. Astrophys J 580:459–467. https://doi.org/10.1086/343037
Gordon MA (1969) 94-α recombination lines in Orion B. Bull Am Astron Soc 1:190
Gordon MA (1994) The nature of the radio recombination line emission from MWC 349A. Astrophys J 421:314–317. https://doi.org/10.1086/173649
Gradshteyn IS, Ryzhik IM (1994) Table of integrals, series and products, 5th edn. Academic Press, New York
Gueth F, Guilloteau S (1999) The jet-driven molecular outflow of HH 211. Astron Astrophys 343:571–584
Guidi G, Tazzari M, Testi L, de Gregorio-Monsalvo I, Chandler CJ, Pérez L, Isella A, Natta A, Ortolani S, Henning T, Corder S, Linz H, Andrews S, Wilner D, Ricci L, Carpenter J, Sargent A, Mundy L, Storm S, Calvet N, Dullemond C, Greaves J, Lazio J, Deller A, Kwon W (2016) Dust properties across the CO snowline in the HD 163296 disk from ALMA and VLA observations. Astron Astrophys 588:A112. https://doi.org/10.1051/0004-6361/201527516
Guzmán AE, Garay G, Brooks KJ, Rathborne J, Güsten R (2011) A hot molecular outflow driven by the ionized jet associated with IRAS 16562–3959. Astrophys J 736:150. https://doi.org/10.1088/0004-637X/736/2/150
Guzmán AE, Garay G, Brooks KJ, Voronkov MA (2012) Search for ionized jets toward high-mass young stellar objects. Astrophys J 753:51. https://doi.org/10.1088/0004-637X/753/1/51
Guzmán AE, Garay G, Rodríguez LF, Moran J, Brooks KJ, Bronfman L, Nyman L-Å, Sanhueza P, Mardones D (2014) The slow ionized wind and rotating disklike system that are associated with the high-mass young stellar object G345.4938+01.4677. Astrophys J 796:117. https://doi.org/10.1088/0004-637X/796/2/117
Haikala LK, Laureijs RJ (1989) CO and IR in L 1228: extended bipolar molecular outflow and strongly self-absorbed ^{12}CO emission. Astron Astrophys 223:287–292
Hara C, Shimajiri Y, Tsukagoshi T, Kurono Y, Saigo K, Nakamura F, Saito M, Wilner D, Kawabe R (2013) The rotating outflow, envelope, and disk of the class-0/I protostar [BHB2007]#11 in the Pipe Nebula. Astrophys J 771:128. https://doi.org/10.1088/0004-637X/771/2/128
Hartigan P, Morse JA, Raymond J (1994) Mass-loss rates, ionization fractions, shock velocities, and magnetic fields of stellar jets. Astrophys J 436:125–143. https://doi.org/10.1086/174887
Harvey PM, Wilking BA, Joy M (1984) Infrared observations of dust cloud structure in young R associations: NGC 1333 S68, and NGC 7129. Astrophys J 278:156–169. https://doi.org/10.1086/161777
Harvey PM, Wilking BA, Joy M, Lester DF (1985) An infrared study of the bipolar outflow region GGD 12–15. Astrophys J 288:725–730. https://doi.org/10.1086/162839
Hasegawa TI, Mitchell GF (1995) CO J = 3–2 and HCO + J = 4–3 observations of the GL 2591 molecular outflow. Astrophys J 451:225. https://doi.org/10.1086/176214

Hasegawa TI, Mitchell GF, Matthews HE, Tacconi L (1994) Submillimeter observations of CO in the W3 core. Astrophys J 426:215–233. https://doi.org/10.1086/174056
Heathcote S, Reipurth B, Raga AC (1998) Structure, excitation, and kinematics of the luminous Herbig–Haro objects 80/81. Astron J 116:1940–1960. https://doi.org/10.1086/300548
Herbig GH, Jones BF (1981) Large proper motions of the Herbig–Haro objects HH 1 and HH 2. Astron J 86:1232–1244. https://doi.org/10.1086/113003
Hirano N, Liu S-Y, Shang H, Ho PTP, Huang H-C, Kuan Y-J, McCaughrean MJ, Zhang Q (2006) SiO J = 5–4 in the HH 211 protostellar jet imaged with the Submillimeter Array. Astrophys J 636:L141–L144. https://doi.org/10.1086/500201
Hirota T, Bushimata T, Choi YK, Honma M, Imai H, Iwadate K, Jike T, Kameya O, Kamohara R, Kan-Ya Y, Kawaguchi N, Kijima M, Kobayashi H, Kuji S, Kurayama T, Manabe S, Miyaji T, Nagayama T, Nakagawa A, Oh CS, Omodaka T, Oyama T, Sakai S, Sasao T, Sato K, Shibata KM, Tamura Y, Yamashita K (2008) Astrometry of H_2O masers in nearby star-forming regions with VERA. II. SVS13 in NGC1333. Publ Astron Soc Jpn 60:37–44. https://doi.org/10.1093/pasj/60.1.37
Hirota T, Honma M, Imai H, Sunada K, Ueno Y, Kobayashi H, Kawaguchi N (2011) Astrometry of H_2O masers in nearby star-forming regions with VERA. IV. L 1448 C. Publ Astron Soc Jpn 63:1–8. https://doi.org/10.1093/pasj/63.1.1
Hoare MG (2006) An equatorial wind from the massive young stellar object S140 IRS 1. Astrophys J 649:856–861. https://doi.org/10.1086/506961
Hoare MG, Drew JE, Muxlow TB, Davis RJ (1994) Mapping the radio emission from massive young stellar objects. Astrophys J 421:L51–L54. https://doi.org/10.1086/187185
Hofner P, Cesaroni R, Rodríguez LF, Martí J (1999) A double system of ionized jets in IRAS 20126+4104. Astron Astrophys 345:L43–L46
Hofner P, Cesaroni R, Olmi L, Rodríguez LF, Martí J, Araya E (2007) Sub-arcsecond resolution radio continuum observations of IRAS 20126+4104. Astron Astrophys 465:197–205. https://doi.org/10.1051/0004-6361:20065770
Hofner P, Cesaroni R, Kurtz S, Rosero V, Anderson C, Furuya RS, Araya ED, Molinari S (2017) High-resolution observations of the massive protostar in IRAS 18566+0408. Astrophys J 843:99. https://doi.org/10.3847/1538-4357/aa7459
Hogerheijde MR, van Dishoeck EF, Blake GA, van Langevelde HJ (1998) Envelope structure on 700 AU scales and the molecular outflows of low-mass young stellar objects. Astrophys J 502:315–336. https://doi.org/10.1086/305885
Hughes VA (1988) Radio observations of Cepheus A. I. The evolving pre-main-sequence stars in Cepheus A East? Astrophys J 333:788–800. https://doi.org/10.1086/166787
Hughes VA, Cohen RJ, Garrington S (1995) High-resolution observations of Cepheus A. Mon Not R Astron Soc 272:469–480. https://doi.org/10.1093/mnras/272.2.469
Hunter TR, Taylor GB, Felli M, Tofani G (1994) Water masers embedded in ultracompact H II regions: the W 75N cloud core. Astron Astrophys 284:215–226
Hunter TR, Testi L, Taylor GB, Tofani G, Felli M, Phillips TG (1995) A multiwavelength picture of the AFGL 5142 star-forming region. Astron Astrophys 302:249
Hunter TR, Phillips TG, Menten KM (1997) Active star formation toward the ultracompact H II regions G45.12+0.13 and G45.07+0.13. Astrophys J 478:283–294. https://doi.org/10.1086/303775
Hunter TR, Brogan CL, MacLeod GC, Cyganowski CJ, Chibueze JO, Friesen R, Hirota T, Smits DP, Chandler CJ, Indebetouw R (2018) The extraordinary outburst in the massive protostellar system NGC6334I-MM1: emergence of strong 6.7 GHz methanol masers. Astrophys J 854:170. https://doi.org/10.3847/1538-4357/aaa962
Imai H, Kameya O, Sasao T, Miyoshi M, Deguchi S, Horiuchi S, Asaki Y (2000) Kinematics and distance of water masers in W3 IRS 5. Astrophys J 538:751–765. https://doi.org/10.1086/309165
Itoh Y, Kaifu N, Hayashi M, Hayashi SS, Yamashita T, Usuda T, Noumaru J, Maihara T, Iwamuro F, Motohara K, Taguchi T, Hata R (2000) A pair of twisted jets of ionized iron from L 1551 IRS 5. Publ Astron Soc Jpn 52:81. https://doi.org/10.1093/pasj/52.1.81
Jiménez-Serra I, Martín-Pintado J, Báez-Rubio A, Patel N, Thum C (2011) Extremely broad radio recombination maser lines toward the high-velocity ionized jet in Cepheus A HW2. Astrophys J 732:L27. https://doi.org/10.1088/2041-8205/732/2/L27
Jiménez-Serra I, Báez-Rubio A, Rivilla VM, Martín-Pintado J, Zhang Q, Dierickx M, Patel N (2013) A new radio recombination line maser object toward the MonR2 H II region. Astrophys J 764:L4. https://doi.org/10.1088/2041-8205/764/1/L4

Johnston KG, Shepherd DS, Robitaille TP, Wood K (2013) The standard model of low-mass star formation applied to massive stars: a multi-wavelength picture of AFGL 2591. Astron Astrophys 551:A43. https://doi.org/10.1051/0004-6361/201219657

Kauffmann J, Bertoldi F, Bourke TL, Myers PC, Lee CW, Huard TL (2011) Confirmation of the VeLLO L1148-IRS: star formation at very low (column) density. Mon Not R Astron Soc 416:2341–2358. https://doi.org/10.1111/j.1365-2966.2011.19205.x

Kounkel M, Hartmann L, Loinard L, Ortiz-León GN, Mioduszewski AJ, Rodríguez LF, Dzib SA, Torres RM, Pech G, Galli PAB, Rivera JL, Boden AF, Evans NJ II, Briceño C, Tobin JJ (2017) The Gould's belt distances survey (GOBELINS) II. Distances and structure toward the Orion Molecular Clouds. Astrophys J 834:142. https://doi.org/10.3847/1538-4357/834/2/142

Krist JE, Stapelfeldt KR, Hester JJ, Healy K, Dwyer SJ, Gardner CL (2008) A multi-epoch HST study of the Herbig-Haro flow from XZ Tauri. Astron J 136:1980–1994. https://doi.org/10.1088/0004-6256/136/5/1980

Kristensen LE, van Dishoeck EF, Bergin EA, Visser R, Yıldız UA, San Jose-Garcia I, Jørgensen JK, Herczeg GJ, Johnstone D, Wampfler SF, Benz AO, Bruderer S, Cabrit S, Caselli P, Doty SD, Harsono D, Herpin F, Hogerheijde MR, Karska A, van Kempen TA, Liseau R, Nisini B, Tafalla M, van der Tak F, Wyrowski F (2012) Water in star-forming regions with Herschel (WISH). II. Evolution of 557 GHz 1_{10}–1_{01} emission in low-mass protostars. Astron Astrophys 542:A8. https://doi.org/10.1051/0004-6361/201118146

Kun M, Prusti T (1993) Star formation in L 1251: distance and members. Astron Astrophys 272:235

Kurtz S, Churchwell E, Wood DOS (1994) Ultracompact H II regions. II. New high-resolution radio images. Astrophys J Suppl Ser 91:659–712. https://doi.org/10.1086/191952

Lada CJ (1991) The formation of low mass stars: observations. In: Lada CJ, Kylafis ND (eds) The Physics of Star Formation and Early Stellar Evolution. NATO ASI Series C, vol 342, p 329

Ladd EF, Adams FC, Casey S, Davidson JA, Fuller GA, Harper DA, Myers PC, Padman R (1991) Far-infrared and submillimeter-wavelength observations of star-forming dense cores. I. Spectra. Astrophys J 366:203–220. https://doi.org/10.1086/169553

Launhardt R, Pavlyuchenkov Y, Gueth F, Chen X, Dutrey A, Guilloteau S, Henning T, Piétu V, Schreyer K, Semenov D (2009) Rotating molecular outflows: the young T Tauri star in CB 26. Astron Astrophys 494:147–156. https://doi.org/10.1051/0004-6361:200810835

Lee C-F (2010) A Change of Rotation Profile in the Envelope in the HH 111 Protostellar System: A Transition to a Disk? Astrophys J 725:712–720. https://doi.org/10.1088/0004-637X/725/1/712

Lee C-F, Hirano N, Palau A, Ho PTP, Bourke TL, Zhang Q, Shang H (2009) Rotation and outflow motions in the very low-mass class 0 protostellar system HH 211 at subarcsecond resolution. Astrophys J 699:1584–1594. https://doi.org/10.1088/0004-637X/699/2/1584

Levreault RM (1984) Interactions between pre-main-sequence objects and molecular clouds. II. PV Cephei. Astrophys J 277:634–639. https://doi.org/10.1086/161734

Levreault RM (1988) A search for molecular outflows toward the pre-main-sequence objects. Astrophys J Suppl Ser 67:283–371. https://doi.org/10.1086/191275

Lim J, Takakuwa S (2006) Properties and formation of the multiple protostellar system L1551 IRS 5. Astrophys J 653:425–436. https://doi.org/10.1086/508510

Lim J, Hanawa T, Yeung PKH, Takakuwa S, Matsumoto T, Saigo K (2016) Formation of the unequal-mass binary protostars in L1551NE by rotationally driven fragmentation. Astrophys J 831:90. https://doi.org/10.3847/0004-637X/831/1/90

Liseau R, Fridlund CVM, Larsson B (2005) Physics of Outflows: The Binary Protostar L1551 IRS 5 and its Jets. Astrophys J 619:959–967. https://doi.org/10.1086/426783

Little LT, Heaton BD, Dent WRF (1990) The outflow and compact core of the molecular cloud GGD 12–15. Astron Astrophys 232:173–183

Liu HB, Ho PTP, Zhang Q (2010) The high-velocity molecular outflows in massive cluster-forming region G10.6−0.4. Astrophys J 725:2190–2208. https://doi.org/10.1088/0004-637X/725/2/2190

Loinard L, Rodríguez LF, D'Alessio P, Wilner DJ, Ho PTP (2002) Orbital proper motions in the protobinary system L1527/IRAS 04368+2557? Astrophys J 581:L109–L113. https://doi.org/10.1086/345940

Loinard L, Rodríguez LF, Gómez L, Cantó J, Raga AC, Goodman AA, Arce HG (2010) A reassessment of the kinematics of PV Cephei based on accurate proper motion measurements. Rev Mex Astron Astrof 46:375–383

Lugo J, Lizano S, Garay G (2004) Photoevaporated disks around massive young stars. Astrophys J 614:807–817. https://doi.org/10.1086/423924

Lyutikov M, Pariev VI, Gabuzda DC (2005) Polarization and structure of relativistic parsec-scale AGN jets. Mon Not R Astron Soc 360:869–891. https://doi.org/10.1111/j.1365-2966.2005.08954.x
Macías E, Anglada G, Osorio M, Calvet N, Torrelles JM, Gómez JF, Espaillat C, Lizano S, Rodríguez LF, Carrasco-González C, Zapata L (2016) Imaging the photoevaporating disk and radio jet of GM Aur. Astrophys J 829:1. https://doi.org/10.3847/0004-637X/829/1/1
Maheswar G, Lee CW, Dib S (2011) Distances to dense cores that contain very low luminosity objects. Astron Astrophys 536:A99. https://doi.org/10.1051/0004-6361/201116438
Margulis M, Lada CJ, Snell RL (1988) Molecular outflows in the Monoceros OB1 molecular cloud. Astrophys J 333:316–331. https://doi.org/10.1086/166748
Marti J, Rodriguez LF, Reipurth B (1993) HH 80–81: a highly collimated Herbig-Haro complex powered by a massive young star. Astrophys J 416:208. https://doi.org/10.1086/173227
Marti J, Rodriguez LF, Reipurth B (1995) Large proper motions and ejection of new condensations in the HH 80–81 thermal radio jet. Astrophys J 449:184. https://doi.org/10.1086/176044
Martí J, Rodríguez LF, Reipurth B (1998) Proper motions of the inner condensations in the HH 80–81 thermal radio jet. Astrophys J 502:337–341. https://doi.org/10.1086/305900
Martin-Pintado J, Bachiller R, Thum C, Walmsley M (1989) A radio recombination line maser in MWC349. Astron Astrophys 215:L13–L16
Masqué JM, Girart JM, Estalella R, Rodríguez LF, Beltrán MT (2012) Centimeter continuum observations of the northern head of the HH 80/81/80N jet: revising the actual dimensions of a parsec-scale jet. Astrophys J 758:L10. https://doi.org/10.1088/2041-8205/758/1/L10
Masqué JM, Rodríguez LF, Araudo A, Estalella R, Carrasco-González C, Anglada G, Girart JM, Osorio M (2015) Proper motions of the outer knots of the HH 80/81/80N radio-jet. Astrophys J 814:44. https://doi.org/10.1088/0004-637X/814/1/44
Maud LT, Moore TJT, Lumsden SL, Mottram JC, Urquhart JS, Hoare MG (2015) A distance-limited sample of massive molecular outflows. Mon Not R Astron Soc 453:645–665. https://doi.org/10.1093/mnras/stv1635
Mayen-Gijon JM (2015) Kinematic study of the molecular environment in the early phases of massive star formation: ammonia observations and modeling. PhD Thesis, University of Granada
Menten KM, Reid MJ, Forbrich J, Brunthaler A (2007) The distance to the Orion Nebula. Astron Astrophys 474:515–520. https://doi.org/10.1051/0004-6361:20078247
Mezger PG, Henderson AP (1967) Galactic H II regions. I. Observations of their continuum radiation at the frequency 5 GHz. Astrophys J 147:471. https://doi.org/10.1086/149030
Mezger PG, Hoglund B (1967) Galactic H II regions. II. Observations of their hydrogen 109α recombination-line radiation at the frequency 5009 MHz. Astrophys J 147:490. https://doi.org/10.1086/149031
Mitchell GF, Hasegawa TI, Dent WRF, Matthews HE (1994) A molecular outflow driven by an optical jet. Astrophys J 436:L177–L180. https://doi.org/10.1086/187661
Mizuno A, Fukui Y, Iwata T, Nozawa S, Takano T (1990) A remarkable multilobe molecular outflow: Rho Ophiuchi East, associated with IRAS 16293–2422. Astrophys J 356:184–194. https://doi.org/10.1086/168829
Molinari S, Brand J, Cesaroni R, Palla F (1996) A search for precursors of ultracompact HII regions in a sample of luminous IRAS sources. I. Association with ammonia cores. Astron Astrophys 308:573–587
Morata O, Palau A, González RF, de Gregorio-Monsalvo I, Ribas Á, Perger M, Bouy H, Barrado D, Eiroa C, Bayo A, Huélamo N, Morales-Calderón M, Rodríguez LF (2015) First detection of thermal radiojets in a sample of proto-brown dwarf candidates. Astrophys J 807:55. https://doi.org/10.1088/0004-637X/807/1/55
Morgan JA, Bally J (1991) Molecular outflows in the L1641 region of Orion. Astrophys J 372:505–517. https://doi.org/10.1086/169996
Morgan JA, Snell RL, Strom KM (1990) Radio continuum emission from young stellar objects in L1641. Astrophys J 362:274–283. https://doi.org/10.1086/169264
Morgan JA, Schloerb FP, Snell RL, Bally J (1991) Molecular outflows associated with young stellar objects in the L1641 region of Orion. Astrophys J 376:618–629. https://doi.org/10.1086/170310
Moriarty-Schieven GH, Snell RL (1989) High-resolution observations of the B335 and L723 bipolar molecular outflows. Astrophys J 338:952–962. https://doi.org/10.1086/167247
Moriarty-Schieven GH, Butner HM, Wannier PG (1995) The L1551NE molecular outflow. Astrophys J 445:L55–L58. https://doi.org/10.1086/187888
Moscadelli L, Sánchez-Monge Á, Goddi C, Li JJ, Sanna A, Cesaroni R, Pestalozzi M, Molinari S, Reid MJ (2016) Outflow structure within 1000 au of high-mass YSOs. I. First results from a combined study

of maser and radio continuum emission. Astron Astrophys 585:A71. https://doi.org/10.1051/0004-6361/201526238
Mozurkewich D, Schwartz PR, Smith HA (1986) Luminosities of sources associated with molecular outflows. Astrophys J 311:371–379. https://doi.org/10.1086/164778
Mundy LG, Wilking BA, Myers ST (1986) Resolution of structure in the protostellar source IRAS 16293–2422. Astrophys J 311:L75–L79. https://doi.org/10.1086/184801
Myers PC, Heyer M, Snell RL, Goldsmith PF (1988) Dense cores in dark clouds. V. CO outflow. Astrophys J 324:907–919. https://doi.org/10.1086/165948
Nisini B, Antoniucci S, Alcalá JM, Giannini T, Manara CF, Natta A, Fedele D, Biazzo K (2018) Connection between jets, winds and accretion in T Tauri stars. The X-shooter view. Astron Astrophys 609:A87. https://doi.org/10.1051/0004-6361/201730834
Osorio M, Anglada G, Lizano S, D'Alessio P (2009) Collapsing hot molecular cores: a model for the dust spectrum and ammonia line emission of the G31.41+0.31 hot core. Astrophys J 694:29–45. https://doi.org/10.1088/0004-637X/694/1/29
Osorio M, Díaz-Rodríguez AK, Anglada G, Megeath ST, Rodríguez LF, Tobin JJ, Stutz AM, Furlan E, Fischer WJ, Manoj P, Gómez JF, González-García B, Stanke T, Watson DM, Loinard L, Vavrek R, Carrasco-González C (2017) Star formation under the outflow: the discovery of a non-thermal jet from OMC-2 FIR 3 and its relationship to the deeply embedded FIR 4 protostar. Astrophys J 840:36. https://doi.org/10.3847/1538-4357/aa6975
Pacholczyk AG (1970) Radio astrophysics. Freeman, San Francisco
Padovani M, Hennebelle P, Marcowith A, Ferrière K (2015) Cosmic-ray acceleration in young protostars. Astron Astrophys 582:L13. https://doi.org/10.1051/0004-6361/201526874
Padovani M, Marcowith A, Hennebelle P, Ferrière K (2016) Protostars: forges of cosmic rays? Astron Astrophys 590:A8. https://doi.org/10.1051/0004-6361/201628221
Palau A, de Gregorio-Monsalvo I, Morata Ò, Stamatellos D, Huélamo N, Eiroa C, Bayo A, Morales-Calderón M, Bouy H, Ribas Á, Asmus D, Barrado D (2012) A search for pre-substellar cores and proto-brown dwarf candidates in Taurus: multiwavelength analysis in the B213–L1495 clouds. Mon Not R Astron Soc 424:2778–2791. https://doi.org/10.1111/j.1365-2966.2012.21390.x
Palau A, Zapata LA, Rodríguez LF, Bouy H, Barrado D, Morales-Calderón M, Myers PC, Chapman N, Juárez C, Li D (2014) IC 348-SMM2E: a class 0 proto-brown dwarf candidate forming as a scaled-down version of low-mass stars. Mon Not R Astron Soc 444:833–845. https://doi.org/10.1093/mnras/stu1461
Panoglou D, Cabrit S, Forêts Pineau Des (2012) Molecule survival in magnetized protostellar disk winds. I. Chemical model and first results. Astron Astrophys 538:A2. https://doi.org/10.1051/0004-6361/200912861
Parker ND (1991) Infrared properties of IRAS sources associated with nearby dark molecular clouds. Mon Not R Astron Soc 251:63–75. https://doi.org/10.1093/mnras/251.1.63
Parker ND, Padman R, Scott PF, Hills RE (1988) New bipolar outflows in dark molecular clouds. Mon Not R Astron Soc 234:67P–72P. https://doi.org/10.1093/mnras/234.1.67P
Patel NA, Curiel S, Sridharan TK, Zhang Q, Hunter TR, Ho PTP, Torrelles JM, Moran JM, Gómez JF, Anglada G (2005) A disk of dust and molecular gas around a high-mass protostar. Nature 437:109–111. https://doi.org/10.1038/nature04011
Pech G, Loinard L, Chandler CJ, Rodríguez LF, D'Alessio P, Brogan CL, Wilner DJ, Ho PTP (2010) Confirmation of a recent bipolar ejection in the very young hierarchical multiple system IRAS 16293–2422. Astrophys J 712:1403–1409. https://doi.org/10.1088/0004-637X/712/2/1403
Pech G, Zapata LA, Loinard L, Rodríguez LF (2012) A rotating molecular jet from a Perseus protostar. Astrophys J 751:78. https://doi.org/10.1088/0004-637X/751/1/78
Pesenti N, Dougados C, Cabrit S, Ferreira J, Casse F, Garcia P, O'Brien D (2004) Predicted rotation signatures in MHD disc winds and comparison to DG Tau observations. Astron Astrophys 416:L9–L12. https://doi.org/10.1051/0004-6361:20040033
Persi P, Tapia M, Smith HA (2006) Mid-infrared images of the massive star forming region W75 N. Astron Astrophys 445:971–978. https://doi.org/10.1051/0004-6361:20053251
Pety J, Gueth F, Guilloteau S, Dutrey A (2006) Plateau de Bure interferometer observations of the disk and outflow of HH 30. Astron Astrophys 458:841–854. https://doi.org/10.1051/0004-6361:20065814
Plunkett AL, Arce HG, Corder SA, Mardones D, Sargent AI, Schnee SL (2013) CARMA observations of protostellar outflows in NGC 1333. Astrophys J 774:22. https://doi.org/10.1088/0004-637X/774/1/22

Purser SJD, Lumsden SL, Hoare MG, Urquhart JS, Cunningham N, Purcell CR, Brooks KJ, Garay G, Gúzman AE, Voronkov MA (2016) A search for ionized jets towards massive young stellar objects. Mon Not R Astron Soc 460:1039–1053. https://doi.org/10.1093/mnras/stw1027

Pyo T-S, Hayashi M, Kobayashi N, Tokunaga AT, Terada H, Tsujimoto M, Hayashi SS, Usuda T, Yamashita T, Takami H, Takato N, Nedachi K (2005) Fast [Fe II] Wind with a Wide Opening Angle from L1551 IRS 5. Astrophys J 618:817–821. https://doi.org/10.1086/426103

Qin S-L, Wang J-J, Zhao G, Miller M, Zhao J-H (2008) Massive molecular outflows associated with UCHII/HII regions. Astron Astrophys 484:361–369. https://doi.org/10.1051/0004-6361:20078483

Quireza C, Rood RT, Balser DS, Bania TM (2006) Radio recombination lines in galactic H II regions. Astrophys J Suppl Ser 165:338–359. https://doi.org/10.1086/503901

Reid MJ, Menten KM, Greenhill LJ, Chandler CJ (2007) Imaging the ionized disk of the high-mass protostar Orion I. Astrophys J 664:950–955. https://doi.org/10.1086/518929

Reipurth B (1989) The HH111 jet and multiple outflow episodes from young stars. Nature 340:42–45. https://doi.org/10.1038/340042a0

Reipurth B, Bally J (1986) First light from a young star? Nature 320:336–338. https://doi.org/10.1038/320336a0

Reipurth B, Olberg M (1991) Herbig-Haro jets and molecular outflows in L1617. Astron Astrophys 246:535–550

Reipurth B, Chini R, Krugel E, Kreysa E, Sievers A (1993) Cold dust around Herbig-Haro energy sources: a 1300-μm survey. Astron Astrophys 273:221

Reipurth B, Rodríguez LF, Anglada G, Bally J (2002) Radio continuum maps of deeply embedded protostars: thermal jets, multiplicity, and variability. Astron J 124:1045–1053. https://doi.org/10.1086/341172

Reipurth B, Rodríguez LF, Anglada G, Bally J (2004) Radio continuum jets from protostellar objects. Astron J 127:1736–1746. https://doi.org/10.1086/381062

Reynolds SP (1986) Continuum spectra of collimated, ionized stellar winds. Astrophys J 304:713–720. https://doi.org/10.1086/164209

Rivilla VM, Chandler CJ, Sanz-Forcada J, Jiménez-Serra I, Forbrich J, Martín-Pintado J (2015) Short- and long-term radio variability of young stars in the Orion Nebula Cluster and Molecular Cloud. Astrophys J 808:146. https://doi.org/10.1088/0004-637X/808/2/146

Roccatagliata V, Ratzka T, Henning T, Wolf S, Leinert C, Bouwman J (2011) Multi-wavelength observations of the young binary system Haro 6–10: the case of misaligned discs. Astron Astrophys 534:A33. https://doi.org/10.1051/0004-6361/201116805

Rodriguez LF (1995) Subarcsecond observations of radio continuum from jets and disks. Rev Mex Astron Astrof Ser Conf 1:1

Rodriguez LF (1996) Thermal jets in star-forming regions: high-mass cases. Rev Mex Astron Astrof Ser Conf 4:7

Rodríguez LF (1997) Thermal radio jets. In: Reipurth B, Bertout C (eds) Herbig–Haro flows and the birth of stars. IAU Symposium, vol 182, pp 83–92

Rodríguez LF (2011) Radio observations of jets from massive young stars. In: Romero GE, Sunyaev RA, Belloni T (eds) Jets at all scales. IAU Symposium, vol 275, pp 367–373. https://doi.org/10.1017/S174392131001642X

Rodriguez LF, Bastian TS (1994) Rotation in the ionized envelope of MWC 349A. Astrophys J 428:324–328. https://doi.org/10.1086/174243

Rodríguez LF, Reipurth B (1989) Detection of radio continuum emission from the Herbig–Haro objects 80 and 81 and their suspected energy source. Rev Mex Astron Astrof 17:59–63

Rodriguez LF, Reipurth B (1994) The exciting source of the Herbig–Haro 111 jet complex: VLA detection of a one-sided radio jet. Astron Astrophys 281:882–888

Rodríguez LF, Reipurth B (1996) VLA detection of the exciting sources of HH 34, HH 114, and HH 199. Rev Mex Astron Astrof 32:27

Rodriguez LF, Reipurth B (1998) VLA detection of the exciting sources of HH 83, HH 117, HH 124, HH 192, HH 300, HH 366, and HH 375. Rev Mex Astron Astrof 34:13

Rodriguez LF, Ho PTP, Moran JM (1980a) Anisotropic mass outflow in Cepheus A. Astrophys J 240:L149–L152. https://doi.org/10.1086/183342

Rodríguez LF, Moran JM, Ho PTP, Gottlieb EW (1980b) Radio observations of water vapor, hydroxyl, silicon monoxide, ammonia, carbon monoxide, and compact H II regions in the vicinities of suspected Herbig-Haro objects. Astrophys J 235:845–865. https://doi.org/10.1086/157687

Rodriguez LF, Carral P, Ho PTP, Moran JM (1982) Anisotropic mass outflow in regions of star formation. Astrophys J 260:635–646. https://doi.org/10.1086/160285
Rodriguez LF, Canto J, Torrelles JM, Ho PTP (1986) The double radio source associated with L1551 IRS 5: binary system or ionized circumstellar torus? Astrophys J 301:L25–L28. https://doi.org/10.1086/184616
Rodriguez LF, Curiel S, Moran JM, Mirabel IF, Roth M, Garay G (1989a) Large proper motions in the remarkable triple radio source in Serpens. Astrophys J 346:L85–L88. https://doi.org/10.1086/185585
Rodriguez LF, Myers PC, Cruz-Gonzalez I, Terebey S (1989b) Radio continuum observations of IRAS sources associated with dense cores. Astrophys J 347:461–467. https://doi.org/10.1086/168134
Rodriguez LF, Ho PTP, Torrelles JM, Curiel S, Canto J (1990) VLA observations of the Herbig–Haro 1–2 system. Astrophys J 352:645–653. https://doi.org/10.1086/168567
Rodriguez LF, Canto J, Torrelles JM, Gomez JF, Anglada G, Ho PTP (1994a) Subarcsecond VLA maps of the disk and the jet in HL Tauri. Astrophys J 427:L103–L106. https://doi.org/10.1086/187375
Rodriguez LF, Garay G, Curiel S, Ramirez S, Torrelles JM, Gomez Y, Velazquez A (1994b) Cepheus A HW2: a powerful thermal radio jet. Astrophys J 430:L65–L68. https://doi.org/10.1086/187439
Rodriguez LF, Anglada G, Raga A (1995) Radio continuum detection of the exciting sources of the DG Tauri B and L1551NE outflows. Astrophys J 454:L149. https://doi.org/10.1086/309797
Rodríguez LF, Anglada G, Curiel S (1997) Is SVS 13 the exciting source of the HH 7–11 Flow? Astrophys J 480:L125–L128. https://doi.org/10.1086/310636
Rodríguez LF, D'Alessio P, Wilner DJ, Ho PTP, Torrelles JM, Curiel S, Gómez Y, Lizano S, Pedlar A, Cantó J, Raga AC (1998) Compact protoplanetary disks around the stars of a young binary system. Nature 395:355–357. https://doi.org/10.1038/26421
Rodríguez LF, Anglada G, Curiel S (1999) The nature of the radio continuum sources embedded in the HH 7–11 region and its surroundings. Astrophys J Suppl Ser 125:427–438. https://doi.org/10.1086/313283
Rodríguez LF, Delgado-Arellano VG, Gómez Y, Reipurth B, Torrelles JM, Noriega-Crespo A, Raga AC, Cantó J (2000) New VLA observations of the HH 1–2 region: evidence for density enhancements moving along the axis of the VLA 1 radio jet. Astron J 119:882–889. https://doi.org/10.1086/301231
Rodríguez LF, Curiel S, Cantó J, Loinard L, Raga AC, Torrelles JM (2003a) Very Large Array observations of proper motions in L1551 IRS 5. Astrophys J 583:330–333. https://doi.org/10.1086/344833
Rodríguez LF, Porras A, Claussen MJ, Curiel S, Wilner DJ, Ho PTP (2003b) The binary jet in L1551 IRS 5. Astrophys J 586:L137–L139. https://doi.org/10.1086/374882
Rodríguez LF, Garay G, Brooks KJ, Mardones D (2005) High angular resolution observations of the collimated jet source associated with a massive protostar in IRAS 16547–4247. Astrophys J 626:953–958. https://doi.org/10.1086/430268
Rodríguez LF, Moran JM, Franco-Hernández R, Garay G, Brooks KJ, Mardones D (2008) The collimated jet source in IRAS 16547–4247: time variation, possible precession, and upper limits to the proper motions along the jet axis. Astron J 135:2370–2379. https://doi.org/10.1088/0004-6256/135/6/2370
Rodríguez LF, Gómez Y, Loinard L, Mioduszewski AJ (2010) On the size of the non-thermal component in the radio emission from Cyg OB2 #5. Rev Mex Astron Astrof 46:215–219
Rodríguez LF, Dzib SA, Loinard L, Zapata LA, Raga AC, Cantó J, Riera A (2012a) Radio and optical observations of DG Tau B. Rev Mex Astron Astrof 48:243–249
Rodríguez LF, González RF, Raga AC, Cantó J, Riera A, Loinard L, Dzib SA, Zapata LA (2012b) Radio continuum emission from knots in the DG Tauri jet. Astron Astrophys 537:A123. https://doi.org/10.1051/0004-6361/201117991
Rodríguez LF, Zapata LA, Dzib SA, Ortiz-León GN, Loinard L, Macías E, Anglada G (2014a) An ionized outflow from AB Aur, a Herbig Ae star with a transitional disk. Astrophys J 793:L21. https://doi.org/10.1088/2041-8205/793/1/L21
Rodríguez LF, Zapata LA, Palau A (2014b) JVLA observations of IC 348 SW: compact radio sources and their nature. Astrophys J 790:80. https://doi.org/10.1088/0004-637X/790/1/80
Rodríguez LF, Zapata LA, Palau A (2017) JVLA observations of young brown dwarfs. Astron J 153:209. https://doi.org/10.3847/1538-3881/aa6681
Rodríguez-Kamenetzky A, Carrasco-González C, Araudo A, Torrelles JM, Anglada G, Martí J, Rodríguez LF, Valotto C (2016) Investigating particle acceleration in protostellar jets: the triple radio continuum source in Serpens. Astrophys J 818:27. https://doi.org/10.3847/0004-637X/818/1/27

Rodríguez-Kamenetzky A, Carrasco-González C, Araudo A, Romero GE, Torrelles JM, Rodríguez LF, Anglada G, Martí J, Perucho M, Valotto C (2017) The highly collimated radio jet of HH 80–81: structure and nonthermal emission. Astrophys J 851:16. https://doi.org/10.3847/1538-4357/aa9895

Rosero V, Hofner P, Claussen M, Kurtz S, Cesaroni R, Araya ED, Carrasco-González C, Rodríguez LF, Menten KM, Wyrowski F, Loinard L, Ellingsen SP (2016) Weak and compact radio emission in early high-mass star-forming regions. I. VLA observations. Astrophys J Suppl Ser 227:25. https://doi.org/10.3847/1538-4365/227/2/25

Rygl KLJ, Brunthaler A, Sanna A, Menten KM, Reid MJ, van Langevelde HJ, Honma M, Torstensson KJE, Fujisawa K (2012) Parallaxes and proper motions of interstellar masers toward the Cygnus X star-forming complex. I. Membership of the Cygnus X region. Astron Astrophys 539:A79. https://doi.org/10.1051/0004-6361/201118211

Sadavoy SI, Di Francesco J, André P, Pezzuto S, Bernard J-P, Maury A, Men'shchikov A, Motte F, Nguyễn-Lu'o'ng Q, Schneider N, Arzoumanian D, Benedettini M, Bontemps S, Elia D, Hennemann M, Hill T, Könyves V, Louvet F, Peretto N, Roy A, White GJ (2014) Class 0 protostars in the Perseus Molecular Cloud: a correlation between the youngest protostars and the dense gas distribution. Astrophys J 787:L18. https://doi.org/10.1088/2041-8205/787/2/L18

Safron EJ, Fischer WJ, Megeath ST, Furlan E, Stutz AM, Stanke T, Billot N, Rebull LM, Tobin JJ, Ali B, Allen LE, Booker J, Watson DM, Wilson TL (2015) HOPS 383: an outbursting class 0 protostar in Orion. Astrophys J 800:L5. https://doi.org/10.1088/2041-8205/800/1/L5

Sánchez-Monge Á, Palau A, Estalella R, Beltrán MT, Girart JM (2008) Survey of intermediate/high mass star-forming regions at centimeter and millimeter wavelengths. Astron Astrophys 485:497–515. https://doi.org/10.1051/0004-6361:20078406

Sandell G, Goss WM, Wright M (2005) Protostars and outflows in the NGC 7538 IRS 9 cloud core. Astrophys J 621:839–852. https://doi.org/10.1086/427625

Sandell G, Goss WM, Wright M, Corder S (2009) NGC 7538 IRS 1: an ionized jet powered by accretion. Astrophys J 699:L31–L34. https://doi.org/10.1088/0004-637X/699/1/L31

Sanna A, Reid MJ, Carrasco-González C, Menten KM, Brunthaler A, Moscadelli L, Rygl KLJ (2012) Clustered star formation and outflows in AFGL 2591. Astrophys J 745:191. https://doi.org/10.1088/0004-637X/745/2/191

Sanna A, Surcis G, Moscadelli L, Cesaroni R, Goddi C, Vlemmings WHT (2015) Velocity and magnetic fields within 1000 AU of a massive YSO. Astron Astrophys 583:L3. https://doi.org/10.1051/0004-6361/201526806

Sanna A, Moscadelli L, Surcis G, van Langevelde HJ, Torstensson KJE, Sobolev AM (2017) Planar infall of CH_3OH gas around Cepheus A HW2. Astron Astrophys 603:A94. https://doi.org/10.1051/0004-6361/201730773

Santiago-García J, Tafalla M, Johnstone D, Bachiller R (2009) Shells, jets, and internal working surfaces in the molecular outflow from IRAS 04166+2706. Astron Astrophys 495:169–181. https://doi.org/10.1051/0004-6361:200810739

Sato F, Mizuno A, Nagahama T, Onishi T, Yonekura Y, Fukui Y (1994) A new look at the dark cloud L1251: sensitive observations of the molecular emission. Astrophys J 435:279–289. https://doi.org/10.1086/174813

Schwartz PR, Simon T, Campbell R (1986) The T Tauri radio source. II. The winds of T Tauri. Astrophys J 303:233–238. https://doi.org/10.1086/164069

Sekimoto Y, Tatematsu K, Umemoto T, Koyama K, Tsuboi Y, Hirano N, Yamamoto S (1997) Molecular outflows from X-ray-emitting protostars in the ρ Ophiuchi dark cloud. Astrophys J 489:L63–L66. https://doi.org/10.1086/310961

Shepherd DS, Churchwell E (1996) High-velocity molecular gas from high-mass star formation regions. Astrophys J 457:267. https://doi.org/10.1086/176727

Shepherd DS, Testi L, Stark DP (2003) Clustered star formation in W75 N. Astrophys J 584:882–894. https://doi.org/10.1086/345743

Shepherd DS, Yu KC, Bally J, Testi L (2000) The molecular outflow and possible precessing jet from the massive young stellar object IRAS 20126+4104. Astrophys J 535:833–846. https://doi.org/10.1086/308873

Shirley YL, Claussen MJ, Bourke TL, Young CH, Blake GA (2007) The detection and characterization of centimeter radio continuum emission from the low-mass protostar L1014-IRS. Astrophys J 667:329–339. https://doi.org/10.1086/520570

Skinner SL, Brown A, Stewart RT (1993) A high-sensitivity survey of radio continuum emission from Herbig Ae/Be stars. Astrophys J Suppl Ser 87:217–265. https://doi.org/10.1086/191803
Skinner SL, Rebull L, Güdel M (2014) An X-ray and infrared survey of the Lynds 1228 cloud core. Astron J 147:88. https://doi.org/10.1088/0004-6256/147/4/88
Smirnov GT, Sorochenko RL, Pankonin V (1984) Stark broadening in radio recombination lines towards the Orion Nebula. Astron Astrophys 135:116–121
Snell RL, Loren RB, Plambeck RL (1980) Observations of CO in L 1551: evidence for stellar wind driven shocks. Astrophys J 239:L17–L22. https://doi.org/10.1086/183283
Snell RL, Scoville NZ, Sanders DB, Erickson NR (1984) High-velocity molecular jets. Astrophys J 284:176–193. https://doi.org/10.1086/162397
Sridharan TK, Beuther H, Schilke P, Menten KM, Wyrowski F (2002) High-mass protostellar candidates. I. The sample and initial results. Astrophys J 566:931–944. https://doi.org/10.1086/338332
Stojimirović I, Snell RL, Narayanan G (2008) Multiple parsec-scale outflows in the NGC 2071 cluster. Astrophys J 679:557–569. https://doi.org/10.1086/586688
Strelnitski V, Bieging JH, Hora J, Smith HA, Armstrong P, Lagergren K, Walker G (2013) The parsec-scale environment and the evolutionary status of MWC 349A. Astrophys J 777:89. https://doi.org/10.1088/0004-637X/777/2/89
Surcis G, Vlemmings WHT, Dodson R, van Langevelde HJ (2009) Methanol masers probing the ordered magnetic field of W75N. Astron Astrophys 506:757–761. https://doi.org/10.1051/0004-6361/200912790
Surcis G, Vlemmings WHT, van Langevelde HJ, Goddi C, Torrelles JM, Cantó J, Curiel S, Kim S-W, Kim J-S (2014) Rapidly increasing collimation and magnetic field changes of a protostellar H_2O maser outflow. Astron Astrophys 565:L8. https://doi.org/10.1051/0004-6361/201423877
Takahashi S, Saito M, Ohashi N, Kusakabe N, Takakuwa S, Shimajiri Y, Tamura M, Kawabe R (2008) Millimeter- and submillimeter-wave observations of the OMC-2/3 region. III. An extensive survey for molecular outflows. Astrophys J 688:344–361. https://doi.org/10.1086/592212
Takahashi S, Ohashi N, Bourke TL (2013) Direct imaging of a compact molecular outflow from a very low luminosity object: L1521F-IRS. Astrophys J 774:20. https://doi.org/10.1088/0004-637X/774/1/20
Takakuwa S, Saigo K, Matsumoto T, Saito M, Lim J, Hanawa T, Yen H-W, Ho PTP (2017) Spiral arms, infall, and misalignment of the circumbinary disk from the circumstellar disks in the protostellar binary system L1551 NE. Astrophys J 837:86. https://doi.org/10.3847/1538-4357/aa6116
Tamura M, Gatley I, Joyce RR, Ueno M, Suto H, Sekiguchi M (1991) Infrared polarization images of star-forming regions. I. The ubiquity of bipolar structure. Astrophys J 378:611–627. https://doi.org/10.1086/170462
Tanaka KEI, Tan JC, Zhang Y (2016) Outflow-confined HII regions. I. First signposts of massive star formation. Astrophys J 818:52. https://doi.org/10.3847/0004-637X/818/1/52
Terebey S, Vogel SN, Myers PC (1989) High-resolution CO observations of young low-mass stars. Astrophys J 340:472–478. https://doi.org/10.1086/167410
Thum C, Neri R, Báez-Rubio A, Krips M (2013) LkHα 101 at millimeter wavelengths. Astron Astrophys 556:A129. https://doi.org/10.1051/0004-6361/201321422
Torrelles JM, Ho PTP, Rodriguez LF, Canto J (1985) VLA observations of ammonia and continuum in regions with high-velocity gaseous outflows. Astrophys J 288:595–603. https://doi.org/10.1086/162825
Torrelles JM, Anglada G, Rodriguez LF, Canto LF, Barral JF (1987) High angular resolution CO mapping of the high velocity gas associated with HL/XZ Tau and V 645 Cygni (GL 2789). Astron Astrophys 177:171–176
Torrelles JM, Gómez JF, Rodríguez LF, Ho PTP, Curiel S, Vázquez R (1997) A radio jet-H_2O maser system in W75N(B) at a 200 AU scale: exploring the evolutionary stages of young stellar objects. Astrophys J 489:744–752. https://doi.org/10.1086/304824
Torrelles JM, Gómez JF, Rodríguez LF, Curiel S, Anglada G, Ho PTP (1998) Radio continuum-H_2O maser systems in NGC 2071: H_2O masers tracing a jet (IRS 1) and a rotating proto-planetary disk of radius 20 AU (IRS 3). Astrophys J 505:756–765. https://doi.org/10.1086/306205
Torrelles JM, Patel NA, Gómez JF, Ho PTP, Rodríguez LF, Anglada G, Garay G, Greenhill L, Curiel S, Cantó J (2001) Spherical episodic ejection of material from a young star. Nature 411:277–280
Torrelles JM, Patel NA, Anglada G, Gómez JF, Ho PTP, Lara L, Alberdi A, Cantó J, Curiel S, Garay G, Rodríguez LF (2003) Evidence for evolution of the outflow collimation in very young stellar objects. Astrophys J 598:L115–L119. https://doi.org/10.1086/380750

Torrelles JM, Patel NA, Curiel S, Estalella R, Gómez JF, Rodríguez LF, Cantó J, Anglada G, Vlemmings W, Garay G, Raga AC, Ho PTP (2011) A wide-angle outflow with the simultaneous presence of a high-velocity jet in the high-mass Cepheus A HW2 system. Mon Not R Astron Soc 410:627–640. https://doi.org/10.1111/j.1365-2966.2010.17483.x

Torrelles JM, Curiel S, Estalella R, Anglada G, Gómez JF, Cantó J, Patel NA, Trinidad MA, Girart JM, Carrasco-González C, Rodríguez LF (2014) A very young, compact bipolar H_2O maser outflow in the intermediate-mass star-forming LkHα 234 region. Mon Not R Astron Soc 442:148–159. https://doi.org/10.1093/mnras/stu847

Trinidad MA (2011) Searching for the Driving Source of the CO Molecular Outflow in the High-mass Star-forming Region G240.31+0.07. Astron J 142:147. https://doi.org/10.1088/0004-6256/142/5/147

Trinidad MA, Curiel S, Migenes V, Patel N, Torrelles JM, Gómez JF, Rodríguez LF, Ho PTP, Cantó J (2005) Very Large Array simultaneous 1.3 cm continuum and H_2O maser observations toward IRAS 20126+4104. Astron J 130:2206–2211. https://doi.org/10.1086/452639

Trinidad MA, Curiel S, Torrelles JM, Rodríguez LF, Migenes V, Patel N (2006) Interferometric observations toward the high-mass young stellar object IRAS 23139+5939: radio continuum and water maser emission. Astron J 132:1918–1922. https://doi.org/10.1086/507127

Trinidad MA, Curiel S, Estalella R, Cantó J, Raga A, Torrelles JM, Patel NA, Gómez JF, Anglada G, Carrasco-González C, Rodríguez LF (2013) Formation and evolution of the water maser outflow event in AFGL 2591 VLA 3-N. Mon Not R Astron Soc 430:1309–1323. https://doi.org/10.1093/mnras/sts707

Tychoniec L, Tobin JJ, Karska A, Chandler C, Dunham MM, Li Z-Y, Looney LW, Segura-Cox D, Harris RJ, Melis C, Sadavoy SI (2018) The VLA Nascent Disk And Multiplicity Survey of Perseus Protostars (VANDAM). III. Extended Radio Emission from Protostars in Perseus. Astrophys J 852:18. https://doi.org/10.3847/1538-4357/aa9980

Uscanga L, Cantó J, Curiel S, Anglada G, Torrelles JM, Patel NA, Gómez JF, Raga AC (2005) A 1 AU expanding water maser circular ring in the W75 N(B)-VLA 2 shell. Astrophys J 634:468–475. https://doi.org/10.1086/491783

van den Ancker ME, The PS, Tjin A, Djie HRE, Catala C, de Winter D, Blondel PFC, Waters LBFM (1997) HIPPARCOS data on Herbig Ae/Be stars: an evolutionary scenario. Astron Astrophys 324:L33–L36

van Kempen TA, van Dishoeck EF, Salter DM, Hogerheijde MR, Jørgensen JK, Boogert ACA (2009) The nature of the class I population in Ophiuchus as revealed through gas and dust mapping. Astron Astrophys 498:167–194. https://doi.org/10.1051/0004-6361/200810445

van Kempen TA, Hogerheijde MR, van Dishoeck EF, Kristensen LE, Belloche A, Klaassen PD, Leurini S, San Jose-Garcia I, Aykutalp A, Choi Y, Endo A, Frieswijk W, Harsono D, Karska A, Koumpia E, van der Marel N, Nagy Z, Pérez-Beaupuits J-P, Risacher C, van Weeren RJ, Wyrowski F, Yıldız UA, Güsten R, Boland W, Baryshev A (2016) Outflow forces in intermediate-mass star formation. Astron Astrophys 587:A17. https://doi.org/10.1051/0004-6361/201424725

Velázquez PF, Rodríguez LF (2001) VLA observations of Z CMa: the orientation and origin of the thermal jet. Rev Mex Astron Astrof 37:261–267

Velusamy T, Langer WD, Marsh KA (2007) Highly collimated jets and wide-angle outflows in HH 46/47: new evidence from Spitzer infrared images. Astrophys J 668:L159–L162. https://doi.org/10.1086/522929

Vig S, Veena VS, Mandal S, Tej A, Ghosh SK (2018) Detection of non-thermal emission from the massive protostellar jet HH80-81 at low radio frequencies using GMRT. Mon Not R Astron Soc 474:3808–3816. https://doi.org/10.1093/mnras/stx3032

Vlemmings WHT, Surcis G, Torstensson KJE, van Langevelde HJ (2010) Magnetic field regulated infall on the disc around the massive protostar Cepheus A HW2. Mon Not R Astron Soc 404:134–143. https://doi.org/10.1111/j.1365-2966.2010.16297.x

Walker CK, Lada CJ, Young ET, Margulis M (1988) An unusual outflow around IRAS 16293–2422. Astrophys J 332:335–345. https://doi.org/10.1086/166659

Walmsley CM (1990) Level populations for millimeter recombination lines. Astron Astrophys Suppl Ser 82:201–206

Ward-Thompson D, Eiroa C, Casali MM (1995) Confirmation of the driving source of the NGC 2264G bipolar outflow: a class 0 protostar. Mon Not R Astron Soc 273:L25–L28. https://doi.org/10.1093/mnras/273.1.L25

Weintroub J, Moran JM, Wilner DJ, Young K, Rao R, Shinnaga H (2008) Submillimeter Array imaging of the maser emission from the H30α radio recombination line in MWC 349A. Astrophys J 677:1140–1150. https://doi.org/10.1086/529132

Wilking BA, Blackwell JH, Mundy LG, Howe JE (1989) A millimeter-wave spectral-line and continuum survey of cold IRAS sources. Astrophys J 345:257–264. https://doi.org/10.1086/167901

Wilner DJ, Reid MJ, Menten KM (1999) The synchrotron jet from the H_2O maser source in W3(OH). Astrophys J 513:775–779. https://doi.org/10.1086/306907

Wootten A, Loren RB (1987) L 1689N: misalignment between a bipolar outflow and a magnetic field. Astrophys J 317:220–230. https://doi.org/10.1086/165270

Wouterloot JGA, Henkel C, Walmsley CM (1989) CO observations of IRAS sources in Orion and Cepheus. Astron Astrophys 215:131–146

Wu YW, Xu Y, Pandian JD, Yang J, Henkel C, Menten KM, Zhang SB (2010) Ammonia and CO observations toward low-luminosity 6.7 GHz methanol masers. Astrophys J 720:392–408. https://doi.org/10.1088/0004-637X/720/1/392

Xu J-L, Wang J-J, Qin S-L (2012) Outflow and accretion detections in the young stellar object IRAS 04579+4703. Astron Astrophys 540:L13. https://doi.org/10.1051/0004-6361/201118657

Yang J, Umemoto T, Iwata T, Fukui Y (1991) A millimeter-wave line study of L 1287: a case of induced star formation by stellar wind compression? Astrophys J 373:137–145. https://doi.org/10.1086/170032

Yıldız UA, Kristensen LE, van Dishoeck EF, Belloche A, van Kempen TA, Hogerheijde MR, Güsten R, van der Marel N (2012) APEX-CHAMP$^+$ high-J CO observations of low-mass young stellar objects. III. NGC 1333 IRAS 4A/4B envelope, outflow, and ultraviolet heating. Astron Astrophys 542:A86. https://doi.org/10.1051/0004-6361/201118368

Yu KC, Billawala Y, Smith MD, Bally J, Butner HM (2000) A multiwavelength study of outflows in OMC-2/3. Astron J 120:1974–2006. https://doi.org/10.1086/301565

Yun JL, Clemens DP (1994) Outflows from young stellar objects in Bok globules: maps. Astrophys J Suppl Ser 92:145–161. https://doi.org/10.1086/191963

Zapata LA, Rodríguez LF, Ho PTP, Beuther H, Zhang Q (2006) In search of circumstellar disks around young massive stars. Astron J 131:939–950. https://doi.org/10.1086/499156

Zapata LA, Schmid-Burgk J, Muders D, Schilke P, Menten K, Guesten R (2010) A rotating molecular jet in Orion. Astron Astrophys 510:A2. https://doi.org/10.1051/0004-6361/200810245

Zapata LA, Lizano S, Rodríguez LF, Ho PTP, Loinard L, Fernández-López M, Tafoya D (2015a) Kinematics of the outflow from the young star DG Tau B: rotation in the vicinities of an optical jet. Astrophys J 798:131. https://doi.org/10.1088/0004-637X/798/2/131

Zapata LA, Palau A, Galván-Madrid R, Rodríguez LF, Garay G, Moran JM, Franco-Hernández R (2015b) ALMA reveals a candidate hot and compact disc around the O-type protostar IRAS 16547–4247. Mon Not R Astron Soc 447:1826–1833. https://doi.org/10.1093/mnras/stu2527

Zhang Q, Hunter TR, Brand J, Sridharan TK, Cesaroni R, Molinari S, Wang J, Kramer M (2005) Search for CO outflows toward a sample of 69 high-mass protostellar candidates. II. Outflow properties. Astrophys J 625:864–882. https://doi.org/10.1086/429660

Zhang Q, Hunter TR, Beuther H, Sridharan TK, Liu S-Y, Su Y-N, Chen H-R, Chen Y (2007) Multiple jets from the high-mass (proto)stellar cluster AFGL 5142. Astrophys J 658:1152–1163. https://doi.org/10.1086/511381

Zhang C-P, Wang J-J, Xu J-L, Wyrowski F, Menten KM (2014) Submillimeter Array and Very Large Array observations in the hypercompact H II region G35.58−0.03. Astrophys J 784:107. https://doi.org/10.1088/0004-637X/784/2/107

Zhang Y, Arce HG, Mardones D, Cabrit S, Dunham MM, Garay G, Noriega-Crespo A, Offner SSR, Raga AC, Corder SA (2016) ALMA cycle 1 observations of the HH46/47 molecular outflow: structure, entrainment, and core impact. Astrophys J 832:158. https://doi.org/10.3847/0004-637X/832/2/158

Zhu L, Zhao J-H, Wright MCH, Sandell G, Shi H, Wu Y-F, Brogan C, Corder S (2013) Subarcsecond observations of NGC 7538 IRS 1: continuum distribution and dynamics of molecular gas. Astrophys J 779:51. https://doi.org/10.1088/0004-637X/779/1/51

Zijlstra AA, Pottasch SR, Engels D, Roelfsema PR, te Lintel Hekkert P, Umana G (1990) Mapping the outflow of OH:5.89−0.39. Mon Not R Astron Soc 246:217